

The Radio and Electronic Engineer

The Journal of the Institution of Electronic and Radio Engineers

A Season of Exhibitions

IN the springtime the engineer's thoughts turn to what the marketing department have been thinking about all through the winter: most of the exhibitions aimed at British engineers concerned with electronics either as producers or users fall between April and June, and this year is no exception, indeed the calendar is fuller in this respect than for some years. Much faith and foresight must be summoned up by the prospective organizer but we should all wish his enterprise success since a busy exhibition, crowded with visitors from home and overseas, promises increased prosperity for the industry.

The exhibition scene this year has been dominated by the opening of the huge new National Exhibition Centre just outside Birmingham. Controversy aroused by the concept, and fuelled by misgivings during its building, continues and will not be immediately resolved. Meanwhile advocates of a much smaller, London-based event promoted 'The All-Electronics Show' at Grosvenor House in April and inevitably one hears conflicting opinions on its success. Generally exhibitors showed limited ranges of equipment, mostly newer models or best-sellers, which could possibly be a disadvantage if a visitor wanted to see a wide range of items. Convenience of access to south-eastern England (and for overseas visitors staying in London) is perhaps justified for the electronics industry which is predominantly based in this quarter of the United Kingdom.

Broader considerations do however apply if an exhibition's aim is to present products to potential users in other industries. Thus Birmingham, where the combined IEA-Electrex (Instruments, Electronics and Automation, and Electrical Engineering Exhibitions) was held early this month is much nearer the geographical centre of industrial Britain. Certainly we saw there numerous exhibits aimed at the electronics industry, notably production techniques, piece parts and materials. The instrumentation and automation themes however could potentially interest almost every manufacturing industry and association with the electrical industry seemed to be both logical and convenient for exhibitors and visitors alike. It does however put this combined event fairly and squarely into the 'big league' and one may question if with just 20% of the 1060 exhibiting firms from 28 countries it yet ranks with the big European fairs, though N.E.C.'s facilities drew favourable comments from many with experience of its overseas competitors. A sizeable section of the electronics industry also took part in HEDA—Home Electronics and Domestic Appliances Exhibition—at the end of May, which continued for the general public over a further four days as 'Sound and Vision 76'. Midlanders and Northerners will have thus a more convenient opportunity to see what has hitherto been a London event (Radiolympia and its successors!).

So much for the big, general shows. In June a more specialized event—Communications 76—opens in Brighton, with which is linked a conference, while previously the IERE Conference on Applications of Electronics in Medicine at Southampton in April included a small specialized exhibition. Even more specialized are the Defence Training Equipment Exhibition (held in April) and the British Army Equipment Exhibition (in June) which are mainly for overseas military purchasers, in a manner analogous to the biennial Greenwich Naval Equipment Exhibition; in all three electronics is but one aspect. Later in this year will be the SBAC Flying Display and Exhibition at Farnborough which has a large 'electronics user' sector.

It will be seen from this brief survey of the 'exhibition season' that almost every professional interest of the electronic and radio engineer is being covered during the space of a few months. This poses the question—can a visit to an exhibition effectively bring the average engineer up-to-date both within and outside his own specialization? To a certain extent we may draw a parallel with the role of an Institution journal: blinkers may help horses pull carts without distractions but the broadening of his horizons must surely be an important part of an engineer's daily life.

Contributors to this issue*



Dr. Ernest Patterson studied Physics at Chelsea College, London University, where he obtained his B.Sc., M.Sc. and Ph.D. From there he joined The General Electric Company Limited in 1969 and worked in the Quantum Electronics Group at the Hirst Research Centre, publishing papers on microwave phonon interactions. He is at present a member of the principal scientific staff and leads a team

carrying out research and development on ultrasonic techniques for signal processing. His principal interest has been in the systems application of surface acoustic wave techniques and he has published a number of papers in this area.



Mr. K. V. Lever studied mathematics at Liverpool University, where he obtained his B.Sc. Honours degree. He then joined the Hirst Research Centre of The General Electric Company Limited in 1966, where he worked on the analysis of various types of communication systems. In 1972 he received the M.Sc. degree in telecommunication systems from Essex University. He is at present with the Microelectronics Division at the Hirst Research Centre where his principal interests and publications are in the areas of component characterization and systems analysis.



Mr. I. M. Wilson obtained an open exhibition to Jesus College Oxford and graduated with a B.A. (Honours) in Physics in 1973. He then joined the Microelectronics Division of The General Electric Company Limited, Hirst Research Centre, and has worked on a number of projects concerned with surface acoustic waves.



Mr. P. C. Stevens read physics at Imperial College, London and obtained a B.Sc. (Hons) and Associateship of the Royal College of Science in 1974. He then joined The General Electric Company Limited, Hirst Research Centre and has worked in the SAW group on signal processing for communications and radar systems.



Dr. G. Alastair Armstrong received the B.Sc. degree in electrical engineering from Queen's University, Belfast, in 1968. He was subsequently awarded the Dunville Research Studentship in Physical Sciences and spent three further years at Queen's University on research concerned with computer modelling of m.o.s. transistors. On the basis of this work, he was awarded the Ph.D. degree in 1971. Since joining

Microwave and Electronic Systems Limited in 1971, he has worked on projects associated with the application of surface acoustic wave devices. Dr. Armstrong is currently in charge of all the company's c.a.d. activities.



Dr. M. B. N. Butler obtained his B.Sc. degree in physics at Newcastle University and studied solid-state physics for his Doctorate. On leaving the University he joined Standard Telecommunication Laboratories and worked on non-linear interactions between charge carriers and acoustic waves in piezoelectric semiconductors and later on the design of surface acoustic wave devices. In 1972 he went

to M.E.S.L. where he has worked throughout on the design of surface wave devices and subsystems. Currently, Dr. Butler is Engineering Manager, concerned with component and surface wave subsystem design and development.



Mr. Hugh Walker graduated from Churchill College, Cambridge in 1969 with an honours degree in mechanical sciences, and the following year received an M.Sc. from Southampton University where he specialized in circuit design. He joined the Research and Development Laboratory of Hewlett-Packard Limited in 1970 and worked on equipment for testing microwave telecommunication systems. More recently he has been concerned with transmission measurements and receiver design and is currently a project leader for selective level measuring sets.

* See also pages 220 and 236.

Second-order effects in acoustic surface-wave filters: design methods

HALVOR SKEIE, M.S., Ph.D.*

and

HELGE ENGAN, M.S., Ph.D.†

SUMMARY

Second-order effects, which may be defined as those effects which prevent acoustic surface-wave filters from behaving as ideal transversal filters, are described systematically. Explicit exact and approximate formulas are given for the effect of acoustic multireflections and external matching circuits on both the main signal response and triple transit echoes. The effect of non-uniform tap coupling across the acoustic beam is described, and weighting methods that provide a more uniform coupling are presented. Other secondary effects like electrostatic or quasistatic end effects, beam diffraction, mass loading and bulk wave excitation are briefly described. A method for the correction of positioning errors or delay errors by experimental means is described.

**Electronics Research Laboratory, University of Trondheim, N7034 Trondheim, NTH, Norway*

†*The Norwegian Institute of Technology, University of Trondheim, N7034 Trondheim, NTH, Norway.*

1 Introduction

An acoustic surface-wave filter where the filter response is shaped by a weighting of finger taps is conceptually a transversal filter. An ideal transversal filter with a periodic distribution of taps may also be realized by digital techniques. A surface-wave filter may thus be analogous to a non-recursive digital filter. The latter type of filters has been quite extensively studied and methods of synthesizing a desired frequency response with a minimum number of taps have been given.¹⁻³ As a starting point in the process of designing a surface-wave filter, results derived from these studies are useful.

Basically, the tap weighting function is determined by the Fourier transform of the specified frequency response (see Fig. 1). The time impulse response derived in this way is of course of infinite extension. In a practical filter the weighting function has to be truncated after a finite number of sidelobes. The truncation gives rise to Gibbs oscillations in the frequency response which may represent a serious degradation at the band edges. A simple truncation of the Fourier transform of an ideal frequency response is equivalent to multiplication with a rectangular window function. By shaping the window function differently, the Gibbs oscillations may be effectively reduced. Several types of window functions have been investigated and of these, the Dolph-Chebyshev functions yield the minimum width for a given sidelobe level which are constant for all sidelobes.²

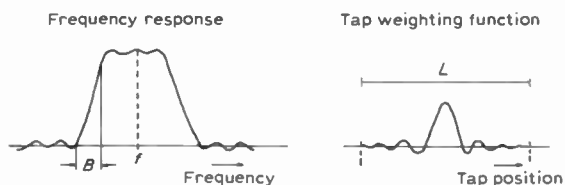


Fig. 1. Specified frequency response and corresponding tap weighting function.

Characteristic quantities in the specified frequency response of band-pass filters are pass-band ripple, stop-band isolation and transition bandwidth. For a particular type of window function, one of these quantities determines the minimum length of the impulse response (number of taps). In cases where the characteristic quantities are specified such that they do not fit the most commonly known window functions in an optimal or near optimal manner, other direct optimization schemes involving numerical iteration procedures may be employed.^{4,5}

Once an optimal or sub-optimal weighting function has been found, the next step might be to choose a basic transducer layout. The weighting may to some extent be implemented on both input and output transducers, the total weighting function being the convolution of two separate weighting functions. It may also be of interest to minimize the number of taps in one or both of the two transducers within the given time impulse duration or transducer lengths. This is done by 'thinning' the transducer structures so that the spacing between adjacent taps becomes more than the conventional half-wavelength.

The thinning gives rise to multiple frequency responses. By choosing different thinning factors for the two transducers, the total filter will exhibit only one or at least a strongly reduced number of frequency responses as shown in Fig. 2.⁶

The detailed transducer layout may further be chosen on the basis of a specified insertion loss. Conventional surface-wave filters are inherently more lossy than their equivalent lumped circuit or distributed electromagnetic counterparts. It is therefore very often desirable to minimize the insertion loss as much as possible. A low insertion loss requires either the use of substrates with a strong piezoelectric coupling, a great number of taps with external tuning, or both.

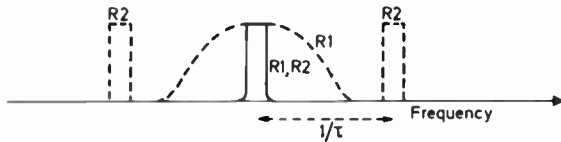


Fig. 2. Frequency response of a filter with different thinning of the input and output transducers used to suppress undesired passbands.

The surface-wave filter is no ideal transversal filter; a number of secondary effects contribute to significant deviations from the ideal response. Some of the most important of these secondary effects tend to increase in importance when low insertion loss is required.

For the design of high performance filters, it is therefore necessary to know these effects fully and to adopt methods for an efficient reduction or compensation of them in the design process. The most important secondary effects are analysed in the following and several methods for compensation are described in detail.

Several of the secondary effects can be included in an equivalent network model^{7,16} for the transducer or they can be taken care of in a more direct numerical calculation of the transducer radiation and detection.¹⁷ In the following we shall not go into details concerning these methods of analysis; instead we will describe the secondary effects more isolated and give approximate quantitative information which can be used in a systematic design procedure.

2 Acoustic Multireflections

The effect of passive acoustic reflections from the taps are most clearly described if we initially assume that the transducer is very weakly coupled to the external circuitry. In most transducer designs, all taps are parallel coupled. In this case the transducer acts as a passive array of reflectors only if the electric terminals are shorted. In the other extreme of weak coupling to the external circuitry, i.e. open electric terminals, the parallel coupled taps cause re-excitation effects which we will describe as an effect caused by the external circuitry.

If the external impedance is very small and purely resistive the acousto-electric transfer is proportional to the sum of the short circuit currents of each individual

tap as induced by an incident surface-wave. Suppose we describe a tap by its three-port scattering matrix (see Fig. 3):

$$S_n = \begin{bmatrix} r_n & t_n & c_n \\ t_n & r_n & c_n \\ c_n & c_n & e_n \end{bmatrix} \tag{1}$$

For simplicity we assume that the tap is symmetric and reciprocal. This can be done without much loss of generality, if we allow for zero coupling taps to be inserted between the 'active' taps. The notation in equation (1) is

- r_n = acoustic reflection coefficient
- t_n = acoustic transmission coefficient
- c_n = acousto-electric transmission
- e_n = electric reflection coefficient.

If acoustic waves of amplitudes a_n and b_n are incident on the two acoustic ports I and II, respectively, the acousto-electric transfer for a nearly shorted tap will be:

$$c'_n \simeq c_n \sqrt{R/R_0}(a_n + b_n) \tag{2}$$

where R is the external load resistance and R_0 the reference impedance (usually 50 Ω).

The tap weighting is included in c_n , so that if the transducer were to behave as an ideal transversal filter with a wave of unit amplitude incident at the beginning of the transducer we should have

$$\begin{aligned} a_n &= e^{-j\phi_n} \\ b_n &= 0 \end{aligned} \tag{3}$$

where ϕ_n is the phase delay of tap n . The presence of b_n is thus caused by acoustic reflections and a_n will be reduced as the wave passes through the transducer because of reflection losses. Very often the transducer

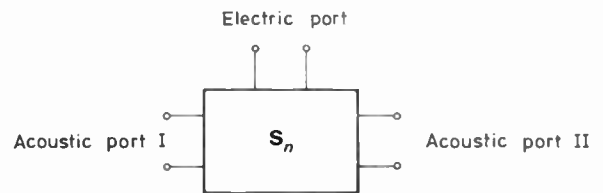


Fig. 3. Transmission line 3-port equivalent of basic transducer element (tap).

can be treated sufficiently accurately as a periodic array with constant reflections at each tap; the waves a_n and b_n can then be described by:

$$a_n = \frac{\cos(N+1-n)\psi + j\left(\frac{z+1/z}{2}\right)\sin(N+1-n)\psi}{\cos N\psi + j\left(\frac{z+1/z}{2}\right)\sin N\psi} \tag{4}$$

$$b_n = \frac{j\left(\frac{z-1/z}{2}\right)\sin(N-n)\psi}{\cos N\psi + j\left(\frac{z+1/z}{2}\right)\sin N\psi} \tag{5}$$

Here, ψ and z are characteristic quantities of the

periodic structure, N is the total number of taps. In our case of symmetric taps we may define:

$$\begin{aligned} \cos \psi &= \frac{\cos \phi}{\sqrt{1-|r|^2}} \\ z &= \sqrt{\frac{\sin \phi \pm |r|}{\sin \phi \mp |r|}} \\ t' &= \frac{e^{-j\phi}}{\sqrt{1-|r|^2}} \end{aligned} \quad (6)$$

where $|r|$ is the absolute value of the acoustic reflection coefficient at each tap and t' is the corresponding acoustic transmission coefficient.

With a large number of taps (N), the distortion of t'_n will be considerable even for weakly piezoelectric materials. At higher frequencies, mass loading due to the finite thickness of the electrodes may enhance this distortion.

If the distortion is reasonably small, it can be described quite accurately by first-order approximations. Thus we write:

$$\begin{aligned} z + 1/z &\simeq 2 \\ z - 1/z &\simeq \frac{\pm 2|r|}{\sin \phi} \end{aligned} \quad (7)$$

and we get

$$a_n \simeq e^{-j(n-1)\phi} \quad (8)$$

$$b_n \simeq \pm j|r| e^{-jn\phi} \frac{\sin(N-n)\phi}{\sin \phi} \quad (9)$$

and

$$\begin{aligned} c'_n &= c_n \sqrt{R/R_0} e^{-j(n-1)\phi} \times \\ &\times \left[1 \pm j|r| e^{-j(N-n+1)\phi} \frac{\sin(N-n)\phi}{\sin \phi} \right]. \end{aligned} \quad (10)$$

If we write the total transducer transfer-function as a sum of a symmetric and an antisymmetric part, the distortion and the unperturbed transfer can be factorized in a convenient way. We write

$$\begin{aligned} T &= \sum_{n=1}^N c_n e^{-j(n-1)\phi} \\ &= e^{-j(N-1)/2\phi} \sum_{p=0}^{(N-1)/2} (a_p \cos p\phi + j b_p \sin p\phi) \end{aligned} \quad (11)$$

where now

$$\begin{aligned} p = N/2 - n + \frac{1}{2}, \quad c_n &= \frac{a_p + b_p}{2} \quad \text{for } n < \frac{N-1}{2} \\ p = -N/2 + n - \frac{1}{2}, \quad c_n &= \frac{a_p - b_p}{2} \quad \text{for } n > \frac{N+1}{2} \end{aligned} \quad (12)$$

and we have assumed that N is an odd number. By substitution of equation (11) into equation (10) and summing, we obtain

$$\begin{aligned} T' &= \sqrt{R/R_0} e^{-j\left(\frac{N-1}{2}\right)\phi} \times \\ &\times \left\{ \sum_{p=0}^{(N-1)/2} a_p \cos p\phi \left(1 \pm j|r| e^{-j\left(\frac{N+1}{2}\right)\phi} \frac{\sin\left(\frac{N-1}{2}\right)\phi}{\sin \phi} \right) + \right. \end{aligned}$$

$$\left. + j \sum_{p=0}^{(N-1)/2} b_p \sin p\phi \left[1 + j|r| e^{-j\left(\frac{N-1}{2}\right)\phi} \frac{\cos\left(\frac{N-1}{2}\right)\phi}{\sin \phi} \right] \right\}. \quad (13)$$

As we see from equation (13) the multi-reflections lead to a superimposed ripple both in the amplitude and phase characteristics of the frequency response.

The most common band-pass filters are specified to have a symmetric or nearly symmetric amplitude frequency response. In this case, the amplitude response may be written

$$|T'| \simeq \sqrt{R/R_0} |T| \left[1 \pm \frac{|r|(\cos \phi - \cos N\phi)}{2 \sin \phi} \right] \quad (14)$$

if $|r|$ is sufficiently small.

In transducers where the taps are spaced by an integer number of acoustic half wavelengths at the resonance frequency, we may for narrow-band operation introduce the approximation:

$$\begin{aligned} \sin \phi &\simeq \pm 2x/N \\ \cos \phi - \cos N\phi &\simeq \pm 2 \sin^2 x \end{aligned} \quad (15)$$

where

$$x = \frac{Nk\pi}{2} \left(\frac{f-f_0}{f_0} \right) \quad (16)$$

k is the tap spacing in number of acoustic half wavelengths, f is the operating frequency and f_0 the resonance frequency. Accordingly, one finds

$$|T'| \simeq \sqrt{R/R_0} |T| \cdot \left(1 \pm |r| \cdot \frac{N \sin^2 x}{2x} \right) \quad (17)$$

The maximum ripple is given by

$$d_{\max} \simeq \pm 0.36 |r| N. \quad (18)$$

If mass loading is neglected, it has been found theoretically⁸ that the reflection $|r|$ from a shorted tap in a conventional interdigital transducer ($\lambda/2$ tap spacing) is given by

$$|r| \simeq 0.36 K_s^2 \quad (19)$$

at the resonance frequency, where $K_{s_i}^2$ is the surface wave coupling constant. This formula also agrees quite well with experiments performed on YZ lithium niobate.⁹

From electrostatic field calculations and perturbation theory it has been found that^{10,7}

$$|r| \simeq 0.41 K_s^2 \quad (20)$$

for a single two-finger tap. This formula should then apply for extensively 'thinned' transducers operating at the fundamental frequency.

The frequency response of a band-pass filter which is distorted by multi-reflections is compared with the response of a distortion-free filter in Fig. 4. In the next Figure (Fig. 5) are shown some design curves which depict the maximum ripple (peak to peak) in dB as function of the number of closely spaced or widely separated taps on several substrates. The curves are based on equations (18)–(20), and thus apply to taps with equal finger width and spacing. Mass loading effects are not included.

We see that for strong coupling materials like lithium niobate, the distortion due to acoustic multi-reflections becomes serious even for quite a small number of taps.

An efficient way of reducing the acoustic multi-reflections is to use double electrodes, or in the case of thinned transducers, extra dummy taps placed between the active taps.

In both cases, the effect on the total amplitude response may be seen by simply reducing the phase angle ϕ by a factor of 2 in equation (14), provided the spacing between the active taps corresponds to an odd number of half wavelengths. We obtain

$$|T'| = \sqrt{R/R_0} |T| \left[1 \pm \frac{|r|(\cos \phi/2 - \cos N\phi)}{2 \sin \phi/2} \right] \quad (21)$$

where $|r|$ now is the reflection from the narrow gap in a double electrode or the reflection as given by equation (20) in the case of widely-spaced taps. N is still taken to be the number of active taps.

For narrow-band operation we approximate

$$\cos \phi/2 \approx 0$$

$$\sin \phi/2 \approx 1$$

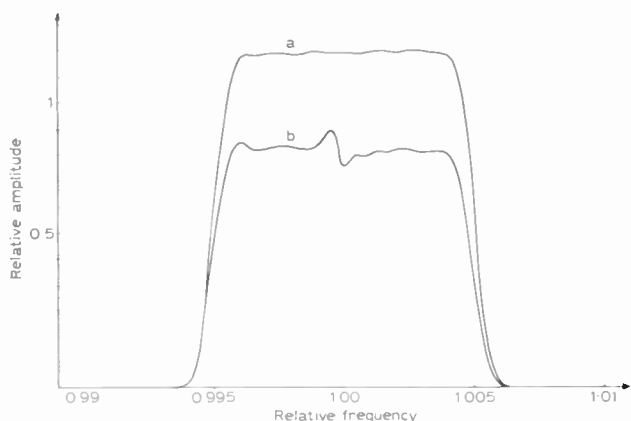


Fig. 4. Frequency responses of (a) distortion free filter, (b) filter with distortion caused by multi-reflections.

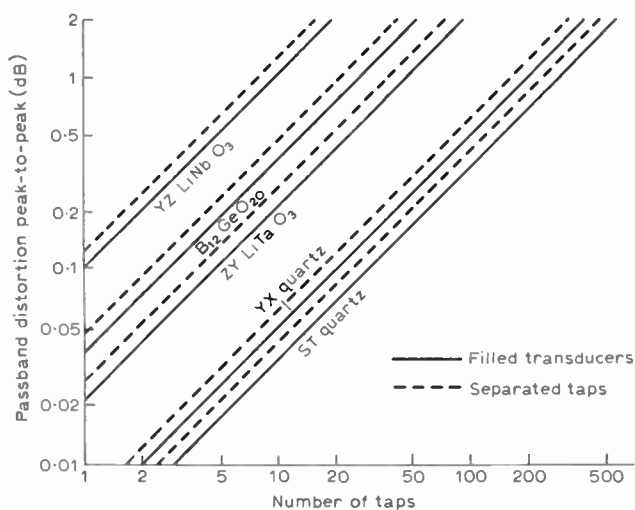


Fig. 5. Pass-band ripple caused by acoustic multi-reflections as function of the number of taps for several substrates.

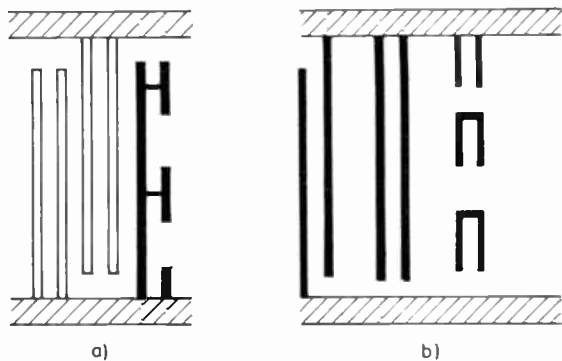


Fig. 6. Two examples of reducing acoustic reflections between a free surface and a transducer area.

(a) Filled double-electrode transducer.

(b) Thinned transducer with dummy taps.

and we see that we get a uniform ripple of amplitude:

$$d = \frac{|r|}{2} \quad (22)$$

For YZ lithium niobate, even this distortion amounts to ± 0.1 dB amplitude ripple in the case of widely-spaced taps.

From the phase factor $N\phi$ we see that in this case the reflection may be regarded as due to a mismatch between the transducer area and the free surface area. In filled double electrode patterns, this mismatch is found to be even greater.¹¹ This ripple is effectively reduced by weighting the last dummy tap or electrode as shown in Fig. 6.

Acoustic multi-reflections are effectively reduced also in transducers with several electrodes in a tap, so-called multi-electrode transducers. Multi-electrode transducers have the disadvantage that they require smaller line widths than single electrode transducers when operated at the fundamental frequency. This drawback can be overcome by operating at higher harmonics. In order to suppress unwanted side-responses and bulk waves, input and output transducers may be chosen to be of different types. An example is shown in Figs. 7-9.²¹

One transducer consists of four electrodes per electrical period and the other consists of six electrodes per

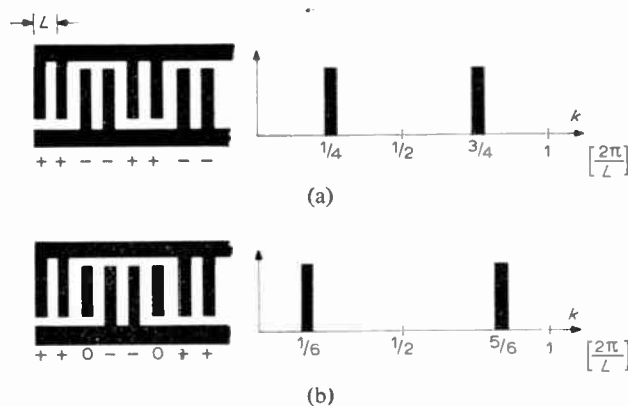


Fig. 7. Physical configurations and transmission spectra for two different multi-electrode transducers. The number of electrodes per electrical period is (a) $S_e = 4$ and (b) $S_e = 6$.

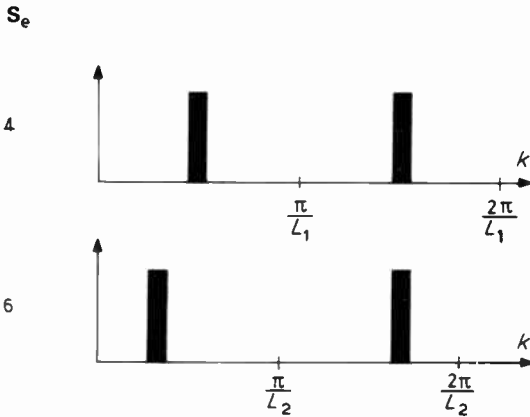


Fig. 8. Overlap of the upper sidebands of two transducers with $S_e = 4$ and 6 , respectively. The overlap is obtained by using different periodicities so that $L_1 = 0.9L_2$.

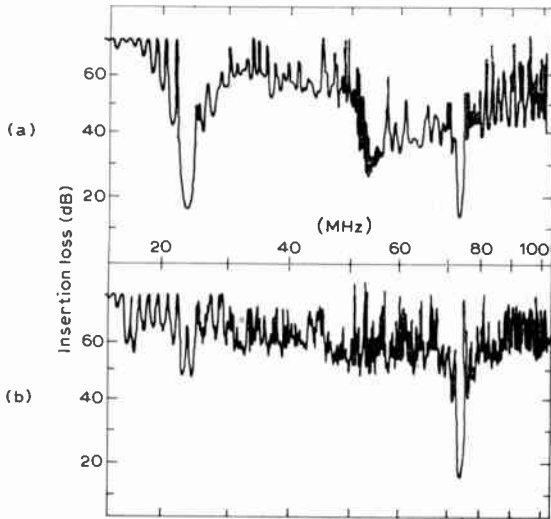


Fig. 9. Measured insertion loss of device with (a) two identical transducers, $S_e = 4$, (b) two different transducers with $S_e = 4$ and 6 and with different periodicities as explained in Fig. 8.

electrical period. The line widths are staggered by a factor of $10/9$ such that the 'upper' sidebands overlap. Thus the line widths are $3/8$ and $5/12$ of an acoustic wavelength, respectively.

In transducers with dummy taps, it is important that the dummy taps are electrically shorted, i.e. the two electrodes must be connected. If they are disconnected, the sign of the reflection coefficient will change, and the dummy taps will enhance the distortion rather than suppress it. This is demonstrated in Fig. 10.

3 Influence of External Matching on Phase and Amplitude Response

An external circuit with an arbitrary impedance will modify the response in equation (13). Suppose the external admittance is given by

$$y_L = \frac{R_0}{Z_L} = g_L + g_d + jb_L \quad (23)$$

and the transducer input admittance by

$$y_t = \frac{R_0}{Z_t} = g_t + jb_t. \quad (24)$$

Here

- g_L = relative load conductance
- g_p = relative dissipation conductance
- b_L = relative load susceptance
- g_t = relative acoustic radiation conductance
- b_t = relative transducer susceptance.

With an acoustic wave incident at the transducer, the short circuit electric current is given by

$$I_s = T'/\sqrt{R} \quad (25)$$

with notations as in the preceding Section.

If the total transducer response is taken to be proportional to the current flowing through the load conductance g_L , it will be given by

$$T'' = T'\sqrt{R_0/R} \cdot \frac{\sqrt{g_L}}{(y_t + y_L)} \quad (26)$$

In addition it is readily found that

$$g_t = \frac{1}{2} \frac{R_0}{R} |T'|^2 \quad (27)$$

if one can assume that the transducer is lossless and perfectly bi-directional.

Both the transducer susceptance b_t and the conductance g_t are also found by a direct calculation of the total transducer scattering matrix from a cascade coupling of individual tap circuits. However, if the simple formula of equation (27) is useful for the calculation of g_t , b_t may be derived from this. We assume b_t to consist of two parts

$$b_t = j\omega C_1 + jb_r \quad (28)$$

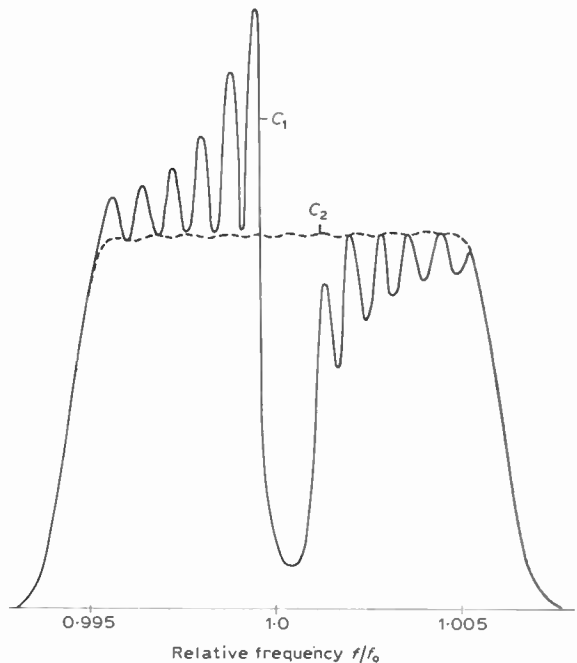


Fig. 10. The effect of dummy taps on the frequency response, C_1 : Electrically 'open' dummy taps. C_2 : Electrically shorted dummy taps.

where C_i is the electrostatic capacitance of the taps and b_r is the acoustic radiation susceptance which can be computed by means of the Hilbert transform:¹²

$$b_r(\omega) = \frac{2\omega}{\pi} \int_0^\infty \frac{g(x)}{x^2 - \omega^2} dx \quad (29)$$

The general influence of the matching circuit on the transducer response is given by equation (26). As we see the modification factor

$$k_m = \frac{\sqrt{g_L}}{(y_i + y_L)} \quad (30)$$

depends on the 'weak coupling' response T' through g_i and b_r , which means that the factor k_m also depends on the shape of the weighting function. Consider two specific cases:

(a) *Band-pass filters with no external tuning*

In this case the modification factor becomes:

$$k_m = \frac{\sqrt{g_L}}{g_i + g_L + jb_r + j\omega C_i} \quad (31)$$

It is obvious that for narrow-band transducers containing a large number of taps which operate on a high-coupling substrate, the distortion caused by k_m can be quite large. In the pass-band, the slope of b_r is of opposite sign as compared to the slope of ωC_i . This means that the total susceptance $b_r + \omega C_i$ may be close to zero or even negative at the high frequency end of the pass-band, while it may be of the order of $2g_i$ at the low frequency end. If, in addition, g_i is significantly larger than g_L the ratio of upper frequency end to lower frequency end conversion may approximate:

$$\frac{k_m(h)}{k_m(l)} \approx 1 + j2 \quad (32)$$

which is equivalent to 7 dB of amplitude distortion. Also the stop band isolation could be seriously reduced. The reduction factor just outside the pass-band on the high frequency side might be

$$\frac{k_m(sh)}{k_m(0)} \approx \frac{g_i(1+j)}{g_L} \rightarrow 20 \log(g_i/g_L) + 3 \text{ dB} \quad (33)$$

In a general case of minor distortions, where we still take the crude approximation

$$b_r(l) - b_r(h) \approx 2g_i,$$

we may write

$$\frac{k_m(h)}{k_m(l)} = \frac{1 + jQ_L(1 + \frac{1}{2}Q_a - 1/Q_e)}{1 + jQ_L(1 - \frac{1}{2}Q_a + 1/Q_e)} \quad (34)$$

which yields the amplitude distortion

$$D_m = \left| \frac{k_m(h)}{k_m(l)} \right| \approx 1 + \frac{Q_L}{1 + Q_L^2} (1/Q_a - 2/Q_e) \quad (35)$$

The Q factors are defined as follows:

loaded $Q_L = \frac{b_i(\omega_0)}{g_L + g_i}$

electric (unloaded) $Q_e = \frac{b_i(\omega_0)}{g_i}$

acoustic $Q_a = \frac{\omega_0}{\Delta\omega}$, $\Delta\omega =$ width of pass-band.

It is of some interest to compare equation (35) with the amplitude conversion:

$$|T''| = \sqrt{\frac{2Q_L(Q_e - Q_L)}{Q_e^2(1 + Q_L^2)}} \quad (36)$$

The first-order approximation which equation (35) is based on rests on the assumption:

$$1/Q_a, 1/Q_e \ll 1.$$

If the transducer is heavily loaded, ($g_L \gg g_i$, $Q_L < 1$) we may approximate:

$$D_m \approx 1 + |T''|^2(Q_e/2Q_a - 1) \quad (37)$$

(b) *Tuned narrow-band filters*

An ideally flat pass-band filter may have a rectangular frequency amplitude response of width 2Δ . If the corresponding transducer conductance is g_0 inside this frequency band, we obtain from equation (29) in the case that $\Delta/\omega_0 \ll 1$:

$$b(\delta) = \frac{g_0}{\pi} \ln \left| \frac{\Delta - \delta}{\Delta + \delta} \right| \quad (38)$$

where $\delta = \omega - \omega_0$.

Curves for $g(\delta)$ and $b(\delta)$ are shown in Fig. 11. For comparison, curves for $g(\delta)$ and $b(\delta)$ for a real filter with a shape factor (ratio of 30 dB bandwidth to 1 dB bandwidth) of 1.25 is shown. The latter curves are derived from computations based on a cascade coupling of 55 taps with an optimized weighting function.¹⁰

$b(\delta)$ is quite linear in most of the pass-band; a linearization around ω_0 corresponds to $b_c = 2g_0/\pi$ at the band edges and we see that $b_c = g_0$ is a reasonable approximation when a practical shape factor is implemented.

When the total susceptance is tuned to zero at resonance, the amplitude response will be symmetric about ω_0 . We get for the amplitude distortion of the band edges:

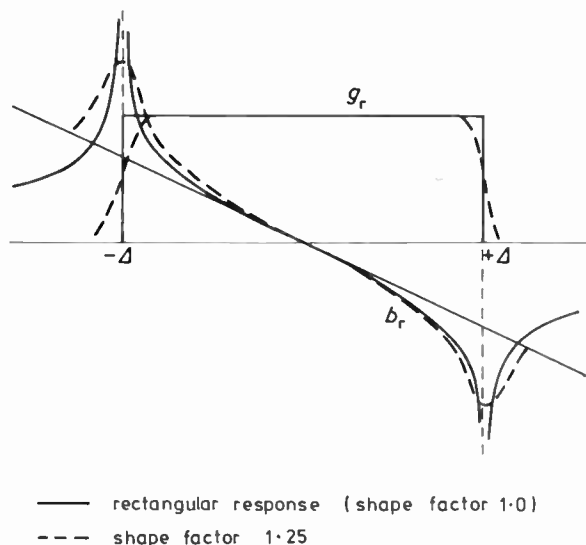


Fig. 11. Immittance of tuned narrow-band filter as function of frequency.

$$D_m = \left| \frac{k_m(l, h)}{k_m(0)} \right| = \left| 1 + Q_L(1/Q_a - 1/Q_c) \right|^{-1} \approx 1 - \frac{1}{2} Q_L^2 (1/Q_a - 1/Q_c)^2. \quad (39)$$

The phase distortion will be essentially linear over the pass-band, and thus represents no serious problem.

For narrow-band filters on high-coupling substrates we have $Q_a \gg Q_c$.

In some cases, most of the amplitude distortion may be removed simply by tuning with a shunt L-C circuit, such that the effective electric Q approaches Q_a . However, if the quality factor of the tuning elements approaches Q_a or becomes less than Q_a , dissipation losses will become significant. In this case the distortion may be compensated for by modifying the tap weighting function such that the radiation conductance gets a slightly parabolic shape in the pass-band as shown in Fig. 12. For this compensation to work satisfactorily, a mismatch loss of 1 to 2 dB at the centre frequency must be allowed.

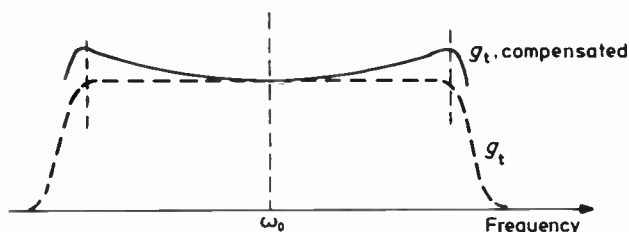


Fig. 12. Distortion compensation by pass-band shaping.

4 Triple Transit Signals

The triple transit echoes which are due to acoustic reflections off both the transmitting and receiving transducers are of major concern in acoustic surface-wave filters of small and moderate bandwidths. In simple designs with one input and one output transducer of the bi-directional type this echo approaches -6 dB compared to the main signal when both transducers are perfectly matched.

If the total acoustic reflection from an externally shorted transducer is r_s , the total reflection with external matching included is readily found from simple circuit theory:

$$r_a = r_s + \frac{1}{2} T'^2 \frac{R_0}{R} \frac{1}{y_L + y_t} \quad (40)$$

with notations as in the previous Sections.

For a periodic array transducer with the same passive reflection at each tap, we obtain r_s from equation (6):

$$r_s = \frac{j \left(\frac{z-1/z}{2} \right) \sin N\psi}{\cos N\psi + j \left(\frac{z+1/z}{2} \right) \sin N\psi}. \quad (41)$$

With small multi-reflection effects we may approximate (cf. equation (9))

$$r_s \approx \pm j |r| e^{-jN\phi} \frac{\sin N\phi}{\sin \phi}. \quad (42)$$

As described in Section 2, r_s is compensated for by the use of multiple electrode taps or by the insertion of additional dummy taps.

If we denote the second term in equation (40) by r_m it can be found that the phase ϕ' of r_m as compared to r_s in the case of regular patterns when mass loading is neglected, is given by⁸

$$\tan \phi' = - \frac{b_L + b_t}{g_L + g_t}. \quad (43)$$

This means that r_s may be partly compensated for by r_m at resonance when the total circuit emittance is largely capacitive. However, this compensation can never be very efficient for narrow bandwidth transducers which will contain a large number of weakly coupled taps. In this case it is preferable to minimize r_s as discussed in Section 2, and then seek to minimize r_m for an otherwise optimal performance. It is useful then to express $|r_m|$ in terms of the transducer conversion amplitude $|T''|$. By comparing equations (40) and (26) we readily obtain

$$|r_m| = \sqrt{\frac{g_t}{2g_L}} |T''|. \quad (44)$$

If we write

$$y_t + y_L = (g_t + g_L)(1 + jq) \quad (45)$$

we may use the combination of equations (40) and (26) to obtain

$$|r_m|^2 = \frac{1 - |T''|^2(1 + q^2) \pm \sqrt{1 - 2|T''|^2(1 + q^2)}}{2(1 + q^2)}. \quad (46)$$

A graphical solution to equations (44) and (46) is shown in Fig. 13. The quantities $|r_m|^{-2}$ and $|T''|^{-2}$ are given in dB so that the graphs can be used to read off directly the triple transit suppression for a delay line with identical input and output transducers if the acoustic propagation loss is negligible. We notice that

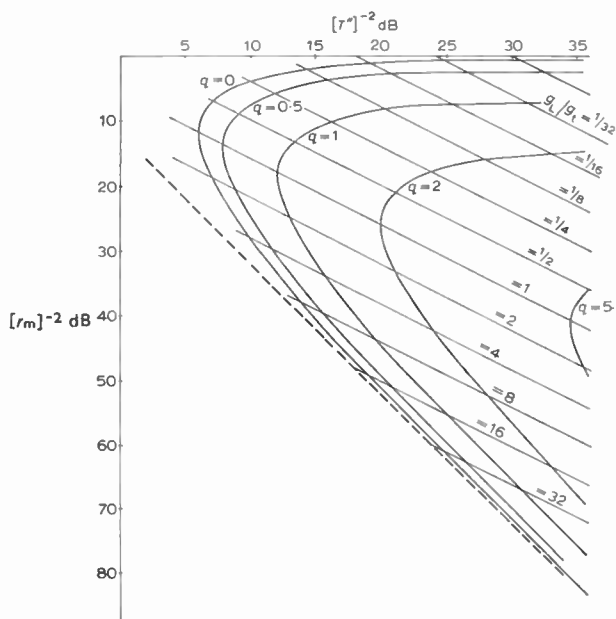


Fig. 13. Triple transit suppression as function of insertion loss for two identical transducers.

for a given insertion loss, the transducers should be tuned, ($q = 0$) and the ratio g_i/g_L should be minimized. By way of example, under these optimal conditions, a triple transit suppression of 30 dB is obtained for approximately 11 dB of insertion loss.

An improved triple transit suppression can be obtained in a number of more or less complicated configurations. A simple useful scheme employs a symmetric 3-transducer configuration as shown schematically in Fig. 14. In a perfectly symmetric pattern, the connection between total acoustic reflection and electro-acoustic conversion is still given by equations (44) and (46) for the output transducers. For the centre transducer, the total acoustic reflection, which now consists of two waves radiating in opposite directions, is given by:

$$r_{ac} = r_s + 2r_m + a \tag{47}$$

where the last term represents the acoustic transmission across an electrically shorted transducer. For a periodic array transducer, we get from equation (5):

$$a = [\cos N\psi + j\left(\frac{z + 1/z}{2}\right) \sin N\psi]^{-1} \tag{48}$$

If the acoustic multi-reflections are fully compensated, we obtain

$$r_{ac} = \frac{T'^2}{|T'|^2} \left(\frac{2g_t}{y_L + y_t} - 1 \right) \tag{49}$$

Perfect cancellation of r_{ac} and hence the triple transit signal is now obtained if the transducer is perfectly matched ($y_L = g_t - jb_t$). However, this cannot be obtained over a finite bandwidth, and in practice, the matching has to be chosen to give a satisfactory overall triple transit suppression across the pass-band. The configuration is useful when a low insertion loss is important.

Other ways of reducing the acoustic reflection is by using directional transducers of either the multi-strip coupler type¹³ or of the phased array type.¹⁴ In some cases, improvements are also obtained by splitting up the transducer in displaced parallel-coupled sections.¹⁵

A scheme which is quite efficient for reasonably narrow band operation is shown in Fig. 15. The trans-

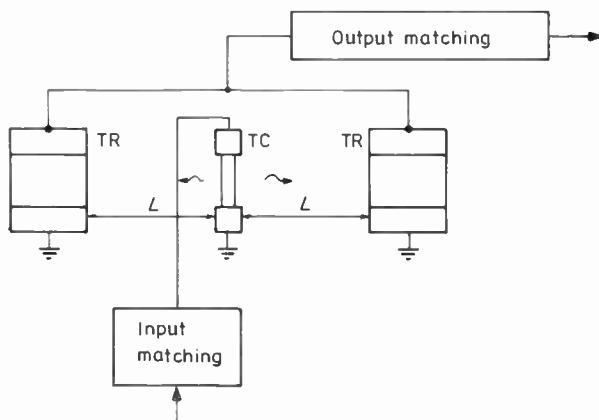


Fig. 14. Symmetric three-transducer configuration for improving the triple transit suppression.

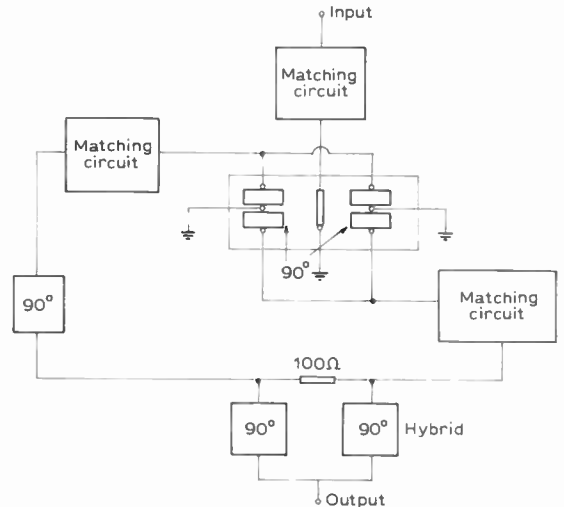


Fig. 15. Scheme for triple transit suppression. The outer transducers of Fig. 14 are here split up into two parts acoustically displaced by 90 degrees of phase which is compensated for electrically in a quadrature hybrid.

ducers are basically arranged in a symmetric 3-transducer configuration where the output transducers are split up into two parts which are mutually displaced by a quarter wavelength. The matched parallel-coupled parts are added through a quadrature hybrid which compensates for the change in delay.⁶

5 Effects of Non-uniform Tap Coupling; Weighting Methods

The simplest and most commonly used method for weighting of taps in surface wave filters is by means of apodization† of the finger overlap. To a first approximation, the tap weighting is then proportional to the length of the finger overlap. However, this simple relation is only reasonably accurate if the other transducer creates an acoustic beam which is uniform over the cross section of the apodized transducer. If the latter transducer also is weighted by apodization this condition is clearly violated. The delay line response can in this case no longer be computed from a simple cascading of the two transducers. An analysis can be carried out by regarding the complete delay line as a parallel-coupling of different transversal filters, each with a uniform and discrete tap weighting.¹⁸ However, it is very difficult to synthesize a specified frequency response effectively even if the weighting of one transducer is kept fixed during the optimization procedure. Also, due to diffraction effects, the method of analysis may be questionable when very small overlaps are involved.

In band-pass filters, the non-uniform tap coupling may lead to an increase of sidelobe levels in the stop-band and may also effect the pass-band ripple.

The problems with non-uniform coupling may be partly overcome by inserting a multi-strip coupler (m.s.c.) between the two transducers.¹¹ The coupler provides a smoothing of the intensity across the aperture,

† Literally, removing the feet.

such that the receiving transducer will couple to a relatively uniform wave.

The insertion of a multi-strip coupler clearly has some disadvantages:

- (a) The m.s.c. increases the width of the delay line by at least a factor of 2 and it normally requires several hundred wavelengths of added substrate area in the direction of propagation.
- (b) It may introduce frequency band limiting effects.
- (c) Additional insertion loss is introduced due to ohmic losses and non-perfect coupling.
- (d) The m.s.c. introduces additional fabrication difficulties for high frequency operation.

A limited form of weighting which in some cases can be very useful is the so-called weighting by selective withdrawal of electrodes.²³ This technique seems to be most useful for dispersive transducers which may contain a large number of fingers.

Newer forms of weighting techniques have recently been investigated which provide an improved uniformity in the tap coupling. A couple of these will be briefly described.

5.1 Weighting by Series Coupling

The tap coupling may be distributed over the transducer cross-section by a series coupling of apodized sections as shown in Fig. 16. The relative weight of a series-coupled tap may be written

$$W_n = \frac{m}{L_{\max} \sum_{p=1}^m 1/l_{n,p}} \quad (50)$$

where m denotes the number of series-coupled sections, L_{\max} is the maximum overlap used and $l_{n,p}$ is the overlap of section p in tap n .

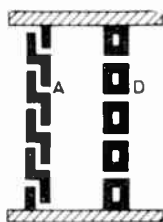


Fig. 16. Weighting by series coupling. A, active tap; D, dummy tap.

If all overlaps $l_{n,p}$ contained in a tap are equal, the weight is simply

$$W_n = \frac{l_n}{L_{\max}} \quad (50b)$$

which is similar to the normal apodization weighting.

If we disregard the effect of the distributed gaps between the overlap regions, a uniform coupling across the transducer is obtained with this method over a large range of weighting factors.¹⁹ However, in a practical realization of a transducer the pattern layout will create a complicated quasi-static field which may be explained as stray capacitances connected between the different series-coupled elements, between an element and a bus-bar, between an element and the ground plane and

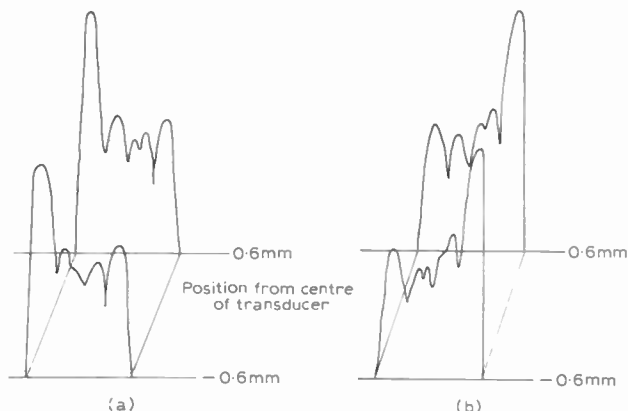


Fig. 17. Beam profiles of a series-weighted transducer with (a) right and (b) left electrode grounded.

between elements of neighbouring taps. If all these stray capacitances could be neglected a uniform coupling would be obtained by implementing equation (51). Especially for extensively thinned transducers containing a large number of weakly coupled taps, the stray capacitances can in fact be quite dominating. This is demonstrated in Fig. 17 which shows the acoustic intensity distribution from a series weighted transducer as measured by means of a laser probe.¹⁰ The transducer layout is shown in Fig. 18. The thinning factor is 9 and even the centre taps are subdivided into four series-coupled sections.

We see from Fig. 17 that the intensity tends to be increased towards the bus-bars, and particularly towards the 'hot' contact. Experiments with filters with filled double electrode transducers²⁰ and less heavily weighted transducers¹⁹ have shown a much more uniform intensity distribution.

It should be noted that even when the stray capacitances are dominating the formula of equation (50) will be approximately valid, and a uniform excitation is conceptually possible to obtain by a correct distribution of overlap lengths $l_{n,p}$ across the aperture. Also, experiments seem to indicate that the effective coupling of a

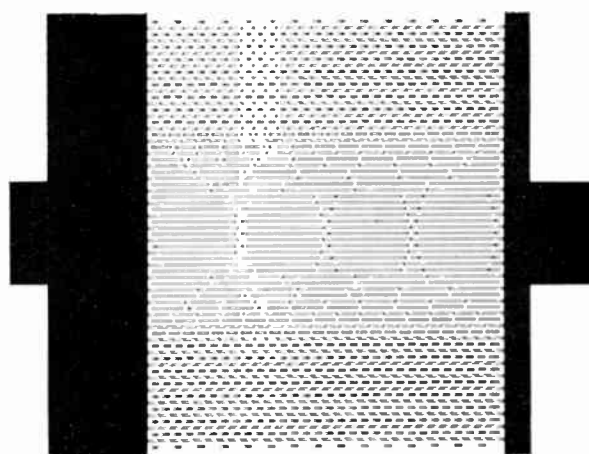


Fig. 18. Layout of transducer referred to in Fig. 17.

series-coupled tap in a uniform beam is more accurately controlled than an ordinary apodized tap.¹⁰

5.2 Position Weighting

A uniform amplitude coupling is obtained by modulating the finger positions over the transducer cross section as shown in Fig. 19. Two forms of modulation have been experimentally investigated.²² One employs a rectangular form of modulation, the other a sinusoidal form.

If the modulation periodicity p is constant over the transducer width, the coupling to an incoming wave is given by:

Rectangular modulation:

$$W_n = \cos\left(\frac{\beta a_n}{2}\right) \tag{51}$$

Sinusoidal modulation:

$$W_n = I_0\left(\frac{\beta a_n}{2}\right) \tag{52}$$

where I_0 denotes the Bessel function of zero order and $a_n/2$ is the amplitude of the modulation. The transducer width must contain an integer number of complete periods. In both forms of modulation extraordinary waves are radiated in directions which satisfy the Bragg condition

$$\sin \phi_n = \frac{2\pi n}{p\beta} \tag{53}$$

where ϕ_n denotes the direction of the n th-order ray.

The extraordinary waves should not be coupled into the receiving transducer. This is best obtained if the distance L between the transducers can be chosen such that

$$L > L_1 \cdot p/\lambda \tag{54}$$

where L_1 is the transducer width and λ the acoustic wavelength.

On an anisotropic material like lithium niobate, the beam steering effect will reduce the effective angles ϕ_n significantly.

As is seen from equations (51) and (52) the weighting is frequency dependent; particularly for weakly-coupled

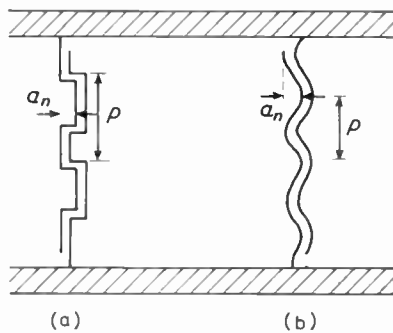


Fig. 19. Two examples of position weighting, (a) rectangular modulation, (b) sinusoidal modulation.

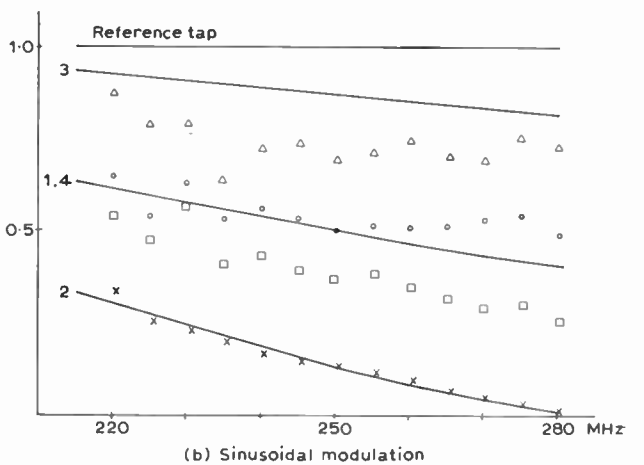
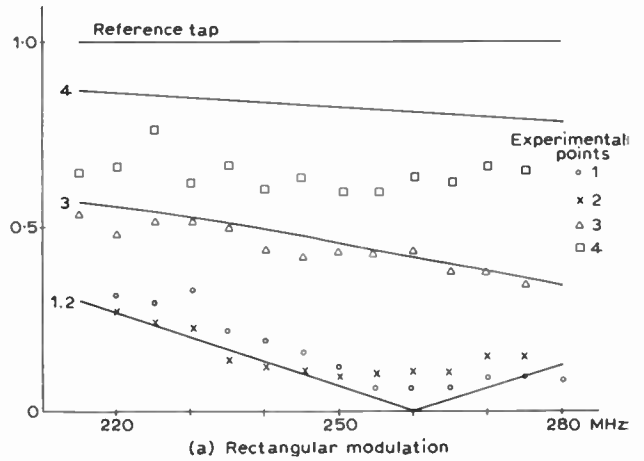


Fig. 20. Responses from two-finger taps in rectangular and sinusoidal modulation. The numbers refer to the taps specified in Table I. Theoretical curves are fully drawn.

taps. The methods are therefore suitable only for narrow-band filters and cannot be applied to all taps.

Experimental results obtained from r.f. response measurements on simple two-fingers taps weighted by rectangular and sinusoidal modulation are shown in Fig. 20.²² The different curves are numbered according to the taps specified in Table I.

Table 1

Specification of taps used for measurements of the effective weighting factor as given in Fig. 20

Form of weighting	No.	Mod. amplitude a/λ	Periodicity p/λ	Number of periods W/p
Rectangular modulation	4	0.39	5	10
	3	0.71	5	10
	2	1.0	5	10
	1	1.0	3	17
Reference tap		0	—	—
Sinusoidal modulation	1	1.0	3	17
	2	1.43	3	17
	3	0.51	10	5
	4	1.02	10	5

6 Other Secondary Effects

A number of secondary effects other than those treated in the previous Sections are present in surface-wave devices. The effects of these on the filter performance may in some cases be suppressed by simple means; in other cases they cannot easily be removed and it is important that they are accurately accounted for in the design. For relatively narrow band-pass filters, the most important secondary effects are, however, believed to be those already described. Other secondary effects are described in the following Sections.

6.1 Transducer End Effects and Neighbour Coupling Effects

These effects are due to the fact that the driving forces in a finger transducer are essentially proportional to the electric field, or equivalently, the electric charge distribution in the transducer area as derived from an electrostatic or quasi-electrostatic field model. Since electrostatic fields caused by a line charge decay quite slowly as a function of the distance, the charge on an electrode will depend quite strongly on the position, shape, and polarity of neighbouring electrodes. Some typical examples of the approximate charge distribution as determined from electrostatic field calculations are shown in Fig. 21.

In a conventional filled transducer with no phase reversal and equally-spaced fingers, the charge distribution deviates significantly from that of an infinite array only for the outermost (end) electrodes. If the acousto-electric coupling is referred to each electrode, the coupling of the end electrodes are reduced by a factor of approximately 0.75 as compared to an infinite array electrode.²⁴ A transducer tap usually refers to the gap between two fingers, and by that notation the tap efficiency at the ends is increased by a factor of ~ 1.5 . This can of course be easily compensated for through the tap weighting.

When there is a phase reversal ((d) of Fig. 21), the charge is redistributed in a similar manner, and some frequency dependent coupling will remain in the phase reversed tap. Most of these simple end effects and phase reversal effects can be dealt with in a systematic manner.²⁵ However, if the transducer exhibits large variations of the weighting between neighbouring taps which would be the case for weighted non-dispersive wide-band transducers, stray fields induced at the ends of short overlap sections which are coupled to neighbouring taps will tend to further distort the picture.

6.2 Surface Velocity Loading

The metallization of the surface causes additional delay of the acoustic signal. In transducers with a periodic distribution of taps, this represents a small problem, since the result of the additional delay will simply be a small shift in the filter resonance frequency. This can be corrected for by a corresponding change in the reduction factor in the last stage of the transducer mask fabrication process. In apodized transducers, it is important to use dummy electrodes outside the coupling region so that the metallization density remains constant

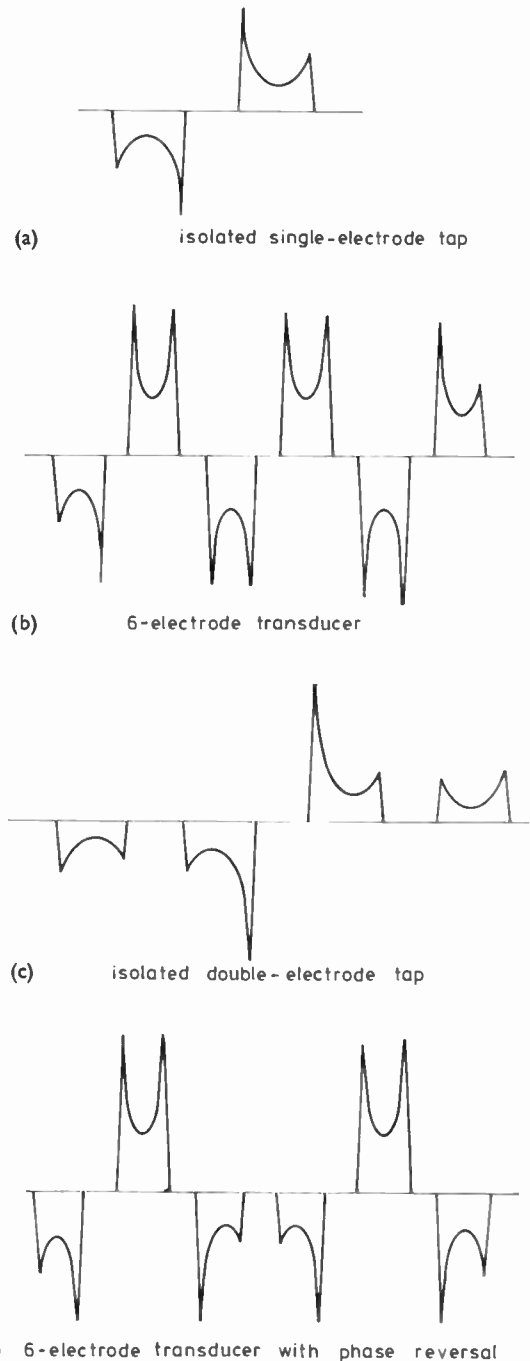


Fig. 21. Electrostatic charge distribution for various transducer configurations.

across the acoustic beam. Otherwise serious distortions of the phase front may occur.²⁶

In transducers where selective withdrawal of electrodes or other ways of non-periodic tap separation is used in the weighting implementation, the velocity loading may be somewhat more difficult to control accurately. If the additional delay is not accurately compensated for in the mask layout, distortions of the filter characteristics may result and this distortion may also depend on line-width and metal film thickness variations caused by fabrication inaccuracies.

Errors in the effective tap position caused by velocity loading effects or by errors in the mask fabrication procedure, may sometimes be corrected for in the final transducer mask. Positioning errors may be measured by a coherent detection of short r.f. pulses being transmitted into the delay line. After measurements the effective positions may be corrected for by adding or removing metal in the transducer pattern. This can be obtained by means of the equipment shown in Fig. 22.

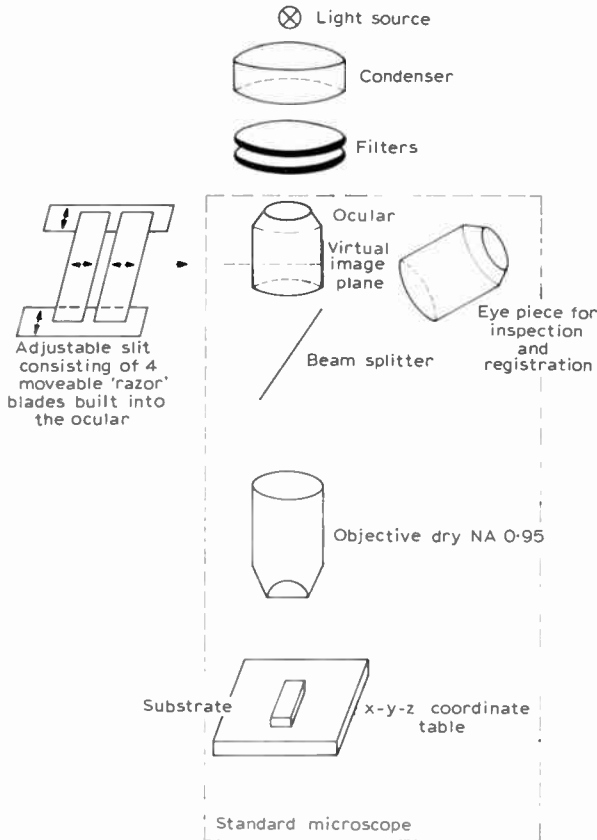


Fig. 22. Equipment for insertion of trimming strips and repair of breaks or shorts in a transducer.

An adjustable rectangular slit is exposed on the substrate through a microscope. Excess metal is removed by etching the exposed substrate while metal is added by deposition and lift off.⁶ This equipment may also be used to repair breaks or shorts in a transducer pattern.

6.3 Beam Diffraction and Beam Steering

In a simple theory it is assumed that the acoustic energy radiated from a transducer is confined in a beam of width equal to the transducer overlap length, and that it is uniform in amplitude and phase across this width. Since we are dealing with an open structure as opposed to a closed waveguide or transmission line, the filters are subject to phase front and amplitude distortions caused by diffraction effects similar to an optical system. The anisotropy of the substrate may also cause beam steering which is due to the fact that the group and phase velocity may not be collinear in all crystal directions. Diffraction

and beam steering effects have been extensively studied for a variety of substrates based on 1st-order calculations of the radiation patterns.²⁷ In principle, it is also possible to compensate for these effects in the tap layout.²⁸ However, usually it is possible to make the maximum finger overlap large enough for the diffraction effects to be negligible over a distance which cover the maximum delay in the filter. The errors caused by beam steering must be controlled by a sufficiently accurate orientation of the substrate with respect to crystal axis and transducer electrodes.

6.4 Mass Loading

The mass and elastic properties of the transducer electrodes may distort the filter performance for higher frequency operation. The mechanical loading will increase the passive acoustic reflections and the added delay caused by the taps.

For pure mass loading where the film stiffness may be neglected, the relative velocity change and edge reflection at an electrode is approximately given by⁷

$$\left| \frac{\delta v}{v_0} \right| = |\delta r| = \frac{\rho' v_p^2 t}{4P_s} \tag{55}$$

where ρ' is the mass density of the electrode material, v_p is the particle velocity at the surface, t is the film thickness and P_s is the power contained in the surface-wave. A rough estimate may be found from:

$$\left| \frac{\delta v}{v_0} \right| = |\delta r| \simeq \frac{\rho' t}{\rho_s \lambda} \tag{56}$$

when it is assumed that the penetration depth of the surface-wave is equal to an acoustic wavelength and ρ_s denotes the mass density of the substrate.

6.5 Coupling to Electromagnetic Waves and Acoustic Bulk Waves

Spurious responses in a surface-wave filter is often due to direct electrostatic or electromagnetic coupling between input and output transducers and to the excitation and detection of bulk acoustic waves. The direct electromagnetic coupling may in most cases be reduced by a careful shielding of the input and output circuit. The coupling to bulk waves is a lot more complicated problem and often represents a limiting factor in the performance of a surface-wave filter. A number of techniques are used to suppress the bulk wave coupling:

1. Staggering of transducers to avoid bulk wave resonances.²¹
2. Beveling of the back surface to obtain destructive interference.
3. Deposition of absorptive material on the back side of a comparatively thin substrate.
4. Decoupling by the insertion of a multistrip coupler between the input and the output transducer.¹¹
5. Decoupling by the insertion of a metallized area in one of two signal paths.²⁹

Considerable effort has also been spent on finding new crystal orientations with a minimum of coupling to bulk waves.³⁰

7 Conclusions

The design of a surface-wave filter obviously may be pursued in a number of different ways. In the beginning, the process was subject to much trial and error procedure, and because of the complexity involved in the analysis and synthesis of optimized transducer patterns this will in many cases still be a valid procedure.

However, during the last years the knowledge and understanding of secondary effects has been vastly increased, and many design details which suppress or compensate for these effects have been invented.

We have in this paper attempted to describe the most important secondary effects and their influence on the filter performance in a systematic manner. This method of analysis is believed to be useful when the device can be treated basically as a transversal filter so that a natural design procedure would be conducted along the following lines:

1. An optimum weighting function is determined from the specified frequency response by means of procedures valid for an ideal transversal (digital) filter.
2. A basic transducer layout is chosen from the estimated influence of factors such as the number of taps, the number of electrodes in each tap and the uniformity of the weighting on the specific filter performance due to second-order effects.
3. The choice of a basic layout is followed by a more exact analysis by means of an equivalent circuit model or similarly developed computer program.
4. The design is further refined by iterative computational procedures which are based on a combination of calculations and experiments or just trial and error methods.

Specifically, it has been shown in Sections 2 to 4 that the effects of acoustic multi-reflections and external matching circuitry on the filter performance with respect to pass-band ripple and stop-band isolation can be quantitatively predicted in a simple manner.

Further, it has been shown in Section 5 how novel weighting methods can be applied to create a more uniform coupling across the acoustic beam and the limitations of these methods in a practical design are also demonstrated.

Errors due to electrostatic stray fields in the transducer pattern, and the coupling to bulk waves cannot yet be treated in a simple, systematic manner. Significant effort has been put into these areas recently, and at least for some specific configurations first-order estimates and quantitative means of compensation may soon be included in the preliminary design.

8 Acknowledgment

Part of the work reported in this paper was sponsored by INTELSAT; any views expressed in the paper are not necessarily those of INTELSAT. Other parts were sponsored by The Royal Norwegian Council for Scientific and Industrial Research.

9 References

1. Tancrrell, R. H., 'Analytic design of surface-wave band-pass filters', *IEEE Trans. on Sonics and Ultrasonics*, SU-21, pp. 12-22, 1974.
2. Helms, H. D., 'Nonrecursive digital filters. Design methods for achieving specifications on frequency response,' *IEEE Trans. on Audio and Electroacoustics*, AU-16, pp. 336-42, 1968.
3. Rabiner, L. R., 'Techniques for designing finite-duration impulse response digital filters', *IEEE Trans. on Communications Technology*, COM-19, pp. 188-95, 1971.
4. Rabiner, L. R., 'Linear program design of finite impulse response digital filters', *IEEE Trans.*, AU-20, pp. 280-8, 1972.
5. Parks, T. W. and McClellan J. H., 'A program for the design of linear phase finite impulse response digital filters', *IEEE Trans.*, AU-20, pp. 195-9, 1972.
6. Skeie, H., 'Problems in the realization of flat delay narrow band surface-wave filters at u.h.f. and microwave frequencies', Proceedings, 1975 IEEE-MTT International Microwave Symposium.
7. Skeie, H., 'Electrical- and mechanical loading of a piezoelectric surface supporting surface-waves', *J. Acoust. Soc. Am.*, 48, No. 5, (Part 2), pp. 1098-1109, November 1970.
8. Skeie, H., 'Mechanical and electrical reflections in interdigital transducers', Proceedings, 1972 IEEE Ultrasonics Symposium, pp. 408-12.
9. Jones, W. S. and Hartmann, C. S. and Sturdivant, T. D., 'Second order effects in surface wave devices', *IEEE Trans.*, SU-19, pp. 368-77, July 1972.
10. 'Acoustic Wave Filter Study', Final Report, ELAB report STF44 F74164. Electronics Research Laboratory, Trondheim, October 1974.
11. Tancrrell, R. H. and Engan, H., 'Design considerations for s.a.w. filters', Proceedings, 1973 IEEE Ultrasonics Symposium, pp. 419-22.
12. Sunde, E., 'Communication Systems Engineering Theory', p. 460 (Wiley, New York, 1969).
13. Marshall, F. G. and Paige, E. G. S., 'Novel acoustic-surface-wave directional coupler with diverse applications', *Electronics Letters*, 7, pp. 460-2, 12th August 1971.
14. Marshall, F. G., Paige, E. G. S. and Young, A. S., 'New uni-directional transducer and broadband reflection of acoustic surface-waves', *Electronics Letters*, 7, pp. 638-40, 21st October 1971.
15. Nishikawa, K., 'An improved surface-wave filter for a p.c.m. timing tank', Proceedings, 1974 IEEE Ultrasonics Symposium, pp. 164-7.
16. Smith, W. R., Gerard, H. M., Collins, J. H., Reeder, T. M. and Shaw, H. J., 'Analysis of interdigital surface-wave transducers by use of an equivalent circuit model', *IEEE Trans. on Microwave Theory and Techniques*, MIT-17, pp. 856-64, 1969.
17. Milsom, R. F., Heighway, J., Reilly, N. H. C. and Redwood, M., 'Comparison of exact theoretical predictions and experimental results for interdigital transducers', Proceedings, 1974 IEEE Ultrasonics Symposium, pp. 406-11.
18. Tancrrell, R. H. and Holland, M. G., 'Acoustic surface-wave filters', *Proc. IEEE*, 59, pp. 393-409, 1971.
19. Rønnekleiv, A., Skeie, H. and Hanebrette, H., 'Design problems in surface-wave filters', IEE International Specialist Seminar on Component Performance and Systems Applications of Surface Acoustic Wave Devices, 1973, pp. 141-51.
20. Engan, H., 'Series-weighting of surface acoustic wave transducers', Proceedings, 1974 IEEE Ultrasonics Symposium, pp. 422-4.
21. Engan, H., 'High frequency operation of surface acoustic wave multielectrode transducers', *Electronics Letters*, 10, No. 19, pp. 395-6, 19th September 1974.
22. Skeie, H., 'Acoustic Surface-Wave Filter Design, Weighting Methods'. ELAB Report, Trondheim, June 1975.

23. Hartmann, C. S., 'Weighting interdigital surface wave transducers by selective withdrawal of electrodes', Proceedings, 1973 IEEE Ultrasonics Symposium, pp. 423-6.
24. Hartmann, C. S. and Secrest, B. G., 'End effects in interdigital surface-wave transducers'. Proceedings, 1972 IEEE Ultrasonics Symposium, pp. 413-6.
25. Smith, Jr., W. R., 'Circuit model analysis for interdigital transducers with arbitrary stripe to gap ratio, Polarity sequences, and harmonic operation', Proceedings, 1974 IEEE Ultrasonics Symposium, pp. 412-7.
26. Gerard, H. M., Smith, W. R., Jones, W. R. and Harrington, J. B., 'The design and applications of highly dispersive acoustic surface-wave filters', *IEEE Trans.*, SU-20, pp. 94-104, April 1973.
27. Szabo, T. L. and Slobodnik, Jr., A. J., 'The effect of diffraction on the design of acoustic surface-wave devices', *IEEE Trans.* SU-20, pp. 240-50, July 1973.
28. Szabo, T. L. and Slobodnik, Jr., A. J., 'Diffraction compensation in periodic apodized acoustic surface-wave filters', *IEEE Trans.*, SU-21, pp. 114-9, April 1974.
29. La Rosa, R. and Vasile, C. F., 'Broad-band bulk-wave cancellation in acoustic surface-wave devices', *Electronics Letters*, 8, No. 19, p. 478, September 21st 1972.
30. Mitchell, R. F., 'Spurious bulk wave signals in acoustic surface-wave devices', Proceedings, 1974 IEEE Ultrasonics Symposium, pp. 313-20.

Manuscript first received by the Institution on 29th August 1975 and in final form on 17th November 1975. (Paper No. 1714/CC 250).

© The Institution of Electronic and Radio Engineers, 1976

The Authors



Dr. Halvor Skeie received the degree of sivilingenior (M.S.) and the degree of lic. techn. (Ph.D.) in electrical engineering from the Norwegian Institute of Technology in 1959 and 1967 respectively. From 1961 to 1967 he was engaged in research on microwave ferrite devices and on acoustoelectric effects in piezoelectric semiconductors at the Electronics Research Laboratory of the Institute. During this period he

completed the studies towards the licenciat degree and also acted as instituttingenior (assistant professor) for some time. Dr. Skeie then spent a year as a visiting postdoctoral Fellow at the University of California, Berkeley, studying acoustoelectric effects and from 1968 to 1970 worked as a Senior Research Engineer for Litton Industries, Electron Tube Division, San Carlos, California, on acoustic surface wave devices. In 1971 he returned to the Electronics Research Laboratory where he has been engaged in research on micro-

wave acoustics and microwave measurements. He is presently acting as manager of the microwave acoustics group, which is mainly engaged in research and development on surface wave devices



Dr. Helge Engan received the 'siv. ing.' degree in physics in 1962 and the 'lic. techn.' degree in physical electronics in 1967, both from the Norwegian Institute of Technology, Trondheim. Since 1964 he has worked at the Division of Physical Electronics at the Institute, interrupted by periods in the Electronics Research Laboratory in 1968 and 1969, and a year from 1973 to 1974 in the Research Division of

the Raytheon Company, Mass., USA. His main working areas have been electron phonon interactions in semiconductors and surface acoustic waves in solids.

Engineering design and evaluation of s.a.w. pulse compression filters with low time sidelobes

G. A. ARMSTRONG, B.Sc., Ph.D.*

and

M. B. N. BUTLER, Ph.D.*

SUMMARY

A linear f.m. pulse compression sub-system employing surface acoustic wave dispersive filters has been designed. When operated as a coherent pulse compression loop, this sub-system provides a compressed pulse with all time sidelobes suppressed by more than 40 dB. This demanding level of performance which is a significant improvement over previously reported sub-systems has been achieved by the development of a design procedure which permits compensations for the spectral ripples of the transmitted waveform to be incorporated in the design of the compression filter. Measurement of amplitude and phase characteristics of the compression filter indicates very good agreement with theoretical predictions.

1 Introduction

To optimize the detection of small targets at long range many radar systems maximize the pulse length. Since the radar resolution depends on the bandwidth of the transmitted pulse, and hence its duration, range is normally enhanced at the expense of resolution. However, this dilemma may be resolved by encoding the transmitted pulse (usually using linear frequency modulation) and decoding the received signal with a matched filter, so that the received energy is compressed to a time interval short enough to give the required resolution. This technique is known as pulse compression. The advantages of pulse compression have been understood for several years but only since the application of s.a.w. (surface acoustic wave) technology¹⁻³ has it been possible to realize some of the advantages. The key signal processing functions of pulse compression, i.e. the dispersive delay of the matched filter for compression of the transmitted pulse, and frequency filtering for time sidelobe suppression, can both be performed at i.f. with surface wave devices. Indeed it is possible to perform both these functions within the same device. This device is known as a pulse compression filter. The passive generation of an appropriate phase-coded waveform is achieved with a surface wave expansion filter.

Before considering certain aspects of the design of such a filter it is instructive to consider the main advantages of s.a.w. dispersive delay lines for this application:

- Performance: A wide range of time-bandwidth products (up to several thousand) suitable for i.f. processing can be made to military specifications.
- Passive generation: The transmitted waveform may be generated passively using a s.a.w. dispersive delay line with an acceptably low noise level.
- Temperature stability: Temperature coefficient of delay and frequency stability may be reduced to several parts in 10^6 per degC by utilization of the appropriate cut of quartz.
- Fabrication facility: All s.a.w. devices are simple planar structures with fabrication based on standard photolithography which ensures reproducibility of sophisticated designs. The mask production process is similar to that used for electronic integrated circuits.
- Flexibility: Wide flexibility exists in the choice of transmitted waveforms, e.g. linear f.m., non-linear f.m. or phase coded waveforms.

In this paper the discussion is confined to the problems encountered in the design of surface wave dispersive filters required to generate and compress a linear f.m. waveform in order to meet a demanding specification on time sidelobe suppression of the compressed pulse.

A linear f.m. waveform of time duration T and bandwidth B is described by the equation,

$$f(t) = \cos\left(\omega_0 t + \frac{\mu t^2}{2}\right), \quad -\frac{T}{2} < t < \frac{T}{2} \quad (1)$$

$$= 0, \quad |t| > \frac{T}{2}$$

* Microwave and Electronic Systems Limited, Lochend Industrial Estate, Newbridge, Midlothian, Scotland EH28 8LP

where μ is the dispersive slope of the filter, i.e.

$$\mu = \frac{2\pi B}{T},$$

The basic definition of a matched filter⁶ requires that it should have an impulse response $h(t)$ defined by

$$h(t) = k \cos\left(\omega_0 t - \frac{\mu t^2}{2}\right), \quad -\frac{T}{2} < t < \frac{T}{2}$$

i.e. a linear f.m. signal of equal but opposite dispersive slope. The manner in which such a waveform is generated by a surface wave delay line is described in the following Section.

2 Device Design

The basic feature of a surface wave dispersive delay line is to build the dispersive characteristic into the transducer design and in the case of linear f.m. to obtain a time delay which is a linear function of frequency. The simplest method of creating a dispersive characteristic is shown in Fig. 1(a).

The acoustic impulse generated in the interdigital transducer A (i.d.t.), when an electrical impulse is applied, exhibits a frequency change from F_H to F_L over a time $T = T_L - T_H$. Providing the output i.d.t. is of sufficiently wide bandwidth, the electrical impulse response is in one-to-one correspondence with the transducer geometry, in both amplitude and phase.

Clearly it is possible to achieve both expansion and compression matched filters simply by changing the sign of the frequency sweep in the compression filter. Sidelobe suppression is achieved by appropriate spectral weighting of the compression filter. To a first order this effect can be realized by varying the length of the electrode overlap in a controlled fashion, assuming a direct linear relation between frequency and time, as shown in Fig. 1(b). This is referred to as apodization.

In practice, if the fractional bandwidth exceeds approximately 25%, it is difficult to achieve a broadband match to the non-dispersive transducer B shown in Fig. 1(b). A lower loss filter can be realized by producing two complementary transducers as shown in Fig. 1(c). Each transducer spans the total bandwidth in one-half of the dispersive delay required. Design complications however are evident in such structures in that the acoustic impulse generated under one dispersive i.d.t. propagates under the second i.d.t. while generating the device impulse response. The associated convolution process creates amplitude and phase distortion which lead to spurious sidelobes in the compressed pulse waveform. A marked reduction in these spurious effects can be achieved by angling the transducers in a complementary fashion as shown in Fig. 1(d). The acoustic impulse crosses the right-hand transducer at an angle, so limiting the region of interaction at any instant of time. With this structure the electrical impulse response approximates that of the single dispersive delay line of Fig. 1(d).

While the various possible configurations of dispersive interdigital arrays have been briefly outlined, further discussion in this paper is confined to the single-ended

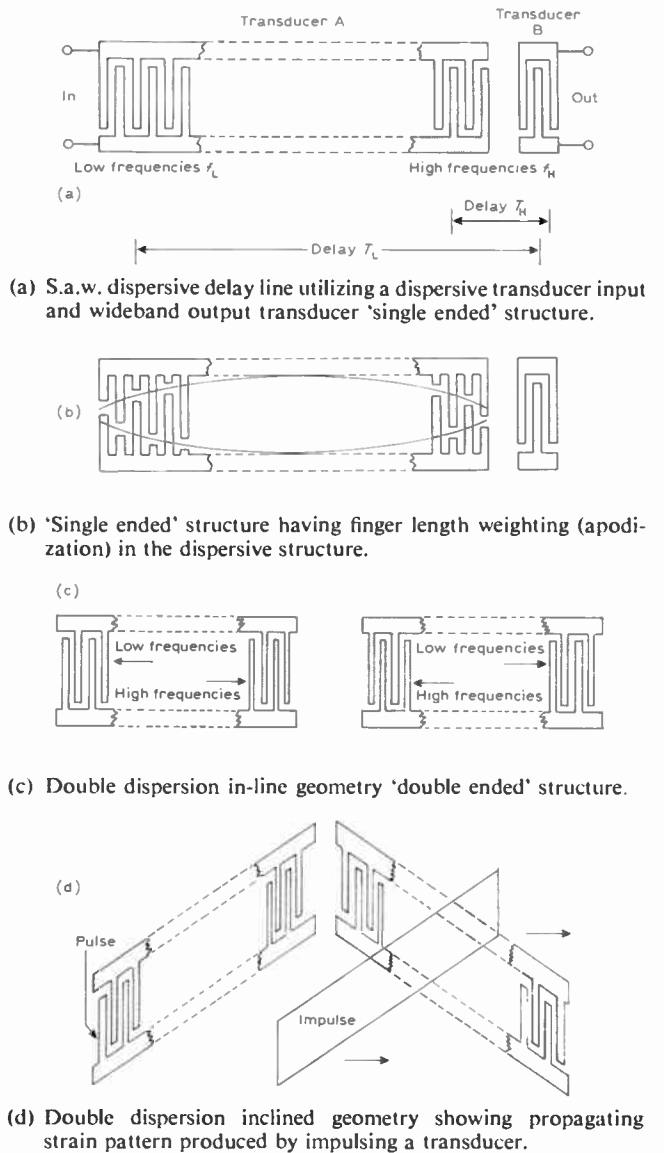


Fig. 1. S.a.w. delay line configurations

transducer design. This structure yields the most straightforward implementation of a dispersive filter since it can be readily implemented from the results of the computer synthesis technique subsequently described.

The weighting function applied to the compression filter depends on the specification of compressed pulse width and range sidelobes. An unweighted matched filter gives a 3 dB pulse width of $0.9/B$, but only -13 dB sidelobes. The most popular form of weighting for pulse compression is Taylor weighting⁴ which offers precise control over sidelobe levels with the least amount of compressed pulse broadening. The variation in compressed pulse-width for different Taylor weighting functions is indicated in Table 1.

To achieve theoretical performance in matched filter design, it is essential to minimize all amplitude and phase distortions in the spectra of the signals being processed. Indeed, it has been shown⁵ that in order to achieve 40 dB sidelobes it is essential that no component of amplitude spectral ripple should be greater than 0.2 dB,

and no component of phase ripple greater than 1° across the bandwidth of the filters.

Table 1

Sidelobe level	-3 dB pulse width
-30 dB	1.16/B
-35 dB	1.2/B
-40 dB	1.25/B
-45 dB	1.33/B

Nevertheless, it is an inevitable consequence of applying a finite time gate to an f.m. waveform as defined in equation (1) that spectral ripples are introduced. The magnitude and periodicity of the spectral ripples depend on the time-bandwidth (TB) product of the chirp. The amplitude spectra of four different chirp signals with time-bandwidth products ranging from 20 to 200 are shown in Fig. 2. The smaller the time-bandwidth product, the larger the amplitude ripple becomes and hence the greater is the sidelobe degradation.

In order to minimize the sidelobe degradation due to these spectral ripples it is necessary to provide appropriate compensation in the design of the compression filter weighting function. Such a design can only be effected using a synthesis technique on a high-speed computer. The use of the computer is hence an integral part of the design process.

If the chirp waveform has a spectrum $P(\omega)$ and the desired compressed pulse a spectrum $W(\omega)$, then the compression filter spectrum is given by

$$H(\omega) = \frac{W(\omega)}{P(\omega)}$$

where $P(\omega)$, $W(\omega)$ and $H(\omega)$ are complex quantities because of the dispersive nature of the filter. The filter time domain impulse response $h(t)$ is obtained by computing the inverse Fourier transform of $H(\omega)$. Since there is a direct one-to-one correspondence between a transducer apodization pattern and its impulse response,⁷ the required transducer apodization can be specified in both amplitude and phase.

A more detailed description of this process is now considered, with reference to the design of a specified pulse compression filter to give better than 40 dB range sidelobe suppression for a time bandwidth product of 56.

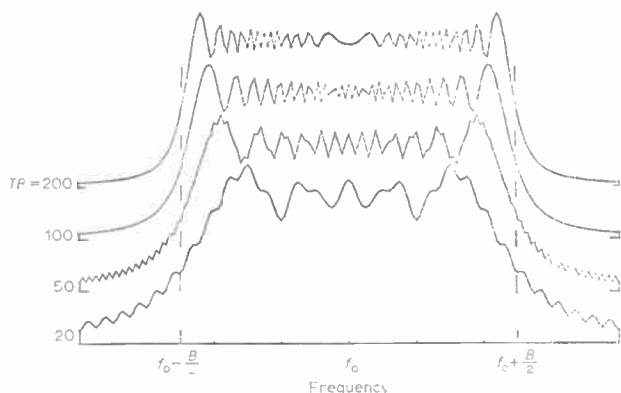


Fig. 2. Chirp spectra.

The following design parameters were chosen to give a compressed pulse 3 dB width less than 100 ns:

- Centre frequency f_0 60 MHz
- Bandwidth B 14 MHz
- Time duration T 4 μ s
- Integral weighting $W(\omega)$ -45 dB Taylor function

The compression filter spectrum $H(\omega)$ is given by dividing the required spectrum by the input spectrum.

$$H(\omega) = \frac{W(\omega)}{P(\omega)} \quad \text{for } \omega_0 - \frac{\Delta\omega}{2} < \omega < \omega_0 + \frac{\Delta\omega}{2} \quad (2)$$

$$H(\omega) = 0 \text{ elsewhere}$$

where $\Delta\omega = 2\pi B$ and $\omega_0 = 2\pi f_0$.

Since a surface wave device comprises an input and an output transducer, $H(\omega)$ represents the composite frequency response of input and output transducers, i.e.

$$H(\omega) = H_i(\omega)H_o(\omega) \quad (3)$$

where $H_i(\omega)$ represents the frequency response of a constant aperture input transducer and $H_o(\omega)$ the frequency response of the synthesized transducer.

For fractional bandwidths less than approximately 25%, the input transducer may be an N finger pair non-dispersive transducer of constant periodicity, in which case

$$H_i(\omega) = \frac{\sin X}{X} \quad \text{where } X = \frac{N\pi(\omega - \omega_0)}{\omega_0} \quad (4)$$

For the device considered in this paper, however, a four-finger pair input transducer was used for both expander and compressor. The required impulse response $h_o(t)$ is given by the inverse Fourier transform of $H_o(\omega)$ where

$$H_o(\omega) = \frac{W(\omega)}{P(\omega)H_i(\omega)} \quad (5)$$

The design process can best be understood by reference to Figs. 3-8. The diagrams, all taken from a computer-driven plotter illustrate the application of the c.a.d. approach to pulse compression filter design. The continuous waveforms are represented on the computer in a sampled form. The sampling rate must be greater than $1/B$ in order to conform to sampling theory. In practice it is advisable to sample the waveform at a higher rate than critical sampling. The sampling process explains the spiked nature of several of the diagrams.

A broad spectrum impulse centred at 60 MHz is applied to the expansion filter. After passive expansion a linear f.m. signal with a time envelope as shown in Fig. 3 appears at the expander output. Before transmission this signal is gated to $\pm 2.0 \mu$ s and then has the spectrum $P(\omega)$, as shown in Fig. 4. To obtain a compressed pulse with sidelobes suppressed to 45 dB, we require an output spectrum $W(\omega)$ from the compressor as shown in Fig. 5, corresponding to a smooth reduction in signal towards the edges of the band. This implies the design of a filter which cancels out the Fresnel ripples in the spectrum of the transmitted chirp. The required filter spectrum $H(\omega)$ is shown in Fig. 6. This function has a sharp truncation at the band edges, and

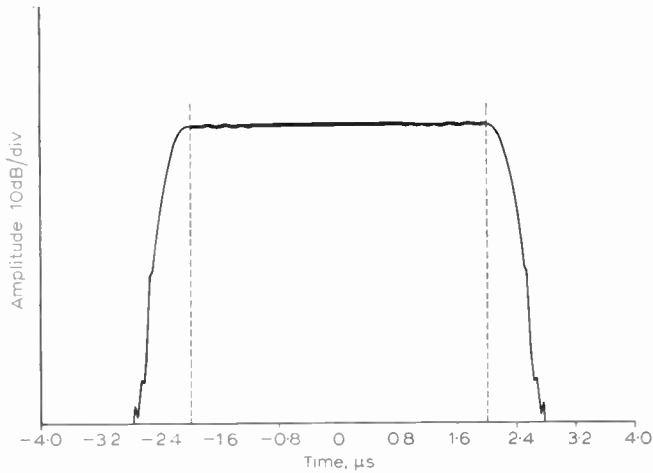


Fig. 3. Expander output signal.

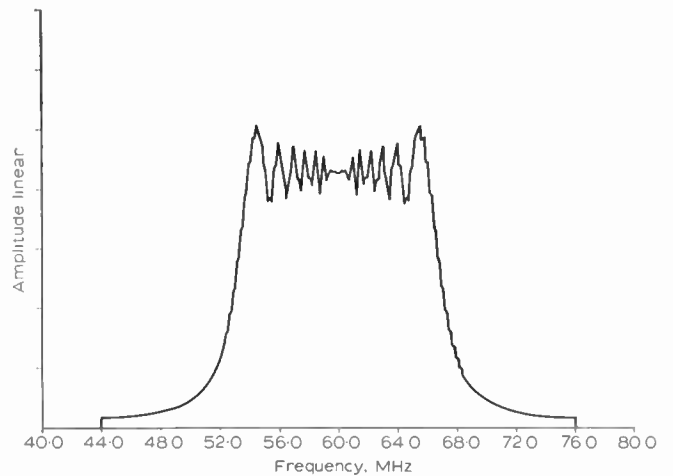


Fig. 4. Expanded signal spectrum.

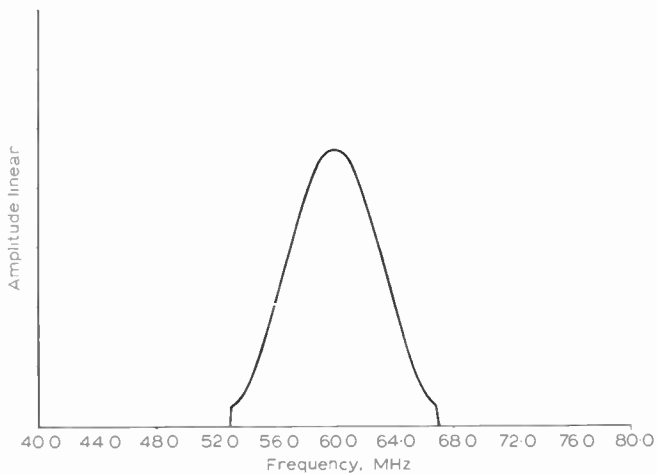


Fig. 5. Desired compressed signal spectrum.

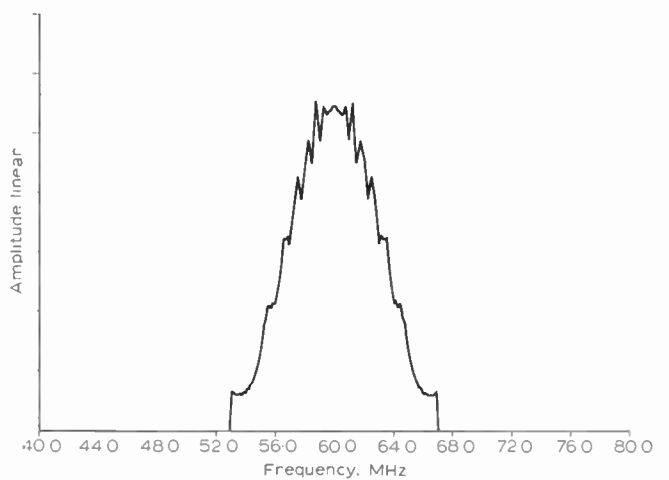


Fig. 6. Desired compressor spectrum.

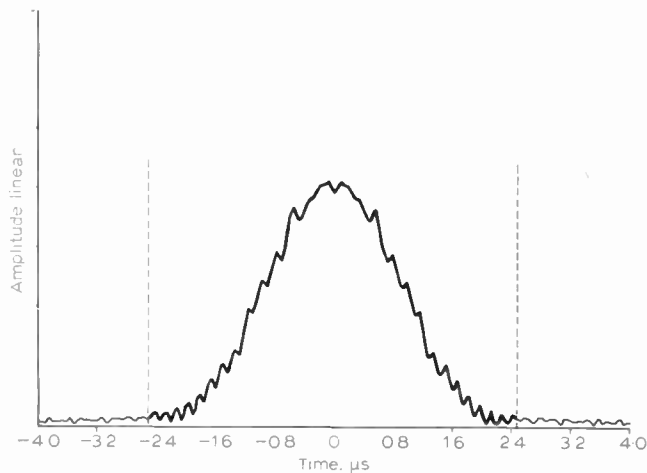


Fig. 7. Required compressor impulse response.

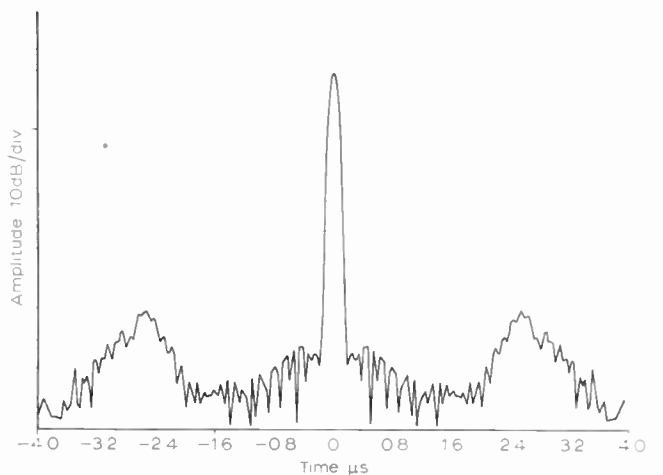


Fig. 8. Compressed pulse envelope.

so has an infinitely long time domain impulse response, the envelope of which is shown in Fig. 7. When this impulse response is truncated to $\pm 2.5 \mu\text{s}$, as indicated, some in-band spectral ripple is introduced. This ripple causes time sidelobes of the compressed pulse at $\pm 2.5 \mu\text{s}$ as shown in Fig. 8. These sidelobes are commonly referred to as gating sidelobes. With a compression filter designed to compensate spectral ripples, computer

simulation indicates that the close-in sidelobes are at their theoretical level of -45 dB while the gating sidelobes are at -41 dB . The magnitude of the gating sidelobes are directly related to the length of the utilized time domain response. For this example, the maximum time domain response was limited by the maximum size of transducer artwork that could be produced, prior to photographic reduction, as explained in Section 3.

Once the basic impulse response $h_0(t)$ has been synthesized, further modifications must be made to the weighting function to take into account:

- (a) finger density variations within the array,
- (b) diffraction of the acoustic beam along the delay path.

The finger density correction is necessary since there are more resonant transducer fingers at the high-frequency end of the array than at the low-frequency end. This correction⁷ is implemented by computing the function, $g(t)$ where

$$g(t) = \frac{|f_0|^{\frac{3}{2}}}{|f_t|} h_0(t) \quad (6)$$

and f_t is the instantaneous frequency at a given point in time.

The effect of acoustic diffraction is best understood with reference to Fig. 9, which shows the variation in beam profile with distance L along the delay path for an aperture of 100 wavelengths. A further synthesis procedure similar to that of Maines *et al.*⁸ has been devised to compensate for beam spreading. This procedure calculates the voltage received for each frequency within the bandwidth of the transmitted signal. The average finger length of the resonant section of the apodized transducer is then adjusted until the voltage output conforms to the required weighting function as defined by equation (6).

3 Device Fabrication

Device fabrication falls into two distinct stages: the initial production of a mask in chrome on glass and the replication of this pattern on to the chosen piezoelectric substrate.

3.1 Mask Preparation

The final stage of the c.a.d. process generates data for use on a precision draughting machine. In this process the individual transducers are drawn as separate artworks at many times the final size. For the devices designed in this work the initial magnification factor was $80\times$, and the final size and full array structure were achieved through separate, first reductions by $20\times$ and a second $4\times$ reduction process in which the arrays were composed into the full pattern.

During the initial artwork preparation, plotting errors can occur. These will introduce phase errors in the device characteristic but can be minimized by using an adequate reduction factor. When $80\times$ reduction is used for a device at 60 MHz the estimated spurious sidelobes resulting from plotting errors reach a maximum at least 50 dB below the compressed pulse.

Reduction can be inaccurate but with care an overall double reduction factor of $80\times$ can be achieved to within 1 part in 10^3 . Providing expansion and compression devices are processed under similar circumstances and as near as possible simultaneously the resultant match is very much better than 1 part in 10^3 .

3.2 Device Replication

All devices in this system are replicated on to ST-X quartz. In this cut the acoustic delay passes through a

minimum, as a function of temperature, at 25°C . The substrates are cut to size and given a specified, fine polish by the supplier. During preparation the interdigital electrode patterns are aligned with reference edges on the crystal and etched into thin aluminium films that have been evaporated on to the substrates in a vacuum chamber. The aluminium films have a thickness less than 10% of the acoustic wavelength to minimize mass loading of the acoustic material. The replication process is carefully controlled to give arrays in which the finger widths and spaces are in the same ratio across the whole pattern.

3.3 Device Mounting

After final cleaning, the processed quartz substrates are mounted in packages which provide screening between input and output and when hermetically sealed provide the s.a.w. devices with an environment which is not subject to dust and condensation. Within the packages the devices are mounted by means of soft-setting epoxy and the substrate ends are loaded to absorb acoustic energy which passes outside the primary area between and underneath the transducer patterns.

4 Device Measurements

Both expansion and compression filters are each provided with matching to the external circuitry through the use of a circuit consisting of a series tuning coil and an inverter as shown in Fig. 10. When correctly aligned this type of circuit provides a constant mismatch, usually of high v.s.w.r., into the required circuit impedance, usually 50 ohms. The matching networks are initially aligned to give either a simulated impulse response—the expander, or a bandpass characteristic—

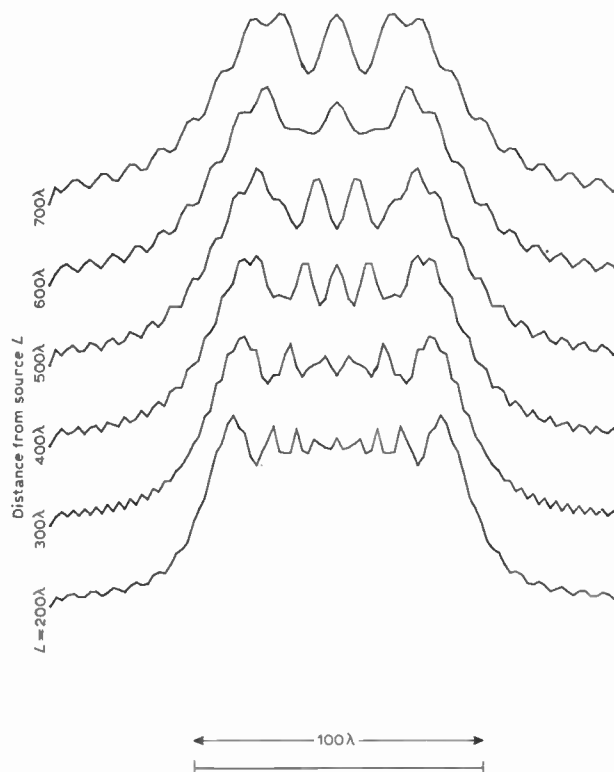


Fig. 9. Beam profile due to diffraction.

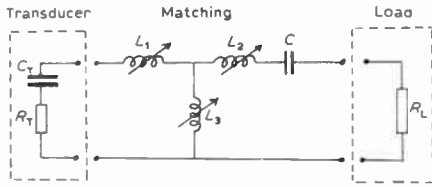


Fig. 10. Schematic of matching circuit. C_T , R_T , transducer capacitance and midband resistance; L_1 , 1st series resonator; L_2 , C , 2nd series resonator; L_3 , shunt resonator; R_L , load resistance.

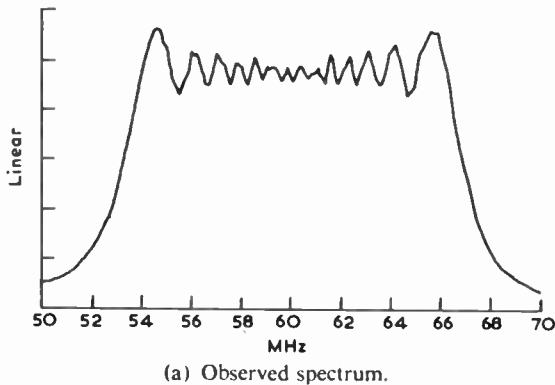
compressor. In a second stage of examination the phase characteristic of each device was measured by means of the π -point method and compared with theory.

4.1 Initial Alignment

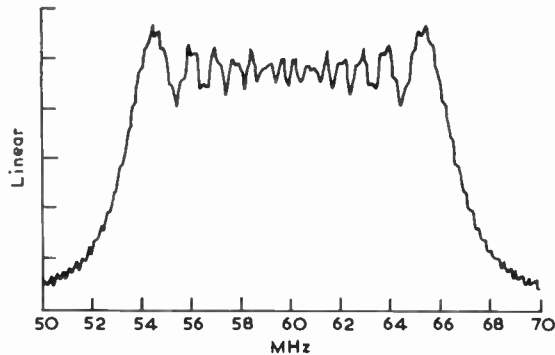
(a) Expander: The expander was designed to give a flat impulse response over the required 14 MHz bandwidth when impulsed with a signal having a symmetrical 1 dB roll-off at each band edge. The impulse response was observed when aligning this device. Following this alignment the expander was found to have slight ripple within the time period used. The observed ripple was 0.4 dB peak to peak which compares well with the theoretical prediction of 0.3 dB peak to peak.

At this stage the 4 μ s part of the signal centred on 60 MHz was gated out and its spectrum examined. The experimental spectrum, shown in Fig. 11(a), compared very closely with the predicted spectrum shown in Fig. 11(b).

(b) Compressor: The compressor was designed to operate with a flat input signal in the time domain.

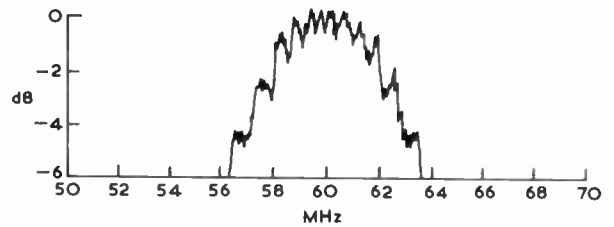


(a) Observed spectrum.

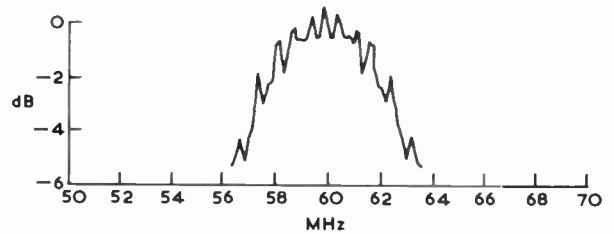


(b) Theoretical spectrum.

Fig. 11. Expander spectrum.



(a) Observed midband spectrum.



(b) Theoretical midband spectrum.

Fig. 12. Compressor spectrum.

In order to determine the response of this device and achieve satisfactory initial alignment, the response to a flat input spectrum was calculated. The detailed characteristic of the central portion of the compressor characteristic is examined in detail in Fig. 12. While there is clearly some distortion at the centre of the band, the general character of the ripple on the bandpass characteristic is in close agreement with the theoretical design.

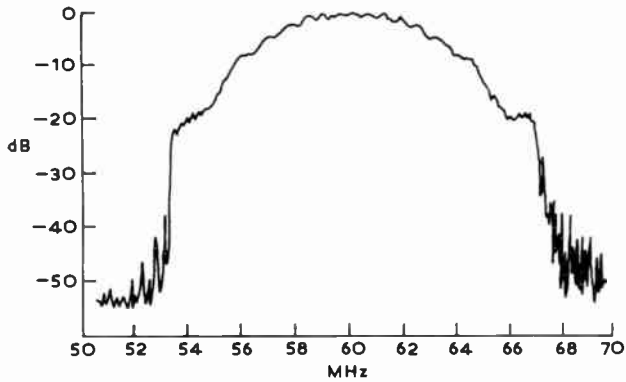
Figure 13 shows a comparison of theory and observation for the full compressor spectrum. The measured characteristic shows out of band rejection greater than 40 dB relative to the centre of the band. The ultimate out-of-band rejection is at -50 dB, which in conjunction with 40 dB device insertion loss indicates more than 90 dB electromagnetic screening of the output.

4.2 Phase Measurements

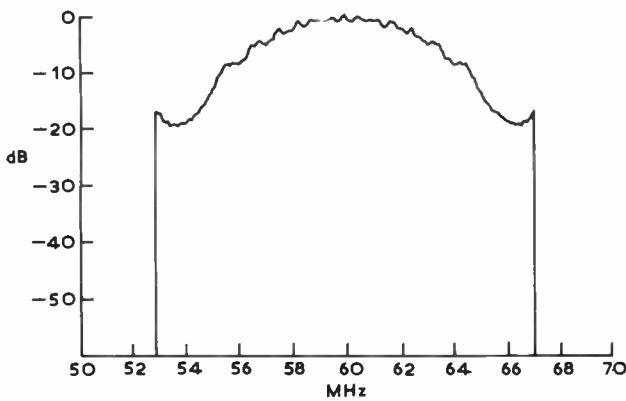
Dispersive devices are aligned as described above and then measured for departures from anticipated phase characteristic using the π -point method. In this the frequency is measured when the phase delay is an integer multiple of π . In practice, the interval is chosen to be $2n\pi$ in longer devices, where n is such as to give between 50 and 100 points across the band.

The result obtained from one of a series of measurements on the compressor device are shown in Fig. 14. In this plot only the quadratic phase behaviour has been eliminated and thus the corrections introduced to compensate for Fresnel ripple should still be observed. The anticipated phase corrections are shown by a continuous line which exhibits generally good agreement with the measurement data. The observed phase zeros in the correction occur at the anticipated frequencies and except at the band edges the amplitudes of the measurement data are in satisfactory agreement.

Even allowing for the rapid variation discussed in the Section on expander phase, there would appear to be a slight error at the band edges. Measurements in these



(a) Observed spectrum.



(b) Theoretical spectrum.

Fig. 13. Fullband compressor spectrum.

areas are made difficult by the 20 dB attenuation introduced by Taylor weighting. Although direct breakthrough is >30 dB below the transmitted and delayed signal other spurious signals can contribute to phase errors in a c.w. measurement of this type.

When the observed data are compared directly with the corrected phase law for the device, no wide range errors are observed. In fact, when the resultant data are Fourier analysed to give details of components which

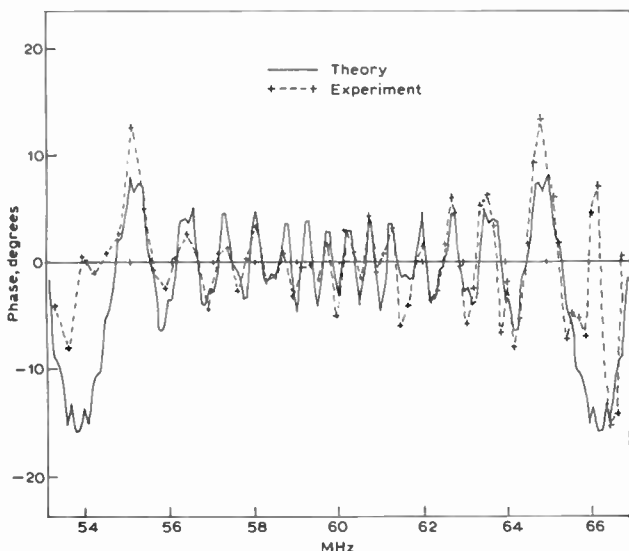


Fig. 14. Compressor phase characteristics.

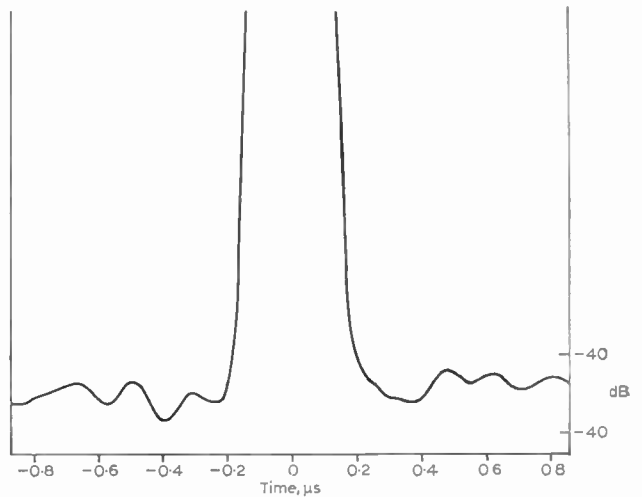
would contribute to individual sidelobe pairs, no component exhibits a peak phase error in excess of 1.0 degrees.

4.3 Loop Performance

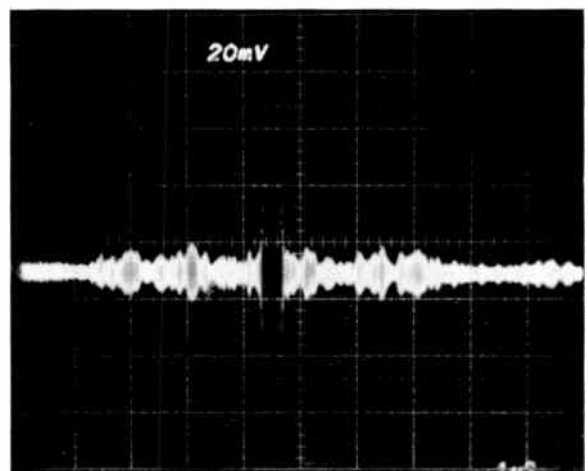
A photograph of the compressed pulse obtained by passing the time-gated output from the expander through the compression filter is shown in Fig. 15(b). All time sidelobes are below the -40 dB level and the compressed pulse has a 3 dB width of 100 ns, compared to a theoretical value of 96 ns.

The degradation in close-in sidelobes from the theoretical prediction of -45 dB is expected. It is due to amplitude and phase distortions caused by electrical matching networks and buffer amplifiers. It may be recalled that less than 1° of periodic phase ripple across the band is sufficient to give this level of sidelobe degradation.

Details of the phase detected pulse are shown in Fig. 15. Slight pulse broadening occurs at the -40 dB level; the observed width is $0.38 \mu\text{s}$ (cf. $0.265 \mu\text{s}$ for a perfect Taylor weighted signal of this bandwidth). Near-in sidelobes are below the -40 dB level and have a maximum peak of -43 dB within $\pm 1 \mu\text{s}$ of the compressed pulse.



(a) Compressed pulse.



(b) Sidelobe detail.

Fig. 15. Close-in sidelobe detail of the compressed pulse.

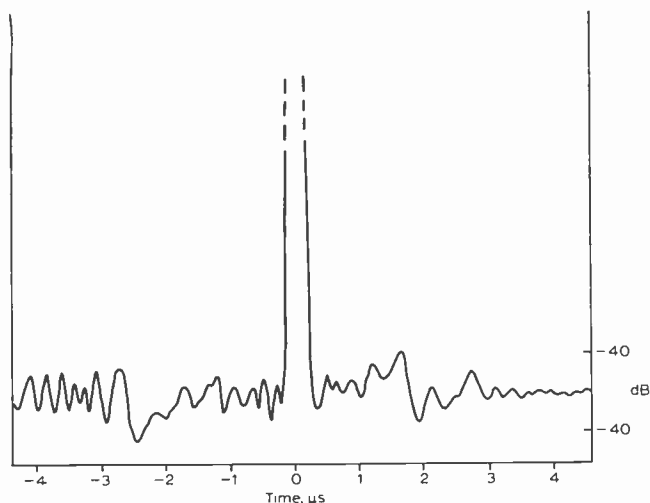


Fig. 16. Phase-detected compressed pulse.

Figure 16 shows the phase detected output over the whole correlation period. Maximum sidelobes, at -39 dB result from a beat between direct breakthrough and sidelobes at -2.5 μs , and -40 dB sidelobes occur at $+1.7$ μs .

4.4 Summary of Device Measurements

(a) Expander:

Centre frequency:	60.0 MHz
Centre frequency delay:	5.005 ± 0.003 μs
Mid-band loss:	42 dB
Bandwidth:	14 MHz
Ripple (unlimited):	0.4 dB peak to peak
Dispersive slope:	-0.283 ± 0.002 $\mu\text{s}/\text{MHz}$

(b) Compressor:

Centre frequency:	60.0 MHz
Centre frequency delay:	5.005 ± 0.003 μs
Mid-band loss:	40 dB
Dispersive slope:	$+0.290 \pm 0.002$ $\mu\text{s}/\text{MHz}$

5 Conclusions

A pulse compression sub-system employing passive s.a.w. devices for signal expansion and compression has been developed. Device design techniques have been examined in detail and designs achieved which allow the complete system to operate coherently and provide compressed pulses with sidelobes 40 dB below the primary pulse. In achieving this performance useful advances in the design of interdigital transducers have been demonstrated. At the same time, existing circuit concepts and designs have required only slight development in order to achieve this high performance.

While precise comparisons are difficult because of the wide range of possible matched filter parameters, it is believed that this level of performance shows an advance over previously reported pulse compression systems employing surface wave filters fabricated with interdigital electrodes.^{9,10} The reason for the achievement of such low sidelobes can be attributed to three major factors:

- (a) The use of a low coupling constant material such as quartz. This avoids some of the second-order

distortions which are characteristic of high-coupling materials such as lithium niobate.

- (b) The reciprocal ripple design allows a precise synthesis of both amplitude and phase perturbations which can be implemented in the compression filter.
- (c) Phase errors due to inaccuracies in the artwork plotting table are minimized by the use of the largest possible reduction factor which is consistent with the range of available first- and second-reduction camera lenses.

The main competitive technology to the interdigital transducer for dispersive filter applications is the reflective array compressor.¹¹

In this structure dispersion is introduced by accurate positioning of etched grooves on the surface of the substrate. The control of groove depth to give spectral weighting is a relatively new technology requiring close control in ion-beam etching. In contrast the photo-replication of interdigital arrays is well documented and available through the application of commercial equipment. This advantage makes it particularly significant that 40 dB sidelobe suppression has been demonstrated with interdigital transducers.

6 References

1. Maines, J. D., 'Applications of surface wave devices', Proceedings of the International Specialist Seminar on Component Performance and Systems Applications of Surface Acoustic Wave Devices, pp. 191-201, Aviemore, 1973. (IEE Conference Publication 109).
2. Butler, M. B. N. and Johnston, J. N., 'Engineering of dispersive sub-systems for pulse compression radar', *ibid.*, pp. 202-11.
3. Paige, E. G. S., 'Dispersive filters: their design and application to pulse compression and temporal transformations', *ibid.*, pp. 167-180.
4. Taylor, T. T., 'Design of line-source antennas for narrow beam-widths and low sidelobes', *IRE Trans. on Antennas and Propagation*, AP-3, pp. 16-28, 1955.
5. Nathanson, F. E., 'Radar Design Principles' (McGraw-Hill, New York, 1969).
6. Cook, C. E. and Bernfield, M. E., 'Radar Signals' (Academic Press, New York, 1967).
7. Hartmann, C. S., Bell, D. T. and Rosenfield, R. C., 'Impulse Model Design of Acoustic Surface Wave Filters', *IEEE Trans. on Microwave Theory and Techniques*, MTT-21, pp. 162-75, 1973.
8. Maines, J. D., Moule, G. L. and Ogg, N. R., 'Correction of diffraction errors in acoustic surface wave pulse compression filters', *Electronics Letters*, 8, No. 17, pp. 431-3, 24th August 1972.
9. Judd, G. W., 'A technique for realising low time sidelobe levels in small compression ratio chirp waveforms', Proceedings, 1973 IEEE Ultrasonics Symposium (Cat. 73, CHO 807-8SU).
10. Gerard, H. M., Smith, W. R., Jones, W. R. and Harrington, J. B., 'The design and applications of highly dispersive acoustic surface wave filters', *IEEE Trans. on Sonics and Ultrasonics*, SU-20, pp. 94-104, 1973.
11. Williamson, R. C. and Smith, H. I., 'The use of surface elastic wave reflection gratings in large time-bandwidth pulse compression filters', *IEEE Trans. on Sonics and Ultrasonics*, SU-20, pp. 113-24, 1973.

Manuscript first received by the Institution on 27th June 1975 and in final form on 19th November 1975. (Paper No. 1715/CC 251).

© The Institution of Electronic and Radio Engineers, 1976

Examples of manufactured dispersive delay lines using acoustic surface waves

P. HARTEMANN, Dr.Ing., Lic. ès Sci.*

SUMMARY

Two kinds of dispersive delay lines operating in radars at the present time are described as examples of manufactured acoustic surface-wave components. These lines were designed some years ago for a non-linear chirp impulse response and they are used as pulse expander and weighting matched pulse compressor. These dispersive delay lines consist of metallic interdigital transducers deposited on piezoelectric quartz substrates.

The first kind of line, which was produced in quantity, (about 180 units) has a compression ratio equal to 23.5. The relative sidelobe level of the compressed pulse is -26 dB. The delay varies by 4 μ s in a 7 MHz frequency range, the centre frequency being 30 MHz.

A sampled transducer with variable finger pair spacing is used for the second kind of line in order to limit the number of fingers. The delay change is 25 μ s for a 1 MHz frequency range centred at 30 MHz. The compression ratio and the relative sidelobe level of the compressed pulse are 19.2 and -24 dB respectively.

*Thomson-CSF, Laboratoire Central de Recherches, Domaine de Corbeville, 91401 Orsay, France

1 Introduction

In the pulse compression technique used for increasing the space-resolution or the range measuring capability of many modern radars, a frequency-modulated pulse is transmitted by the antenna and the received signal is processed with a dispersive filter in order to obtain a pulse compressed in the time domain. The frequency modulator and the receiving filter are generally dispersive delay lines and the delay variation versus frequency may be obtained in an analogue fashion by using several techniques. Conventional L-C circuits were employed at first for this purpose but acoustic components are now preferred. Bulk waveguides, bulk wave transducer arrays, Love wave lines and Rayleigh wave (s.a.w.) lines have been used with more or less favourable results. Surface wave (Rayleigh wave) devices were first tested about seven years ago and the high quality of the obtained characteristics have had as consequence a rapid development of the s.a.w. technique. Two types of s.a.w. dispersive delay line, now operating in radars, are described in this paper as examples of industrial components. The lines considered here were designed about five years ago. Then they were industrialized and one type was fabricated in relatively large quantities. Thus recent advances of the s.a.w. technique were not taken in account in designing these lines. As it will be shown later, the delay of lines fluctuates versus frequency around a mean value and the variation of this mean delay is T for a frequency interval equal to B . For line No. 1, T and B are equal to 4 μ s and 7 MHz respectively, and 25 μ s and 1 MHz for the line No. 2. This delay for the two lines is a non-linear function of the frequency in order to obtain a reduced sidelobe level of the compressed pulse without an additional filter, the matched filtering conditions being satisfied. Moreover the interdigital transducer of the line No. 2 is sampled in order to avoid having too many fingers. The operating principles of these lines are presented in Section 2 of this paper. Lines No. 1 and No. 2 are then described and their electrical features reported in Sections 3 and 4 respectively.

2 Surface Wave Dispersive Delay Lines With Non-Linear Time-Frequency Characteristics

The dispersive delay line is designed as a matched filter reducing the sidelobe level of the compressed pulse. The optimum receiver of an echo-pulse with a Gaussian noise is a filter matched to the pulse transmitted by the radar. In this case the impulse response of the filter to a Dirac pulse is similar to the time inverted transmitted signal¹ and the spectrum of the pulse at the filter output is equal to the squared spectrum of the transmitted signal. The envelope of the transmitted signal is rectangular and the frequency is modulated according to a specific law.

2.1 Operating Principle of a Dispersive Delay Line

The matching conditions may be obtained relatively easily by using interdigital transducers of surface waves. A s.a.w. delay line is made of two transducers deposited on a piezoelectric surface, each transducer being composed of two metallic electrodes with interleaved fingers

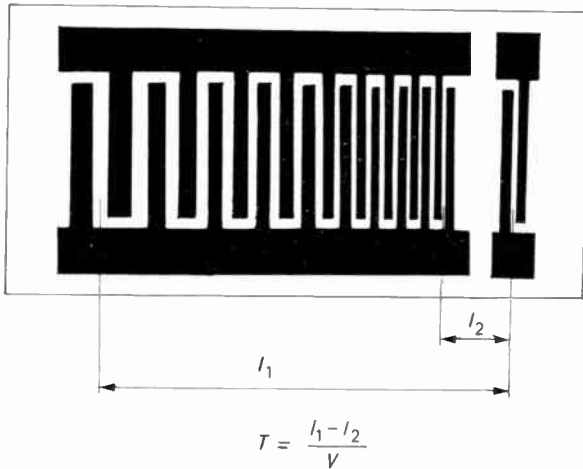


Fig. 1. Sketch of a dispersive delay line using acoustic surface waves.

a quarter acoustic wavelength wide (see Fig. 1). In this case the impulse response of the transducer depends essentially on the dimensional features of the electrodes. The instantaneous frequency of the impulse response varies with time according to the change of the finger spacing and the impulse response amplitude may be made constant by adjusting the finger overlap along the transducer. No wave is launched when the finger overlap is zero and the impulse response envelope may be practically rectangular. A transducer with a variable finger spacing (dispersive transducer) and another transducer with a constant finger spacing are used for both of the lines considered. The finger number of the non-dispersive transducer is limited in order to avoid amplitude distortion of the impulse response launched by the dispersive transducer. For both lines the time t varies with instantaneous frequency f of the impulse response according to a curve equal to the sum of a straight line and a period of a sine curve:

$$t = \frac{T}{2} + (f - f_0) \frac{T}{B} + \frac{T}{2\pi} \left(\frac{1-K}{1+K} \right) \sin 2\pi \left(\frac{f - f_0}{B} \right) \quad (1)$$

where $K \leq 1$ and f_0 is the centre frequency.

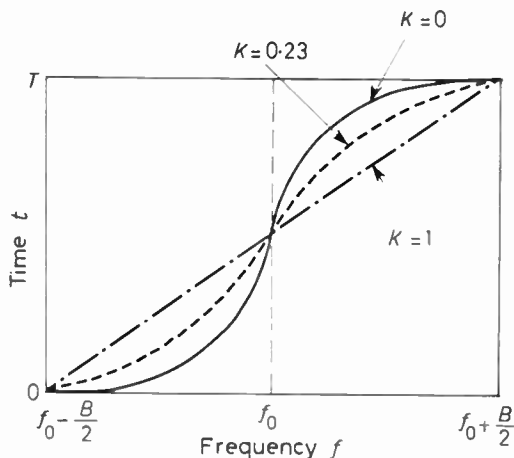


Fig. 2. Typical curves for the non-linear time-frequency characteristics of the impulse response.

The function (1) is shown in Fig. 2 for three values of the parameter K . The mean frequency response curve of such a dispersive delay line may be determined by using the principle of the stationary phase.¹ The effects due to the abrupt sides of the impulse response are neglected. This approach is approximately valid for lines with a large BT product as will be discussed later. The amplitude spectrum $|U(f)|$ of the impulse response, which has the same form as the frequency response, may be calculated according to the following relationship:¹

$$|U(f)| = a \left(\frac{dt}{df} \right)^{1/2} \quad (2)$$

Here a is the constant amplitude of the impulse response. Using equations (1) and (2) the following relationship (3) may be obtained:

$$|U(f)|^2 = 2a^2 \frac{T}{(1+K)B} \left[K + (1-K) \cos^2 \pi \left(\frac{f-f_0}{B} \right) \right] \quad (3)$$

A frequency response similar to $|U(f)|$ is plotted schematically in Fig. 3 for three values of K . This frequency response is bell shaped with a pedestal equal to \sqrt{K} . Because of the matching, $|U(f)|^2$ is equal to the amplitude spectrum of the compressed pulse $E(f)$ and the normalized expression of $E(f)$ is:

$$\frac{E(f)}{E(f_0)} = K + (1-K) \cos^2 \pi \left(\frac{f-f_0}{B} \right) \quad (4)$$

This expression is equal to that of the amplitude spectrum of the compressed pulse obtained using a linear f.m. delay line with amplitude weighting. In this case the impulse response of the compressor is bell shaped and the matching conditions are not satisfied. Formula (4) is identical to the general form of the compressed pulse spectrum obtained with the Hamming amplitude weighting.¹ Thus we have demonstrated that if the stationary phase principle may be used, the sidelobe level of the compressed pulse is reduced without mismatching by using a s.a.w. dispersive delay line, the time-frequency characteristic being S shaped.²

The relative sidelobe level W is a function of K . For example W is -31.4 dB for K equal to zero and a

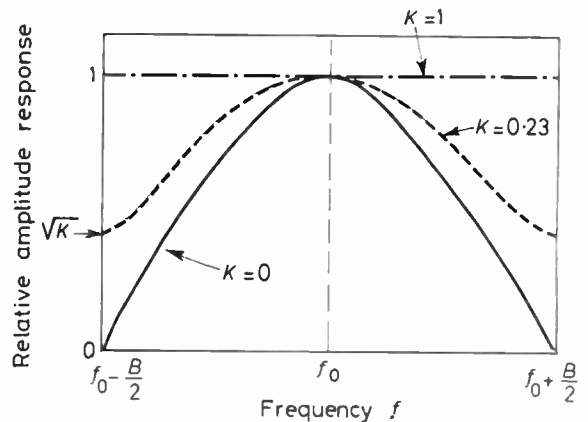


Fig. 3. Normalized frequency responses determined by using the stationary phase principle, the time-frequency characteristics being non-linear as shown in Fig. 2.

minimum value¹ (−42.8 dB) is reached for K equal to 0.08. Then W increases with K and the relative level is about −27 dB for K equal to 0.3. However these levels are not actually obtained because the impulse response envelope of a matched filter is rectangular and the abrupt sides introduce fluctuations of both the frequency response amplitude and the transit time. These effects may be roughly determined without computer aid by considering the behaviour of the dispersive transducer versus frequency.³ Each finger pair is equivalent to a linear elementary source and when a c.w. voltage is applied to this transducer, acoustic wavelets are launched by every finger pair. The wave incident on the receiving transducer is the resultant of the wavelet interference. An active group of cooperating sources consists of a set of finger pairs which launch wavelets having less than $\pm 45^\circ$ phase error from that transmitted by the central member of the set. The transducer may be considered as made up of a main active group and several secondary active groups which are in phase or 180° out of phase. The amplitude of the transducer frequency response at a given frequency is equal to the algebraic sum of waves launched by the groups and the transit time is determined by locating the transmitting source equivalent to the dispersive transducer.

The positions of the active groups change with frequency according to the time-frequency characteristic and the number of elementary sources in phase and 180° out of phase is frequency dependent because the spatial distribution of groups cannot spread outside the geometrical boundaries of the dispersive transducer. Thus the amplitude of the resulting transmitted wave changes with frequency around the value determined by the stationary phase principle. Close to the centre frequency the fluctuations of the frequency response amplitude are due to the displacements of the secondary groups located near the boundaries of the transducer. These fluctuations are essentially as a sine curve³ with a relative amplitude about equal to $((1+K)/(8BT))^{1/2}$. The frequency dependent position of the transmitting source equivalent to the dispersive transducer may be calculated as the ‘centre of gravity’ of all groups with respect to the main group axis. The transit time varies with frequency around the time frequency characteristic and the amplitude of transit time fluctuations relative to T is practically proportional to $(BT)^{-1/2}$.

The fluctuations of the frequency response amplitude and transit time are inherent in a filter matched to a pulse with a rectangular envelope. To obtain the compressed pulse the transmitted pulse is applied to the matched dispersive delay line. The delay fluctuations of the line are compensated by those of the input pulse spectrum. But the relative amplitude ripple of the compressed pulse spectrum is about twice that of the frequency response and imposes a minimum value of the compressed pulse sidelobe level. According to the paired echo-distortion analysis,¹ two spurious pulses with a relative amplitude equal to $((1+K)/(8BT))^{1/2}$ must be added to the main compressed pulse determined by using the stationary phase principle for lines with a relatively large product BT ($BT \geq 50$). The lowest relative sidelobe level of the

compressed pulse is about $0.35/\sqrt{BT}$ for K close to zero. However for lines with a small BT product a modulation of the frequency response amplitude produced by the secondary groups the closest to the main group must be taken into account.

Thus for these lines the sidelobe level may not be reduced below a limit which depends upon the product BT . However this limit may be lowered if the dispersive transducer is specially designed for compensating the frequency response fluctuations.⁴

The sidelobe level obtained using a dispersive delay line with a non-linear time-frequency characteristic is generally more sensitive to the Doppler frequency shift than that of a line with a linear characteristic. As an example the relative sidelobe level increases from −27 dB to −21 dB for a Doppler shift equal to ± 40 kHz, B , T and K being 6 MHz, 15 μ s and 0.23 respectively. However this Doppler shift sensitivity is not a drawback for the applications using these lines.

2.2 Sampled Transducer

The required impulse response is of the dispersive transducer is $h(t)$.

$$h(t) = a(t) \cos(\phi(t)).$$

The linear acoustic sources equivalent to a finger pair are located in positions corresponding to time t_n such that:

$$\phi(t_n) = n\pi$$

where n is an integer. The number of sources is $2Tf_0$.

The samples of the impulse response are equidistant in the phase domain and a development in Fourier series may be used.⁵ The harmonic order m is an odd number because of the symmetry features of the impulse response. The transducer is called ‘sampled’ when the finger pairs are located at positions corresponding to a time t_n such that:

$$\frac{\phi(t'_n)}{Q} = n\pi$$

where Q is an integer (sampling coefficient).

The instantaneous frequency of the m th harmonic of the impulse response of the sampled transducer is f_m

$$f_m = \frac{1}{2\pi} \frac{d(m\phi/Q)}{dt} = m \frac{f}{Q}$$

$$B_m = \frac{m}{Q} B$$

The desired frequency time characteristic is found for m equal to Q . The frequency range B_m of the harmonic Q and that of the $(Q+2)$ th harmonic must not overlap, that is:

$$f_0 + g(T/2) \leq \left(\frac{Q+2}{Q}\right) [f_0 - g(T/2)] \quad (5)$$

with $f = f_0 + g(t)$.

The time origin is in the middle of the impulse response. The maximum Q_{\max} of the sampling coefficient is found by using the equation (5):

$$Q_{\max} = \frac{2f_0}{B} - 1.$$

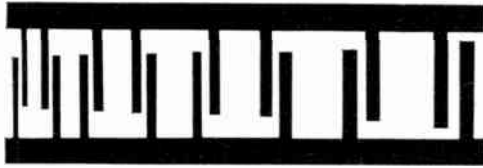


Fig. 4. Sketch of a sampled dispersive transducer for surface waves.

The minimum number of sources (N_{min}) is:

$$N_{min} = \frac{2Tf_0}{Q_{max}} = \frac{BT}{1 - B/(2f_0)}$$

The minimum number of fingers is $2N_{min}$.

A sketch of a sampled dispersive transducer is shown in Fig. 4. Thus the location of finger pairs is determined for a sampled transducer as for one with a frequency range and a centre frequency equal to B/Q and f_0/Q respectively. However the width of the fingers corresponds to the useful harmonic frequency f . This sampling technique is used for line No. 2 in order to avoid the perturbation of the propagation as a consequence of having too many fingers, the acoustic waves launched by the finger pair farthest from the receiving transducer propagating under the total number of fingers.

For a given input voltage the wave amplitude launched by a sampled transducer is Q times smaller than that of an unsampled transducer ($Q = 1$). The parallel radiating resistance of the sampled transducer is equal to $Q^2 R_p$, R_p being the parallel radiating resistance of the unsampled transducer.

3. Line No. 1 ($B = 7 \text{ MHz}$, $T = 4 \mu\text{s}$)

This type of line has been designed to take the place of conventional L-C dispersive delay lines intended for a ground radar. About 27 dispersive delay lines are used in this radar; one for transmitting, 26 for receiving. Some 180 units of this kind of line have been industrialized and fabricated by the Division Tubes Electroniques of Thomson CSF.

3.1 Description

The piezoelectric substrate is a sample of natural quartz (Y cut, X propagating) the dimensions of which are $40 \times 11 \times 2$ (mm). The larger side (40 mm) corresponds to the propagating direction. The dispersive transducer is designed for a K value equal to 0.28 and the lowest frequencies are more delayed than the largest frequencies. The useful finger length is 8 mm and the finger width varies along the transducer from $24 \mu\text{m}$ to $30 \mu\text{m}$, the centre frequency being 30 MHz. The length of this transducer is about 13 mm (264 fingers) (see Fig. 5). This transducer is used as the transmitting one. The non-dispersive transducer is made of 8 equidistant fingers with a width equal to $26.3 \mu\text{m}$ and is employed as the receiving one. The spacing between the two transducers is about 11.5 mm. Conventional photolithography technique is used for realizing the transducers: an 8000 Å thick aluminium coating is deposited on the polished quartz surface and chemically etched. The quartz substrate is glued using araldite on

the bottom of a box made in sheet-metal. Three hermetic bead feed-throughs are soldered on the side of the box for the input and the output. A shielding screen is fixed between the two transducers. Gold wires are thermal compression bonded on the transducer pads. A hybrid integrated circuit with a high impedance input is fastened with araldite on the quartz surface near one end and is connected to the output pads of the receiving

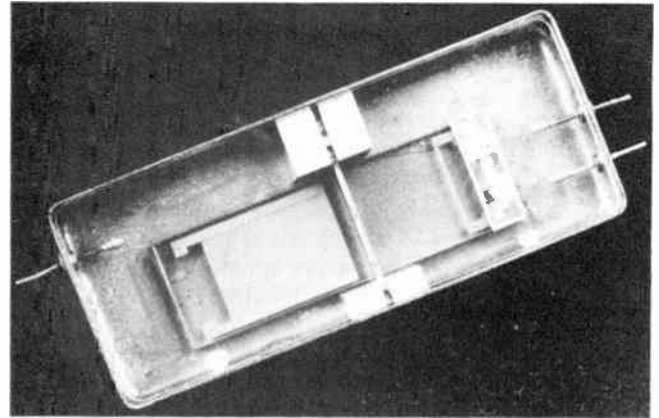


Fig. 5. View of a line No. 1 ($B = 7 \text{ MHz}$, $T = 4 \mu\text{s}$) in its industrialized packaging. The length and the width of the substrate are 40 mm and 11 mm respectively.

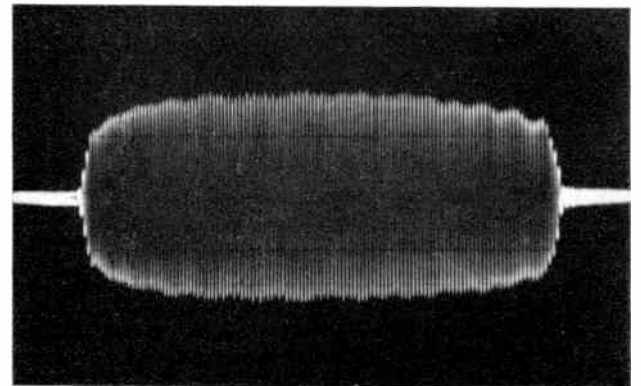


Fig. 6. Impulse response of the line No. 1. Horizontal scale: $0.5 \mu\text{s}/\text{div}$.

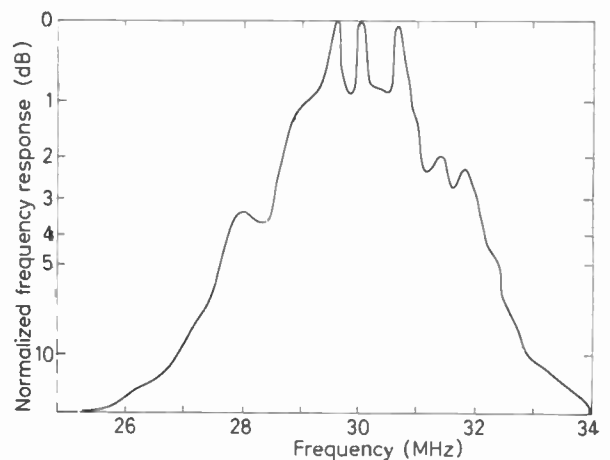
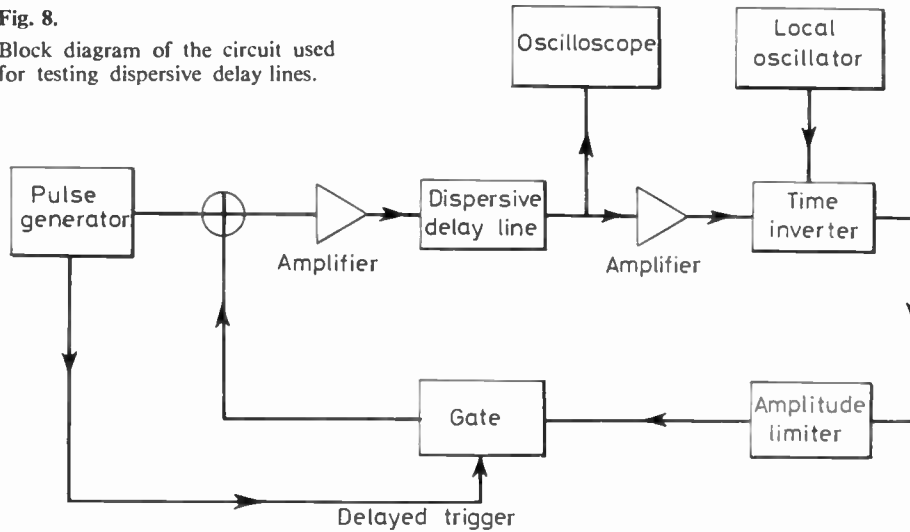


Fig. 7. Normalized frequency response of the line No. 1.

Fig. 8.
Block diagram of the circuit used for testing dispersive delay lines.



transducer. This circuit is used to limit the insertion loss of the line without frequency response distortion, the parallel capacitance and resistance of the output transducer being about equal to 2 pF and 100 k Ω respectively. The circuit consists of a circuit printed on ceramic plate, a field effect transistor 2N4416 and 1 M Ω resistance loading the gate of the transistor. The transistor packaging is the 'Ceratab' kind: the semiconductor chip is bonded on a U-shaped alumina ceramic holder which is soldered to the printed circuit. The source and the drain of the transistor are connected to two bead feed-throughs. One pad of the launching transducer is connected to a bead feed through and the other to the metallic box. The cover of the box is hermetically soldered using silver tin. The box is fixed to a printed card supporting the associated electronic circuits, mainly the impedance matching circuits and the amplifier.

3.2 Electrical Characteristics

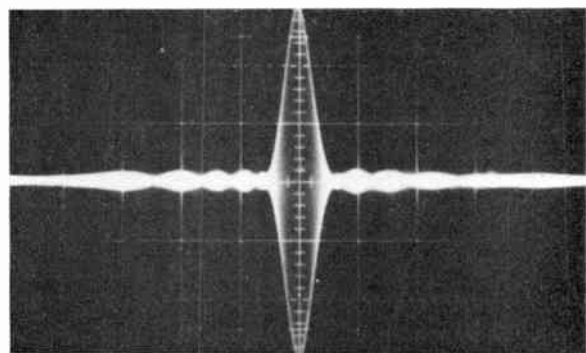
The parallel capacitance and resistance of the transmitting transducer are about equal to 57 pF and 4 k Ω respectively. The insertion loss of the line loaded with a high impedance is 33 dB. The impulse response of the line and the normalized frequency response are shown in Figs. 6 and 7 respectively. The compressed pulse has been observed for each line using the circuit in Fig. 8.

A narrow pulse with a carrier frequency is applied to the line, the expanded pulse at the line output is time-inverted, amplitude levelled and time-gated in order to obtain a pulse with a rectangular envelope. Then this pulse is applied to the line and the compressed pulse may be observed on an oscilloscope screen. The -3 dB and -20 dB widths of the compressed pulse are 170 ns and 370 ns respectively (see Fig. 9). Therefore the compression ratio is 23.5.

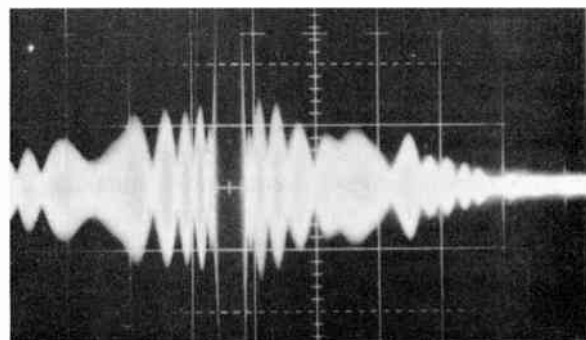
The relative sidelobe level of the compressed pulse lies between -25.5 dB and -26 dB for all fabricated lines. The computed sidelobe level is -24.8 dB in the case of a perfectly matched filter. It is equal to -27.5 dB by using the stationary phase principle. But in fact the impulse

response of the line is not of a perfectly rectangular shape (see Fig. 6) and as a consequence, an extra amplitude weighting reduces the sidelobe level. The sidelobe level computed for a $\sin x/x$ shaped impulse response is -27.2 dB, the normalized amplitude of the impulse response envelope being 0.714 at the time limit of the impulse. In this case the sidelobe shape (see Fig. 10) is in good agreement with the experimental result.

The lines used in a radar must be very nearly identical in time-frequency characteristics, a single local oscillator



(a) Horizontal scale: 0.5 μ s/div. Vertical scale: 0.1 V/div.



(b) Horizontal scale: 1 μ s/div. Vertical scale: 0.01 V/div.

Fig. 9. Compressed pulse obtained with the line No. 1
The compression ratio is 23.5 and the relative sidelobe level -26 dB.

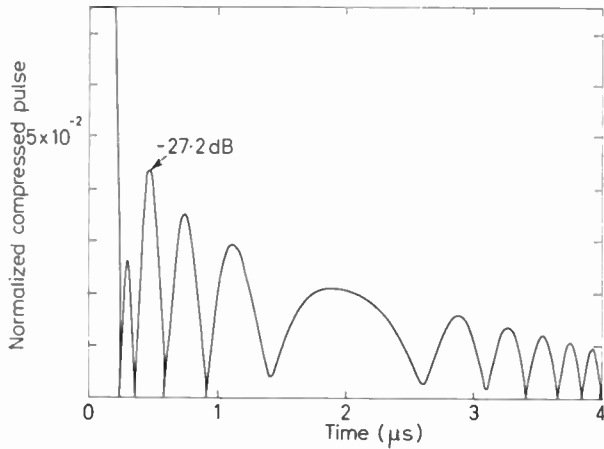


Fig. 10. Computed normalized envelope of the pulse compressed using the line No. 1 ($K = 0.28$). The impulse response of the line is $\sin x/x$ shaped with a normalized amplitude value equal to 0.714 at the limits of this response.

being employed for realizing the time inversion. The sidelobe level of a line with a S-shaped time-frequency characteristic is very sensitive to the local oscillator frequency. The inflection point frequency of this characteristic belonging to the receiving line impulse response must be very close to that of the time-inverted expanded pulse. This inflection point frequency is measured for each line by adjusting the local oscillator frequency in order to obtain the best sidelobe level without gating. The variation of the inflection point frequency was found to be equal to ± 25 kHz around 30.050 MHz for the 180 units. This variation is mainly due to the accuracy of the crystalline axis orientation and of the transducer positioning with respect to these axes.

The lines have successfully undergone environmental tests appropriate to the standards intended for the fixed ground systems. The operating temperature range is from $+10^\circ\text{C}$ to $+50^\circ\text{C}$ in a 95% humid atmosphere. The shelf temperature range is from -40°C to 70°C in a 95% humid atmosphere. The duration of the heating or cooling plateau is equal to 16 hours per temperature cycle.

4. Line No. 2 ($B = 1$ MHz, $T = 25$ μs)

The general structure of this line, about 10 units of which have been fabricated for a ground radar, is identical to that of the line No. 1. The finger number of an unsampled dispersive transducer would be about 1500, the centre frequency being 30 MHz and the acoustic wave propagation would be perturbed by such a finger number. Therefore a sampling technique has been employed in order to reduce this number. The dispersive transducer was designed with a sampling coefficient Q equal to 15; thus the total number of fingers is about 200.

4.1 Description

A quartz plate, the dimensions of which are $95 \times 22 \times 4$ mm, is employed as a substrate. ST cut, X propagating quartz is used because the temperature stability of this

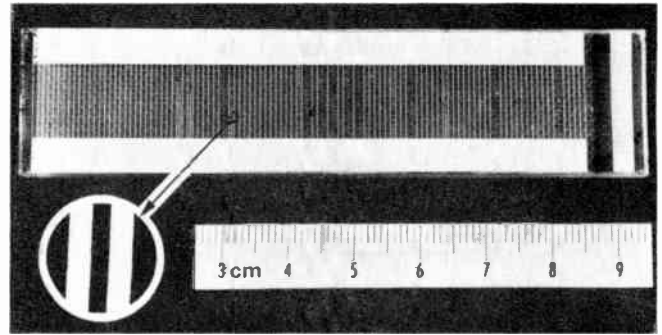


Fig. 11. View of line No. 2 ($B = 1$ MHz, $T = 25$ μs , $Q = 15$) outside its box. The dispersive transducer is sampled. The white lines between the large electrodes are pairs of aluminium fingers 26 μm wide. (See the enlarged inset of the transducer pattern).

cut is very good. The relative delay change is about equal to 140 parts in 10^6 at -40°C , 0 at 28°C and 174 parts in 10^6 at $+100^\circ\text{C}$. The time-frequency characteristic corresponding to the dispersive transducer is non-linear with a coefficient K equal to 0.23. The lowest frequencies are the most delayed. The length of this transducer, which is made of 105 finger pairs, is equal to 81 mm (see Fig. 11). The finger pair spacing varies between 0.827 mm and 0.856 mm along the dispersive transducer. The finger number of the non-dispersive transducer is 60. The constant useful length of fingers is 11 mm.

Conventional photolithography techniques were employed for depositing the transducer. The positions of

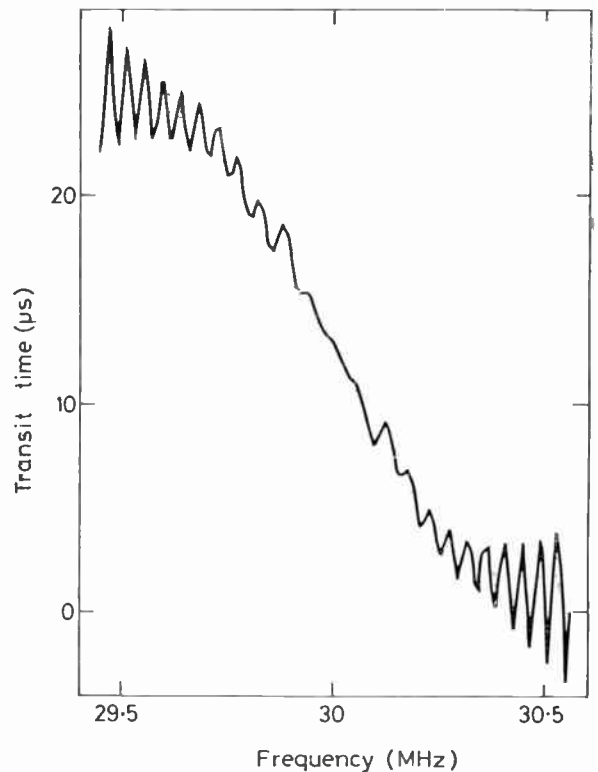


Fig. 12. Transit time versus frequency computed for line No. 2. The time origin corresponds to an end of the transducer.

finger pairs must be carefully controlled on the mask. The geometrical aberration of the reducing lens used for obtaining the mask is not negligible as a consequence of the great length of the line and was taken into account for the calculation of the finger places. The discrepancy between the measured and the theoretical locations of finger pair changes along the transducer between $-3\ \mu\text{m}$ and $+5\ \mu\text{m}$. The line is fixed on the bottom of a metallic box and two hermetic coaxial connectors (subclitic type) are used as the input and the output. The cover of the box is hermetically fixed with screws. No electronic components are located in the box. The line is fixed on a printed card supporting the matching circuits.

4.2 Electrical Characteristics

The transit time, which depends upon the sampling coefficient was computed versus frequency as shown in Fig. 12.

The transit time fluctuations are very important (about $5\ \mu\text{s}$ peak to peak) near the ends of the frequency range as a consequence of the small product BT (25).

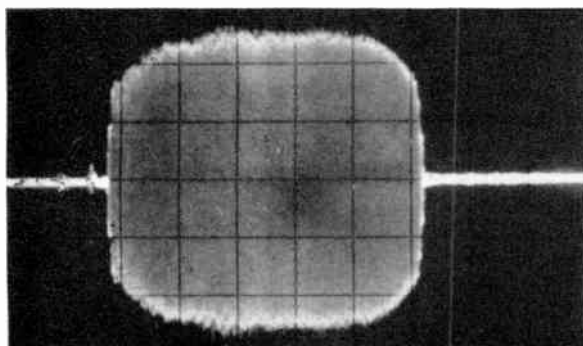
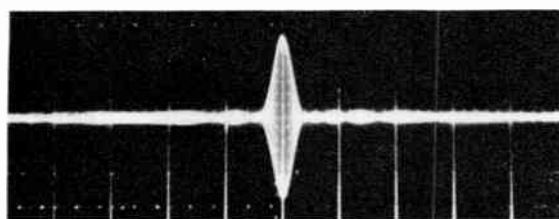
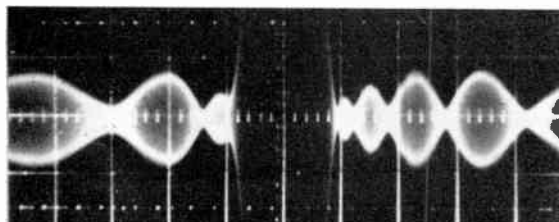


Fig. 13. Impulse response of the line No. 2. Horizontal scale: $5\ \mu\text{s}/\text{div}$.



(a) Horizontal scale: $5\ \mu\text{s}/\text{div}$. Vertical scale: $0.1\ \text{V}/\text{div}$



(b) Horizontal scale: $2\ \mu\text{s}/\text{div}$. Vertical scale: $0.01\ \text{V}/\text{div}$.

Fig. 14. Compressed pulse obtained with line No. 2. The compression ratio is 19.2 and the relative sidelobe level $-24\ \text{dB}$.

Close to the centre frequency the fluctuation is smaller than that of a line with a linear time-frequency characteristic. In this case the transit time variation is about $3\ \mu\text{s}$ peak-to-peak.

The parallel capacitance and resistance are $55\ \text{pF}$ and $5.8\ \text{k}\Omega$ respectively for the dispersive transducer and $23\ \text{pF}$ and $3\ \text{k}\Omega$ respectively for the other transducer. The impulse response duration is $26.5\ \mu\text{s}$ (see Fig. 13). The relative spurious pulse level of the impulse response is about $-25\ \text{dB}$ with bevelled substrate ends. The insertion loss with a high loading impedance is $33\ \text{dB}$. The $-3\ \text{dB}$ and $-6\ \text{dB}$ bandwidths of the frequency response are $0.65\ \text{MHz}$ and $0.8\ \text{MHz}$ respectively. The $-3\ \text{dB}$ and $-20\ \text{dB}$ widths of the compressed pulse are $1.3\ \mu\text{s}$ and $2.9\ \mu\text{s}$ respectively. The compression ratio is 19.2. The experimental relative sidelobe level is $-24\ \text{dB}$ (see Fig. 14). The computed value of this level is $-24.8\ \text{dB}$. It is the lowest level calculated as function of K . The sidelobe level determined according to the stationary phase principle is $-29.7\ \text{dB}$ for K equal to 0.23.

Environmental tests according to the standards for ground systems have been successfully applied to these lines. The sidelobe level of the compressed pulse changes by about $0.5\ \text{dB}$ between -40°C and $+100^\circ\text{C}$. In this experiment the two identical lines used for transmitting and receiving were at the same temperature and the frequency of the time inverter local oscillator and the time position of the gating pulse are fixed. This good result is obtained because the substrate used (ST-cut quartz) is very stable in temperature. The features of the lines are very reproducible as has been demonstrated by using five identical lines. The centre frequencies of these lines measured by observing the sidelobe shape as for the line No. 1 varies from $-2\ \text{kHz}$ to $+4\ \text{kHz}$ around $29.950\ \text{MHz}$. The loss of these lines varies by about $1\ \text{dB}$ around $33\ \text{dB}$. The compressed pulse has been observed with two identical lines for transmitting and receiving, these lines being exchanged for testing the five lines. The maximum variations of the sidelobe level and of the $-3\ \text{dB}$ width of the compressed pulse were found to be equal to $2\ \text{dB}$ and $25\ \text{ns}$ respectively. The delay between the applied expanded pulse and the compressed pulse fluctuates by $40\ \text{ns}$.

5 Conclusion

Two dispersive delay lines have been described in this paper as examples of manufactured acoustic surface wave component. The very good results obtained with these lines show that the s.a.w. dispersive delay lines can effectively replace lines fabricated by other techniques for expanded pulse durations smaller than about $150\ \mu\text{s}$. The dispersive transducer is synthesized relatively easily according to the desired features and the performance is realized with a good accuracy. Because the time-frequency characteristics of the line depend upon the transducer pattern a great diversity of features is possible. A S-shaped time-frequency characteristic has been used in order to reduce the sidelobe level of the compressed pulse. The line is thus a weighting matched filter. Adjustments may be carried out by modifying the

transducer pattern. The technique employed for fabricating the s.a.w. lines is relatively simple and well known because it is currently used for realizing microelectronic components. The reliability of surface wave components is noteworthy and performance is very reproducible, as has been shown in the present paper. This last quality is mainly due to the photoetching of the transducers using a single master mask. The lines with an ST-cut quartz substrate are very stable in temperature and the use of thermostats is not necessary. The overall dimensions of s.a.w. dispersive delay lines are drastically smaller than those of other types of lines. The cost of surface wave lines is relatively low and may be small if the number of the fabricated identical units is great. These features of dispersive delay lines using acoustic surface waves encourage one to design new devices and recent advances (for instance the use of reflective gratings) increase still further the possible applications.

6 Acknowledgments

The author gratefully acknowledges helpful discussions with Mr. F. Genauzeau in the Division Tubes Elec-

troniques of Thomson-CSF. This work has been supported in part by the Service Technique des Télécommunications de l'Air.

7 References

1. Cook, C. E. and Bernfeld, M., 'Radar Signals' (Academic Press, London, 1967).
2. Hartemann, P. and Dieulesaint, E., 'Pondération des lobes secondaires d'une impulsion comprimée par une ligne dispersive à ondes élastiques de Rayleigh', *L'Onde Electrique*, 51, pp. 523-4, June 1971.
3. Hartemann, P., 'Filtres dispersifs à ondes élastiques de Rayleigh', Thésis C.N.R.S. Ref. No. A.O. 8293, April 1973.
4. Judd, G. W., 'Technique for realizing low time sidelobe levels in small compression ratio chirp waveforms', Proceedings, 1973 IEEE Ultrasonics Symposium, pp. 478-81.
5. Atzeni, C., 'Sensor number minimization in acoustic surface wave matched filters', *IEEE Trans. on Sonics and Ultrasonics*, SU-18, No. 4, pp. 193-201, October 1971.

Manuscript first received by the Institution on 14th July 1975 and in final form on 17th November 1975. (Paper No. 1716/CC 252).

© The Institution of Electronic and Radio Engineers, 1976

The Author



Dr. P. Hartemann received the Licence ès Science from the University of Clermont-Ferrand in 1958. In 1960 he obtained the Ingénieur degree from the Ecole Supérieure d'Electricité, and then spent two years at the Research Centre of the Compagnie Générale d'Electricité where he worked on solid state lasers. In 1964 he joined the Research Centre of Thomson-CSF where he studied the yttrium aluminium garnet laser. Since 1968 he has been engaged in research on surface acoustic waves and in 1973 he received the Docteur-Ingénieur degree from the University of Orsay for work on dispersive delay lines using acoustic surface waves.

Surface acoustic wave matched filters for communications systems

K. V. LEVER, B.Sc., M.Sc., C.Eng., M.I.E.E.,*

E. PATTERSON, M.Sc., Ph.D., M.Inst.P.,*

P. C. STEVENS, B.Sc., A.R.C.S.*

and

I. M. WILSON, B.A.*

SUMMARY

The design, fabrication and performance of surface acoustic wave matched filters for particular communication systems are described. Applications are considered for synchronization acquisition by means of m-sequence phase shift keyed correlators, and for demodulation of data in (i) a four-level frequency-shift keyed system and (ii) a differentially coherent phase-shift keyed system.

* The General Electric Company Ltd., Hirst Research Centre, Wembley, Middlesex HA9 7PP.

1 Introduction

The velocity of surface acoustic waves (s.a.w.) is about five orders of magnitude slower than that of electromagnetic waves, and this allows transversal filters of a particularly useful range and size to be realized in s.a.w. technology. Matched filter time intervals up to tens of microseconds are straightforward¹⁻⁶ and even up to milliseconds are possible with special techniques.⁷⁻¹⁰ In addition s.a.w. devices offer advantages of weight, cost, planar thin film fabrication, large dynamic range and stable temperature performance.¹¹⁻¹³ These are the reasons for the increasing interest in s.a.w. components over the past five years and their rapid adoption for some systems applications.¹⁴ A major area of impact to date has been in pulse compression radar where, using s.a.w. devices, generation and matched filter reception of the frequency chirp signals is standard practice.^{5, 15, 16}

The basis for this success has been the spatial realization in a transducer pattern on a piezoelectric crystal surface of the waveform required to be generated and detected, and the close to theoretical performance of such matched filter pairs.⁵ These criteria apply equally well to phase-shift-keyed (p.s.k.) s.a.w. matched filters suitable for communication systems applications.^{2, 7, 8, 17} The design and performance of such devices for several communication systems are described in this paper. The receiver synchronization problem in spread spectrum communications is considered first. This is followed by sections on data demodulation in multi-frequency-shift-keyed (m.f.s.k.) systems and also differentially coherent phase-shift-keyed (d.c.p.s.k.) systems.

2 Receiver Synchronization in Spread Spectrum

2.1 System Description

A spread spectrum communication system employs a bandwidth many times the data bandwidth and this is done principally to provide the following advantages: resistance to interference; tolerance of multi-path signals, and low detectability. However, one of the difficulties introduced by such techniques is the need to lock the phase of the receiver to that of the transmitter in order to demodulate the information. Analogue matched filters are particularly useful in this synchronization role, since a conventional serial search and integrate receiver will, on some occasions, take minutes to achieve synchronization.

The operation of spread spectrum systems and various possible configurations have been well described elsewhere,^{2, 7, 18} and only a brief description will be included here. These systems can be implemented in a number of forms involving frequency hopping and/or phase coding, but a basic element of the system is that the data or bits to be transmitted are multiplied by a suitable fast code, commonly known as the signature of the transmitter. A biphasic pseudo-noise sequence is often used and this results in information being spread over a wide bandwidth with one bit period now sub-divided into many chips. The signal is usually buried in noise

and interfering signals. A multiply-and-integrate procedure can be used at the receiver to demodulate the information, but only once synchronization has been established. The multiply and integrate technique provides signal-to-noise gain (s.n.g.) and so discriminates against noise and other interfering signals which do not possess the relevant fast code format. Similarly, without a knowledge of the code it is difficult to make use of the available s.n.g. and the signal is difficult to detect: this provides message privacy. Synchronization is the key to the rejection of multi-path signals since this allows the receiver phase to be adjusted for only the direct signal delay.

The relatively long lock-up time of the serial search and integrate technique is overcome by using a matched filter as the synchronizing element because this simultaneously searches over a large code interval permitting the receiver to use a much faster search rate. The reduction factor in lock-up time is equal to the number of chips in the matched filter, i.e. the time bandwidth product or the s.n.g. This matched filter application may also be extended to the data demodulation as well as establishing synchronization.⁷ This is elaborated further in Section 2.2. The length of the matched filter required depends on the signal-to-noise ratio (s.n.r.) of the system. This is usually defined in dBHz, the s.n.r. in a 1 Hz bandwidth at the receiver. Typically this will be in the range 50 dBHz to 30 dBHz requiring matched filter periods of 40 μ s to 4 ms respectively for 6 dB s.n.r. at the output.

2.2 The S.A.W. Matched Filter System

The design of s.a.w. devices for generation and matched filtering of biphas coded signals is illustrated in Fig. 1. An input transducer of one chip duration on a piezoelectric substrate is impulsed with the polarity controlled by the data stream. The resulting intermediate frequency burst is sampled by a series of wide bandwidth acoustic taps which form the output transducer and are phase coded according to the required sequence. The insert in Fig. 1 shows the form of such a sequence and a time-expanded section. The data have now been spread over a wide bandwidth and the signal is up-converted and transmitted.

The received signal is down converted and applied to an identical s.a.w. device but from the opposite direction to provide the time reversal necessary for matched filtering. A number of streams of correlation peaks appear at the output transducer, i.e. the direct and multi-path signals. The largest of these is used to set the phase-locked sampler to accept only the direct path signal stream. The data are regenerated by multiplying by a phase-locked carrier. The second insert in Fig. 1 shows an example of such a train of correlation peaks resulting from a negative s.n.r. input signal.

The signal examples used above to illustrate the system are only of 10 μ s duration, while, as mentioned in Section 2.1, at least 50 μ s matched filters are necessary for these devices to be applied to present-day needs. Some solutions to this problem are considered in Section 2.4.

It is necessary to use ST quartz as the substrate material to provide a reasonable range of temperature stable operation.¹⁹ Although this material only provides

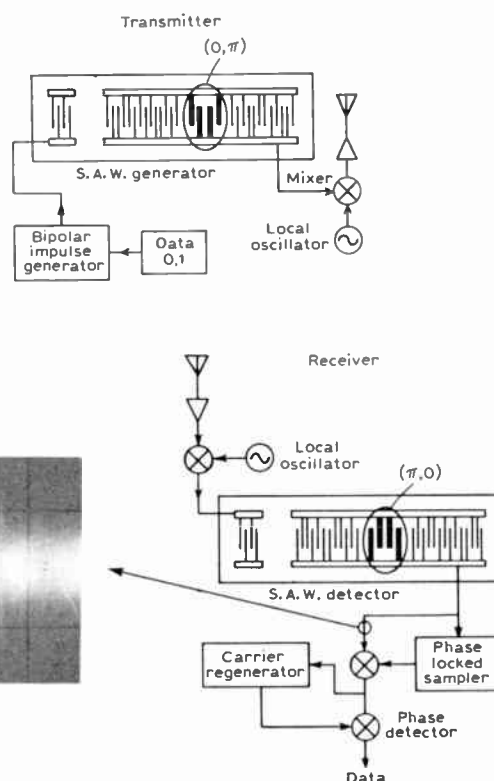
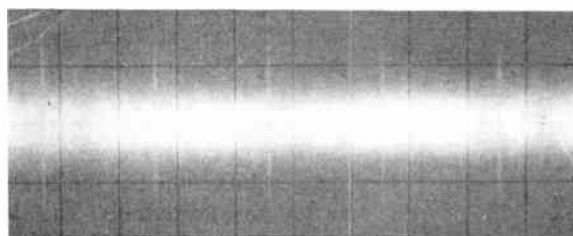
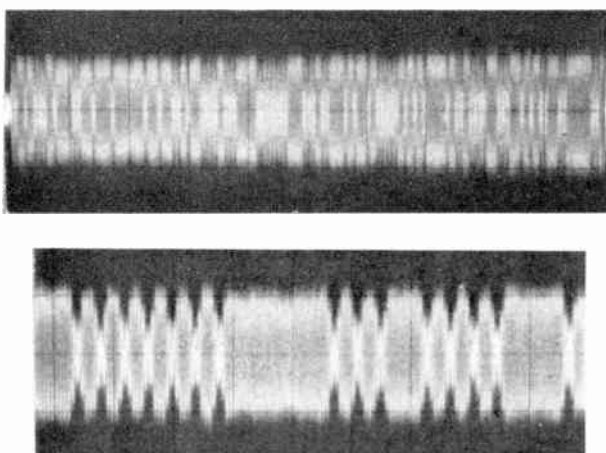


Fig. 1. Biphas coded signal generation and detection with s.a.w. devices.

a parabolic frequency variation with temperature, this is a slowly varying relationship about the turning point. For the longer matched filters required, i.e. 1 ms time duration, the operating temperature range is still greater than $\pm 12^{\circ}\text{C}$.

2.3 S.A.W. Fixed Code P.S.K. Matched Filter Performance

A number of s.a.w. m-sequence biphase coded matched filters have been investigated. The individual devices range from $10\ \mu\text{s}^4$ to $50\ \mu\text{s}^{20}$ and the cascades from $50\ \mu\text{s}^8$ to $350\ \mu\text{s}^{20}$. The peak-to-sidelobe ratio of these devices was found to be close to theoretical for a single burst signal correlation, but the large improvement in sidelobe levels expected when the devices were operated in a continuous mode was not observed. This problem has been analysed, using a delta function model, in terms of phase errors, amplitude variations, taper of the amplitude response, bandlimiting effects and spurious signal levels.^{8, 17} This analysis has been compared with measurements on 127-tap matched filters fabricated on ST quartz. An inclined transducer structure was used on these devices⁴ to avoid the mass loading reflections associated with the quarter wavelength wide transducer lines. The arrangement is shown in Fig. 2. The carrier frequency was 76.8 MHz and the m-sequence code rate 12.8 MHz. Table 1 compares the measured performance with the analysis indicated above and reveals the close agreement between observed peak-to-sidelobe levels and the predicted values in the light of

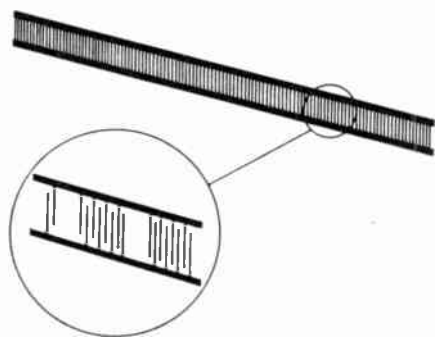
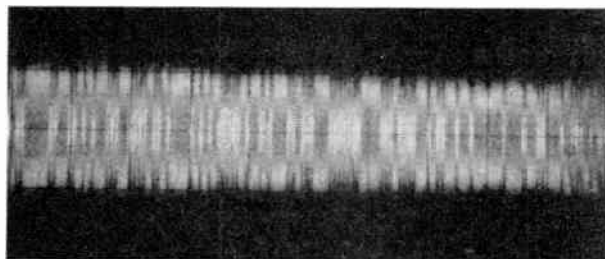


Fig. 2. Inclined transducer structure for 127-tap matched filter.

Table 1. Effect of imperfections on sidelobe level for 127-tap biphase coded matched filter

	Peak-to-sidelobe (dB)	
	burst	periodic
Perfect code	23.0	42.1
1.1 dB taper	22.6	37.9
3% phase errors + 1.1 dB taper	22.5	34.5
3% amplitude errors + 1.1 dB taper	22.5	34.9
Errors + taper + bandlimitation	22.2	32.6
Errors + taper + bandlimitation + spurious	22.1	30.0
Experimental measurement	22.0	28.0

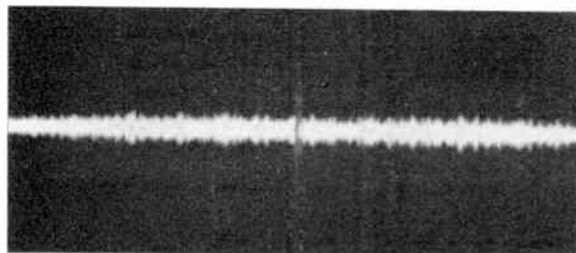
the analysis. Figure 3 shows the observed performance. Displayed is an impulse response with its associated 3% amplitude variations and a small degree of bandlimitation. Also shown is correlation performance for both matched pair operation and for the m-sequence gener-



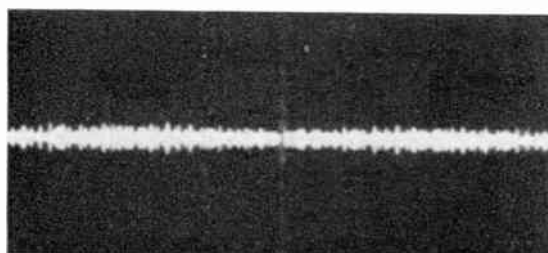
(a) Impulse response (1 $\mu\text{s}/\text{div}$).



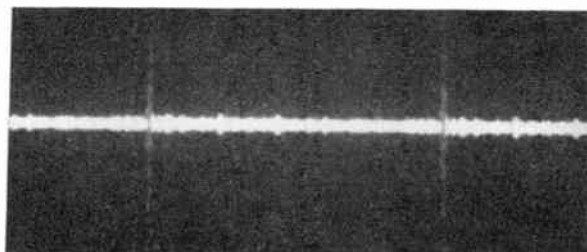
(b) Expanded section of the impulse response (0.25 $\mu\text{s}/\text{div}$).



(c) Matched pair operation (2 $\mu\text{s}/\text{div}$).



(d) Aperiodic active generation (2 $\mu\text{s}/\text{div}$).



(e) Periodic active generation (2 $\mu\text{s}/\text{div}$).

Fig. 3. 127-tap biphase matched filter performances.

ated by a linear feedback shift register arrangement. The lowest photograph illustrates the limited improvement in peak-to-sidelobe levels for periodic operation.

2.4 S.A.W. Programmable P.S.K. Matched Filters

Both the switchable tap^{9, 23, 24} and the convolver^{10, 25, 26} approach to programmability have received attention. However, the implementation of both techniques introduces difficulties with fabrication and system complexity. The authors have recently demonstrated a hybrid 127-tap programmable matched filter suitable for such a system.²⁷ A double-pole, double-throw diode ring switch was used to control the phase of each tap and Fig. 4 shows a schematic of the device arrangement with the tap switching circuit and the correlation performance. Difficulty has been experienced with reliable operation of such hybrid systems, and the more completely integrated systems (aluminium nitride on sapphire for the s.a.w. device, coupled with silicon on sapphire for the switching and data stores,²³ or m.o.s.f.e.t. programmable devices with piezo-resistive taps²⁴) present their own material, fabrication or reliability problems. The increased complexity of programmable

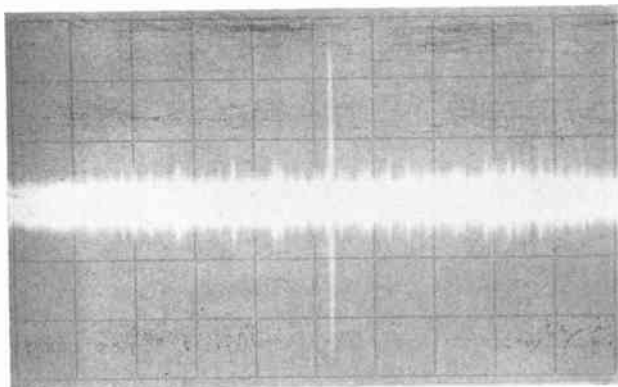
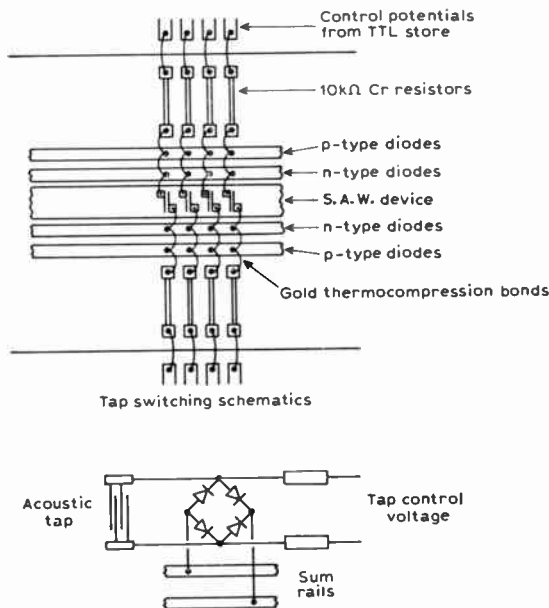


Fig. 4. Programmable biphase s.a.w. matched filters.

approaches is unlikely to produce a reliable and cost-effective technique.

2.5 Large Time Interval S.A.W. Matched Filters

Several techniques have been investigated to achieve large time interval synchronizers. Single devices up to 100 μs are possible²² but substrate size (~20 cm) precludes anything greatly in excess of this and alternative arrangements must be considered. The earliest was a series-parallel processing technique⁷ which made use of a 15-625 μs matched filter and a recirculating integrator to achieve longer integration periods. This provided two orders of magnitude reduction in lock-up time in an 8 MHz code rate system, and used a repeated pseudo-noise sequence with an additional phase coding on the blocks. This is less satisfactory than a non-repeated code because of the susceptibility to an intelligent jammer. The use of a programmable matched filter with a recirculating integrator overcomes this difficulty by resetting the coding in the matched filter after each section of the signal has been correlated.

A cascading method was adopted to increase the attainable matched filter interval. This has been described previously⁸ for a 50 μs system and has now been extended to produce a completely asynchronous 350 μs system.²⁰ While the recirculating arrangements only reduce the lock-up time by the number of taps in the initial matched filter, a cascade of matched filters provides a reduction factor equal to the total number of taps in the system, i.e. the complete s.n.g. available.

The principle of cascading is illustrated in Fig. 5. A transducer is placed appropriately on the s.a.w. substrate in order to transmit the received signal to the

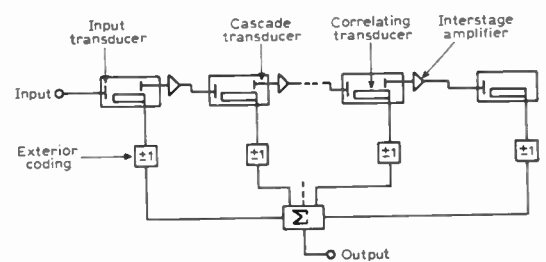


Fig. 5. Schematic of cascading matched filters.

next device and the outputs of the phase-coded transducers on each substrate are summed to provide the matched filter response. Losses introduced by the additional transducers are equalized by the use of wideband amplifiers and the cascade transducers are positioned to allow for the initial delay between the input and phase-coded transducers and delays in the amplifiers and tuning circuits. Fine equalization of the phase of each section is achieved with short lengths of cable where necessary.

It is very important in the application of matched filters for synchronization to analyse the effect of the imperfections mentioned in Section 2.3 on the s.n.g. performance. The authors' work in this area has shown

bandlimiting to be the important factor since the remaining parameters do not have a cumulative effect. This is particularly so in cascading techniques described above where repeated transduction to successive substrates introduces an increasing bandlimiting process. This was analysed for single devices up to 50 μ s duration at 10 MHz chip rates and cascades up to seven stages, again using a delta function model. A full description of the theory can be found in Reference 8 and the results are summarized in Fig. 6. The bandlimiting introduced by one chip transducers for the input and cascade processes has been found not to cause a severe degradation to performance, because the noise is bandlimited

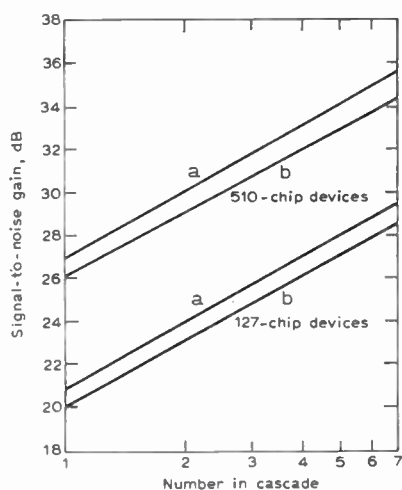


Fig. 6. Theoretical predictions of signal-to-noise gain.
a, Ideal; b, With bandlimiting.

as well. Thus, although the perfect device performance and bandlimited performance lines in Fig. 6 are diverging, this is occurring at a particularly slow rate. Signal-to-noise gains well in excess of 30 dB are therefore possible using this technique.

2.6 350 μ s Cascaded Matched Filter Performance

A 350 μ s matched filter has been constructed using seven 50 μ s sections.²⁰ A schematic of an individual section is shown in Fig. 7. The substrate material was ST quartz. In these devices an in-line tap arrangement

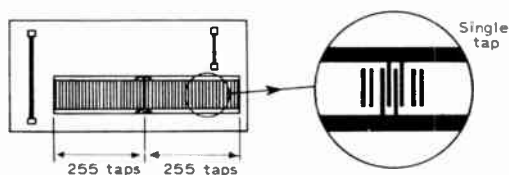


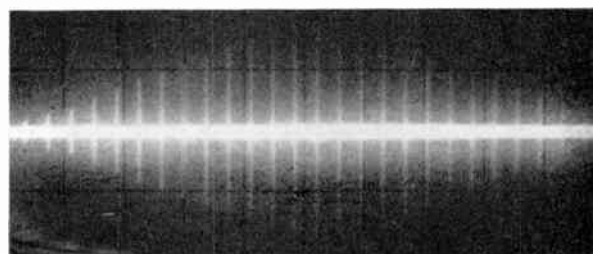
Fig. 7. Schematic of the 50 μ s matched filter.

was used to achieve optimum insertion loss and dummy strips were placed to act as quarter wavelength cancellers of the mass loaded reflection.²⁸ The devices operated at a centre frequency of 72.5 MHz and a chip rate of 10.36 MHz. The 510-chip phase coded structure on each substrate consisted of a 255-chip m-sequence repeated

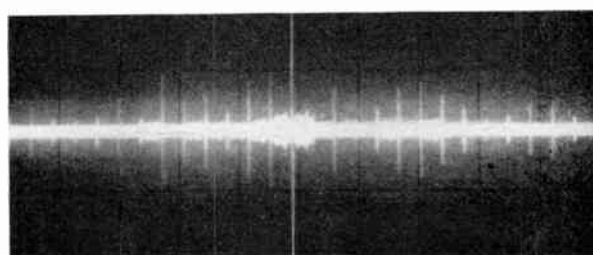
with the aid of alignment crosses, and wire-stitch-bonded in the fabrication process. The input and cascade transducers were one chip long and the phase-coded transducer was terminated at both ends in its characteristic impedance to avoid distortion due to electrical reflections.²⁹ These devices were cascaded as described in Section 2.4 and shown in Fig. 5.

Burst correlation performance is shown in Fig. 8(a) with a 350 μ s input signal made up of a 25 μ s 255-chip m-sequence repeated fourteen times. The sub-correlation peaks, present because of this repeating process, have been reduced below the principal output by applying an exterior coding to the polarities of the individual devices in the cascade. A 14-bit truncated m-sequence was used to allow six of the devices to operate with both 25 μ s sections of the output transducer in phase and only one device with an internal phase reversal, which was realized at the bonding stage of the fabrication process. The correlation performance of this mode is shown in Fig. 8(b) where a central peak-to-sub-peak ratio of 9.1 dB (theoretical 10.9 dB) was achieved. This is sufficient to allow error rate measurements to be made on the system, although it should be noted that in a practical system a non-repetitive code would be used with sidelobes better than 20 dB below the correlation peak. The signal-to-noise gain of the 350 μ s cascade was measured at 34.0 ± 1 dB in close agreement with the theoretical predictions when bandlimiting is included in the analysis (see Fig. 6).

The performance of this system was within 2 dB of the ideal which indicates that the cascading technique can be extended to produce millisecond matched filters. This can be achieved by increasing the number of devices in the cascade and using both faces of the quartz substrate for the phase-coded transducers.¹⁹ In this manner signal-to-noise gains, at 10 MHz code rates, of 40 dB are possible.



(a) Sections uncoded.



(b) Sections coded according to a 14-bit truncated m-sequence (70 μ s/div).

Fig. 8. Burst correlation performance of the 350 μ s cascade.

3 S.A.W. Matched Filters as Demodulators

3.1 Multi-frequency Shift Keyed Systems (M.F.S.K.)

An m.f.s.k. system conveys multi-level input data by transmitting rectangular r.f. pulses at several frequencies, each frequency corresponding to a different input data level. In a four-level system, for example, a burst of a given length at any of four centre frequencies can be transmitted. Conventionally, m.f.s.k. signals are demodulated by the use of quenched resonators.³⁰ These LC circuits are required to be of high Q and are therefore realizable only at relatively low intermediate frequencies (less than 10 MHz). This involves a second down-conversion in some communication links and critical alignment of the circuits is necessary. They are also susceptible to drift and mechanical disturbance. The use of s.a.w. matched filters eliminates most of the difficulties.³¹ They may be operated at the preferred intermediate frequency of 70 MHz and are stable devices requiring little setting up and negligible long-term attention.

The matched filter for a rectangular i.f. burst—a device whose impulse response is a rectangular burst of the same duration and at the same centre frequency as the m.f.s.k. signal—is easily realized using s.a.w. techniques.³² All that is required is a uniform input transducer and an output transducer consisting of a long array of regularly spaced uniform taps (Fig. 9). This arrangement reduces interference from mass loaded reflections and dummy quarter wave cancellers are included to

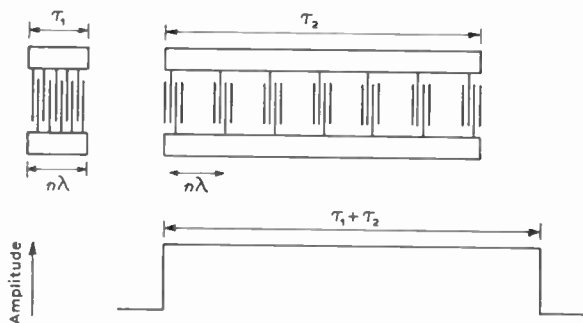


Fig. 9. Schematic of an m.f.s.k. transducer and impulse response.

help further in this respect. On impulsing the n finger pair input transducer an n wavelength burst propagates down the substrate and is detected at each tap in the output transducer. With the number of wavelengths in the input transducer made equal to the spacing of the output taps, the overall response has the rectangular envelope also shown in Fig. 9. Using single finger pair output taps gives an excellent approximation to the desired rectangular envelope.

The frequency response of such a device is of $\sin x/x$ form where

$$x = \pi\tau(f - f_c)$$

and τ is the impulse response duration, with f_c the device centre frequency (determined by the finger periodicity). The nulls of this frequency response falls at frequencies

given by:

$$f_N = \frac{N \pm k}{N} f_c$$

where N is the number of wavelengths in the impulse response and $k = 1, 2, 3, \dots$. Thus, by fitting different integral numbers of wavelengths into filters with impulse responses of the same duration, a family of orthogonal matched filters can be realized. These are precisely the matched filters required for optimum detection of signals in an m.f.s.k. system.³²

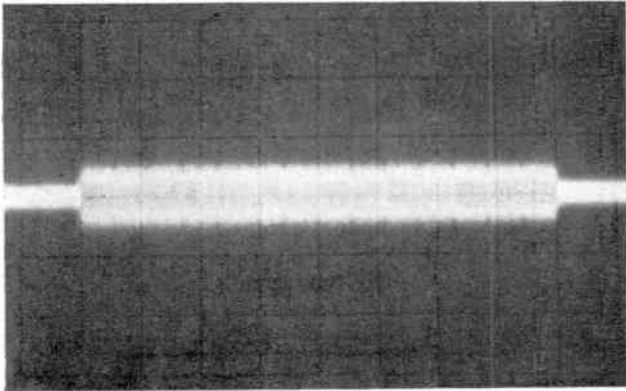
3.2 S.A.W. Matched Filters for a Four Level M.F.S.K. System

A requirement existed for a bank of m.f.s.k. filters with centre frequencies of 70.00, 70.25, 70.50 and 70.75 MHz, with three matched lengths: 4, 12 and 36 μ s. The basic design outlined above was employed: an input transducer having 20 finger pairs, combined with an output transducer having single finger pair taps separated by 20 wavelengths. The 4 μ s filter thus required 14 output taps to achieve a total impulse response length of 280 wavelengths at 70.00 MHz. A result of this 'thinned' structure used to make the device is that the total number of wavelengths in the device cannot be changed arbitrarily. Instead, the devices required to operate at the three other centre frequencies were designed to contain 280 wavelengths at their respective centre frequencies. This caused their matched lengths to deviate by up to 1% from the desired 4 μ s, hence shifting the null positions a few kilohertz from the truly orthogonal positions. Inspection of the $\sin x/x$ curve showed, however, that this would not present any problems. The 12 μ s and 36 μ s filters were designed similarly, with 42 and 126 single finger pair output taps respectively. A 12 μ s glass artwork was used in the mask making process to maintain rigidly the orthogonality of the transducer responses. The mask was designed to allow 4 μ s and 12 μ s devices to be made from this mask and for three 12 μ s sections to be pieced together on the same substrate for the 36 μ s devices. Stable temperature performance was ensured by the use of ST quartz substrates.

3.3 Performance of M.F.S.K. Matched Filters

The impulse response and frequency response of a 70 MHz, 4 μ s f.s.k. filter is shown in Fig. 10. The exponential taper of ~ 0.5 dB, visible on the impulse response, is due to acoustic attenuation. The frequency response shows the characteristic -13 dB sidelobe of the $\sin x/x$ function and deep traps at the expected null frequencies. Orthogonal channel rejection of better than 25 dB was obtained with all four filters. This is shown in Fig. 11 and the time domain responses in Fig. 12 with the correct frequency into channel two.

The 12 μ s and 36 μ s devices exhibited more evident deviation in their frequency responses from the ideal $\sin x/x$ functions. These are shown in Fig. 13 and Fig. 14. The poorer null rejections close to the principal responses do not severely affect the device performance since the adjacent channels in these cases are the third



(a) Impulse response (0.5 μ s/div).

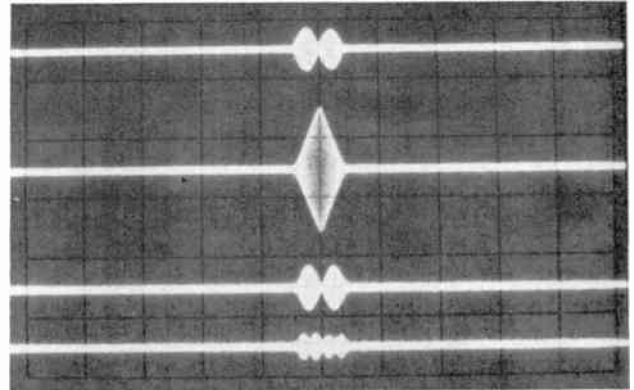
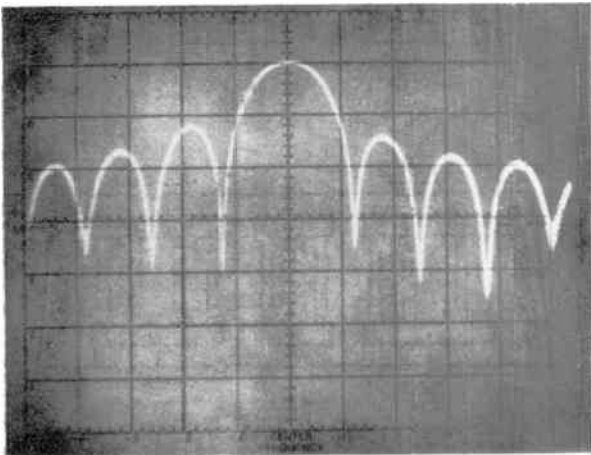


Fig. 12. Time domain responses of the four 4 μ s m.f.s.k. filters with correct frequency injected into channel two (5 μ s/div).



(b) Frequency response (200 kHz/div).

Fig. 10. 4 μ s filter.

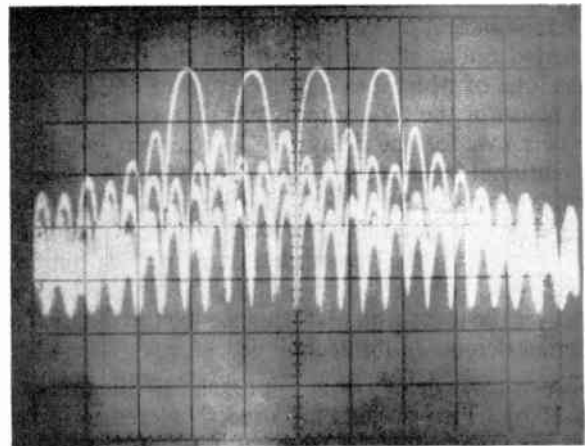


Fig. 13. Superimposed frequency responses for the 12 μ s devices (200 kHz/div).

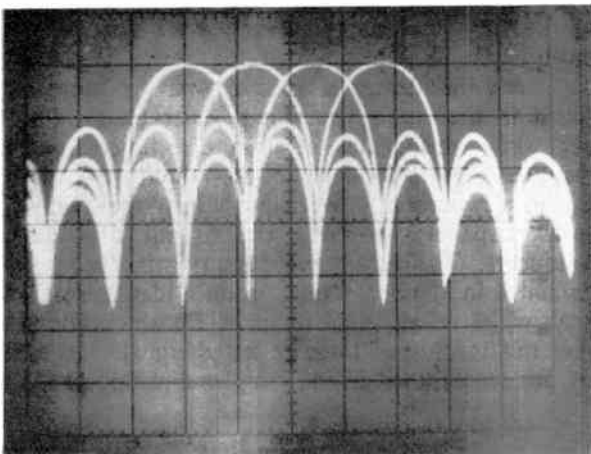


Fig. 11. Frequency responses of the four 4 μ s m.f.s.k. filters superimposed (200 kHz/div).

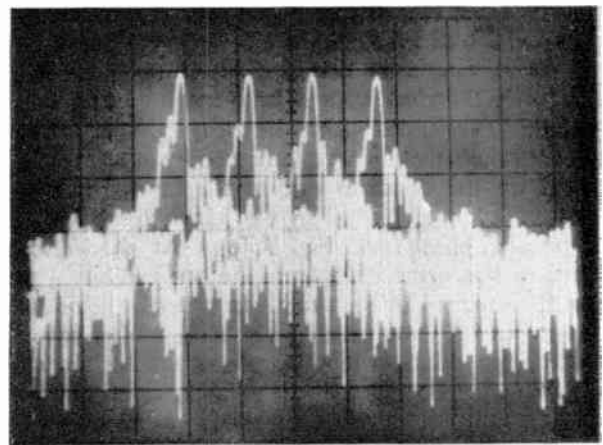


Fig. 14. Superimposed frequency responses for the 36 μ s devices (200 kHz/div).

null of the $\sin x/x$ function for the 12 μ s devices and the ninth one for the 36 μ s devices. Several degrading effects were investigated theoretically³²: piecing accuracy for the 36 μ s devices, tap phase and amplitude errors, electrical propagation effects²⁹ and curvature in the quartz. A combination of the last two was found to be responsible for the amplitude distortion and the filling

in of the nulls. However, better than 25 dB orthogonal channel rejection was achieved on all the devices described. This is adequate for error rate performance within 1 dB of theory,³¹ but the effects of substrate curvature and electrical mismatches require careful consideration whenever the construction of long s.a.w. devices with deep frequency traps is envisaged.

3.4 Differentially Coherent Phase Shift Keyed Systems (D.C.P.S.K.)

D.c.p.s.k. systems transmit a phase-coded carrier and the relative phase of the bits is either 0 or π depending on a baseband data stream. Unlike the p.s.k. modulation described before, the correspondence between the baseband data format and the carrier phase is such that a bit is represented by a phase change. Demodulation of the p.s.k. signal may be by coherent or differentially-coherent detection. Although coherent detection has some theoretical advantage in carrier-to-noise ratio for a given bit error rate, differential detection is preferred in some situations as being easier to implement, and less sensitive to extraneous phase disturbance and traffic content. The latter method has been used, for example, in the 5.9 GHz digital radio system developed by GEC Telecommunications Ltd. for the British Post Office.³³

Demodulation of the differentially phase-coded signal is carried out at the i.f. by splitting the signal into two paths, one of which has a delay equal to one bit length. The phase of the two outputs are then compared. The use of s.a.w. for the delay line has certain merits over conventional techniques: reduced size; bandpass characteristics permit the removal of a filter in the i.f. system; no trimming required. However, surface waves can be used to perform the demodulation, as well as the delay, by using a correlation technique. This method also improves the error rate performance for the differentially coherent demodulation technique.

The s.a.w. delay line approach is illustrated in Fig. 15(a). Two outputs are used staggered in distance from the common input by one bit. These provide the signals for phase comparison. The correlation arrangement is very similar (Fig. 15(b)) except that the two outputs are summed on the substrate. This provides a peak when the two bits to be compared have the same phase and a null when they are of opposite phase. The data are recovered by envelope detection of the signal wave form, followed by a sample-and-hold and a level detector. The improvement in error rate performance for a given signal-to-noise is achieved by using two more outputs on the opposite side of the input transducer. These are again staggered by one bit, but this time are of opposite phase—see Fig. 15(c). At the detection instant in this arrangement one output exhibits a peak when the other is giving a null. In order to demodulate the data stream a comparator is now used, after envelope detection, to decide which output is greater. In effect the system provides a built-in variable threshold level; a state of affairs which will give rise to reduced error rates in a noisy environment.

3.5 Design and Performance of a S.A.W. D.C.P.S.K. Demodulator

The Post Office system mentioned above required a d.c.p.s.k. demodulator at a centre frequency of 70.4 MHz with a bit rate of 6.4 Mb s^{-1} . The temperature specification of the system allowed the use of lithium niobate as the substrate material (temperature coefficient 80 parts in 10^6 per degC) and this enabled a design to be made for the required operating bandwidth without

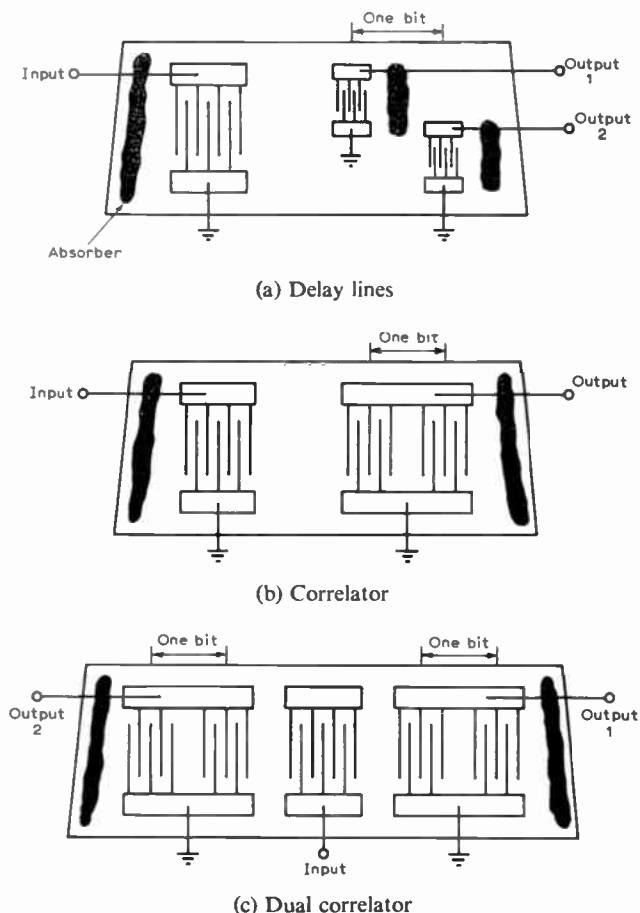


Fig. 15. Surface acoustic wave demodulators.

excessive insertion loss. Good suppression of triple transit signals was achieved using a multi-strip coupler and dummy transducer arrangement for reflection cancelling.³⁴ A schematic of the device is shown in Fig. 16 and the operation is as follows. An input signal applied to the centre transducer generates an acoustic wave which propagates in both directions along the substrate. The multi-strip coupler splits the incident wave into two equal power signals in phase quadrature which propagates towards the output and dummy transducers. The output and dummy transducers, being terminated in identical loads, produce identical reflected signals which return to the coupler. Consideration of the phase relationship of these reflected signals shows that they are recombined in the coupler and appear on the

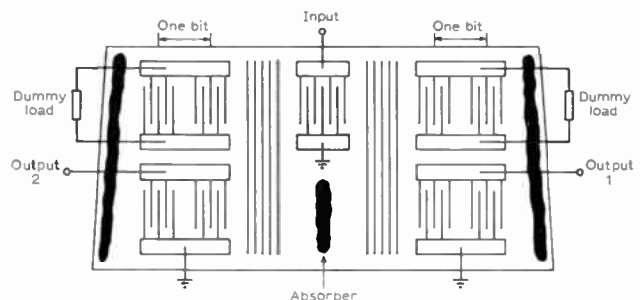
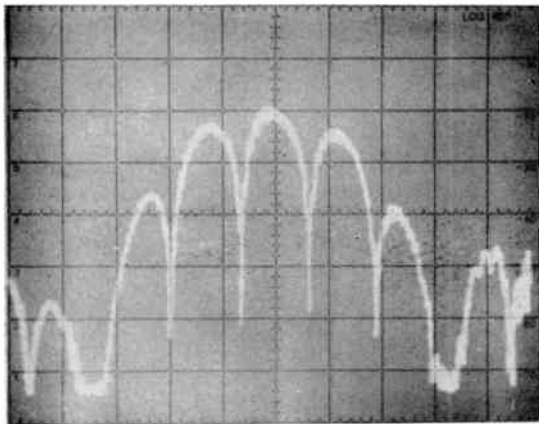


Fig. 16. Schematic of the triple transit suppressed correlating demodulator.

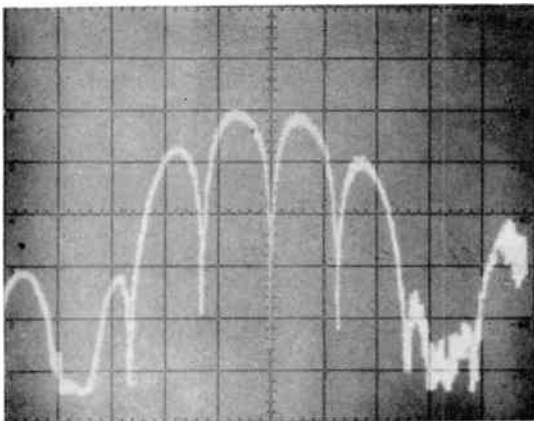
lower track, where they are removed by the absorber. The left and right sections of the device are similar except for the output transducer: one having two in-phase taps separated by a chip, the other having two out-of-phase taps. This design uses to advantage the bi-directionality of the input port.

The frequency responses of the two channels are shown in Fig. 17. The response of the same-phase channel is similar to a $\sin x/x$ function; the other channel exhibits a deep null at the $\sin x/x$ centre frequency. Ripple on the passband is of the order of 0.5 dB peak-peak, which corresponds to the measured triple transit suppression of 30 dB. Outputs from the two channels with a biphasic coded m-sequence input at 70.4 MHz are shown in Fig. 18. The measured peak/null ratio was in excess of 22 dB. Untuned insertion loss was 21 dB in the 75 Ω system: this can be improved to ~ 13 dB by matching.

The error rate performance of this device has been tested by GEC Telecommunications Ltd. They have observed the expected improvement, described above, when demodulation is carried out by comparison of the two envelope detection outputs. The device was more than adequate for the system performance requirements, as well as offering reduced size and complexity. Extension of the s.a.w. d.c.p.s.k. demodulator to much higher



(a) Channel matched to same-phase chip pair.



(b) Channel matched to opposite-phase chip pair.
(5 MHz/horizontal div, 10 dB/vertical div).

Fig. 17. Frequency responses of the two demodulator channels.

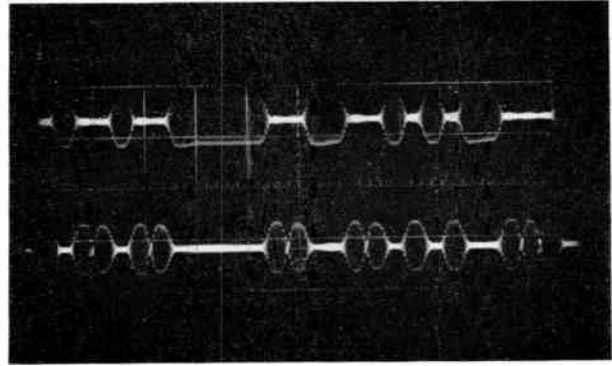


Fig. 18. Outputs from the two-channel correlating demodulator (0.5 μ s/div).

frequencies and bit rates is a straightforward scaling exercise which makes this device particularly attractive for the new experimental systems with intermediate frequencies about 1 GHz.

4 Conclusions

Surface acoustic wave matched filters have been designed, fabricated and tested for use in existing communication links utilizing phase shift keyed and frequency shift keyed waveforms. In each case the use of a s.a.w. device provides substantial improvements in the system performance. Specifically, in spread spectrum phase shift keyed systems, which conventionally employ the serial search receiver for synchronization, s.a.w. matched filters permit a reduction in acquisition time by a factor equal to the time bandwidth product. Cascading of s.a.w. devices provides matched filters up to about a millisecond which covers a large proportion of systems requirements. In those cases where larger integration times are necessary, programmable devices and recirculation techniques may be used to implement matched filters up to several milliseconds.

S.a.w. matched filters in m.f.s.k. systems exhibit several advantages in comparison with the conventional quenched resonator approach. They provide stable, passive operation, and time intervals up to 50 μ s can be easily achieved over the preferred operating frequency range of 10 MHz to 100 MHz. Similarly in d.c.p.s.k. systems there are a number of attractions in demodulators based on s.a.w. matched filters. By combining the outputs from complementary channels the error rate performance of the differentially coherent systems is improved without sacrificing the inherent simplicity permitted by the differential modulation format. The device is passive and considerably smaller than alternative techniques and, in addition, it is applicable to carrier frequencies up to the low gigahertz region.

These examples reveal that s.a.w. matched filters have an important role to play in the development of modern communication systems.

5 Acknowledgment

Part of this work has been carried out with the support of Procurement Executive, Ministry of Defence, sponsored by DCVD.

6 References

1. Jones, W. S., Hartmann, C. S. and Claiborne, L. T., 'Evaluation of digitally coded acoustic surface wave matched filters', *IEEE Trans. on Sonics and Ultrasonics*, SU-18, pp. 21-27, 1971.
2. Collins, J. H. and Grant, P. M., 'The role of surface acoustic wave technology in communication systems', *Ultrasonics*, 10, pp. 59-71, 1972.
3. Williams, R. C. and Smith, H. I., 'Large time bandwidth product surface pulse compression employing reflective gratings', *Electronics Letters*, 8, No. 16, pp. 401-2, 10th August 1972.
4. Fisher, T. S., Patterson, E. and Scotter, D. G., 'Surface wave correlator with inclined transducer', *Electronics Letters*, 9, No. 3, p. 55, 8th February 1973.
5. Maines, J. D. and Johnson, J. N., 'Surface wave devices and applications—2. Pulse compression systems', *Ultrasonics*, 11, pp. 211-7, 1973.
6. Setrin, M., Bell (Jr.), D. T., Schultz, M. B. and Unkauf, M. G., 'An iff system using block programmable surface wave signal expander and compressor', Proceedings IEEE Ultrasonics Symposium, pp. 316-23, 1973.
7. Hunsinger, B. J., 'Surface wave devices in spread spectrum processors', *Ultrasonics*, 11, pp. 254-62, 1973.
8. Lever, K. V., Patterson, E. and Wilson, I. M., 'Cascaded m-sequence saw correlators', Proceedings IEEE Ultrasonics Symposium, pp. 390-2, 1974.
9. Collins, J. H. and Grant, P. M., 'Large time bandwidth product programmable saw psk matched filter module', Proceedings IEEE Ultrasonics Symposium, pp. 382-5, 1974.
10. Hannah, J. M. and Morgan, D., 'Correlation of long sequences by a surface-acoustic-wave convolver, with application to spread-spectrum communication', *Electronics Letters*, 11, No. 9, pp. 193-5, 1st May 1975.
11. *IEEE Trans. on Microwave Theory and Techniques*, MTT-17, No. 11, November 1969.
12. *IEEE Trans. on Microwave Theory and Techniques*, MTT-21, No. 4, April 1973.
13. Proceedings of IEE Conference on 'Component Performance and Systems Applications of Surface Acoustic Wave Devices', Aviemore, Scotland, 1973.
14. Maines, J. D., 'Surface acoustic wave devices: past successes and future prospects', Proceedings IEEE Ultrasonics Symposium, pp. 136-47, 1974.
15. Paige, E. G. S., 'Dispersive filters: their design and application to pulse compressions and temporal transformations', Ref. 13, pp. 167-80.
16. Jones, W. S., Kempf, R. A. and Hartmann, C. S., 'Practical surface wave linear f.m. correlators for modern radar systems', *Microwave Journal*, 15, pp. 43-86, 1972.
17. Lever, K. V., Patterson, E. and Wilson, I. M., 'Analysis of the effects of fabrication errors on performance of surface acoustic wave m-sequence correlators', *Proc. Instn Elect. Engrs*, 22, No. 12, pp. 1333-8, 1975.
18. Bell, D. T., Holmes, J. D. and Ridings, R. V., 'Application of acoustic surface wave technology to spread spectrum communications', *IEEE Trans. on Microwave Theory and Techniques*, MTT-21, No. 4, pp. 263-71, 1973.
19. Carr, P. H., DeVito, P. A. and Szabo, T. L., 'The effect of temperature and Doppler shift on the performance of elastic surface wave encoders and decoders', *IEEE Trans. on Sonics and Ultrasonics*, SU-19, No. 3, pp. 357-67, 1972.
20. Lever, K. V., Patterson, E., Stevens, P. C. and Wilson, I. M., 'S.a.w. 350 μ s binary phase shift keyed matched filter', *Electronics Letters*, 12, No. 5, pp. 116-7, 4th March 1976.
21. Lever, K. V. and Patterson, E., 'VX28004 SAW Biphase Coded Correlators', Hirst Research Centre Memorandum No. CVD 73, 1975.
22. LaRosa, R. and Vasile, C. F., '1000-bit surface-wave matched filter', *Electronics Letters*, 8, No. 19, pp. 479-80, 21st September 1972.
23. Hagon, P. J., 'Programmable analogue matched filters', Ref. 13, pp. 92-101.
24. Staples, E. J. and Claiborne, L. T., 'A review of device technology for programmable surface wave filters', *IEEE Trans. on Microwave Theory and Techniques*, MTT-21, No. 4, pp. 279-87, 1973.
25. Cafarella, J. H., Bers, A. and Stern, E., 'Surface acousto-electric correlators with surface state memory', Proceedings IEEE Ultrasonics Symposium, pp. 216-9, 1974.
26. Reeder, T. M., 'Electrically programmable convolution and correlation using nonlinear delay line filters', Ref. 13, pp. 73-84.
27. Patterson, E. and Wilson, I. M., 'CVD Research Project RP28-3. Integrated Surface Wave Devices. Final Report', Hirst Research Centre, Report No. 16, 108C, October 1974.
28. Lewis, M. F., 'The surface acoustic wave oscillator—a natural and timely development of the quartz crystal oscillator', Proc. 28th Annual Symposium on Frequency Control, Atlantic City, pp. 304-14, 1974.
29. Heighway, T. and Thompson, A., 'SAW devices and their possible implications for novel radar systems design', Ref. 13, pp. 212-21.
30. Robin, H. K., Bayley, D., Murray, T. L. and Ralphs, J. D., 'Multitone signalling system employing quenched resonators for use on noisy radio-teleprinter circuits', *Proc. Instn Elect. Engrs*, 110, No. 9, pp. 1554-68, 1963.
31. Lever, K. V., Patterson, E., Scotter, D. G. and Feasey, B. G., 'Assessment and performance of matched filters for mfsk communications', Ref. 13, pp. 329-32.
32. Lever, K. V., Patterson, E., Stevens, P. C. and Wilson, I. M., 'Surface acoustic wave matched filters for multi-frequency shift keyed communication systems', submitted to *Proc. IEE*.
33. Doe, E. S., 'A digital radio-relay system', *Post Office Elect. Engrs J.*, 65, Part 3, pp. 160-4, 1972.
34. Marshall, F. G., 'New technique for the suppression of triple-transit signals in surface acoustic wave delay lines', *Electronics Letters*, 8, No. 12, pp. 311-2, 15th June 1972.

*Manuscript first received by the Institution on 24th February 1976
and in final form on 29th March 1976. (Paper No. 1717/CC 253.)*

© The Institution of Electronic and Radio Engineers, 1976

Sources of intermodulation in diode-ring mixers

H. P. WALKER, B.A., M.Sc.*

SUMMARY

Intermodulation is known to arise in diode-ring mixers due to non-linearity in the diode switches, and also due to the interference by signal voltages with the local-oscillator switching function. This interference can be reduced by ensuring fast switching with a square-wave local-oscillator. In this paper the relationship between rise-time and intermodulation is investigated in connection with a practical mixer design for use at v.h.f.

* Hewlett Packard Limited, Research and Development Department, South Queensferry, West Lothian, EH30 9TG Scotland.

1 Introduction

Diode-ring modulators have been used for many years in telephone carrier systems and more recently in communications receivers and instruments. The sources of distortion in diode mixers have been studied in several papers and have been identified as firstly current-overload,^{1, 2} due to the exponential characteristic of the forward-biased diode and proportional to the ratio of signal to local-oscillator current, and secondly voltage overload,^{3, 4} due to phase modulation of the switching function in a commutating mixer by the influence of input signal voltage on the instant of switching.

The second effect results from finite commutation time in the diode ring. If the switching could take place instantaneously there would be no possibility of phase modulation. In the case of a sinewave local oscillator, this source of distortion can be minimized by increasing the local oscillator voltage so that the transition time is reduced.

Now that high-speed transistors are available giving sub-nanosecond rise and fall times, it is interesting to investigate the advantages of a square-wave local oscillator in diode-ring modulators. The ideal case has been investigated by Gardiner,⁵ and Poultney⁶ reports an improvement in a practical mixer of over 40 dB in third-order intermodulation products when changing from a sinewave to a square-wave local oscillator having a rise-time of 300 ps.

The purpose of the present paper is to review the sources of intermodulation and to present a theoretical basis for predicting the effect of non-ideal switching in a high-frequency mixer operating at v.h.f. in the region 50–100 MHz. Finally a practical design is described in relation to the preceding theory.

2 Equivalent Circuit of Ring Modulator

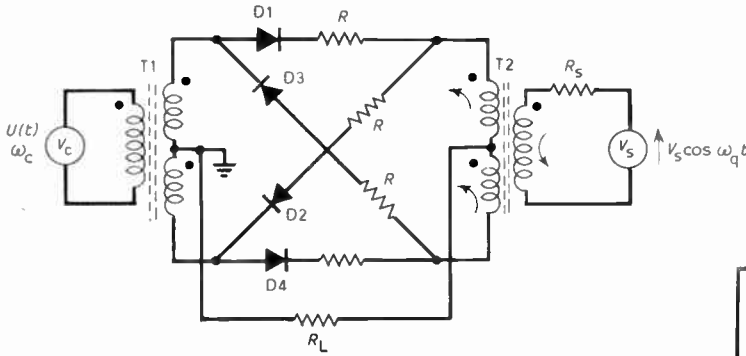
The ring mixer of Fig. 1(a) can be represented by the equivalent circuit of Fig. 1(b). The switching is represented by the function $U(t)$,

$$U(t) = \frac{1}{2} + \frac{2}{\pi} \sum_{n=1}^{\infty} \frac{\sin(2n-1)\omega_c t}{(2n-1)} \quad (1)$$

and the diodes by the ideal switches in series with a resistance r which will be assumed constant for the present analysis. The resistance of reverse bias diodes is represented by r_b shunting the ideal switch.

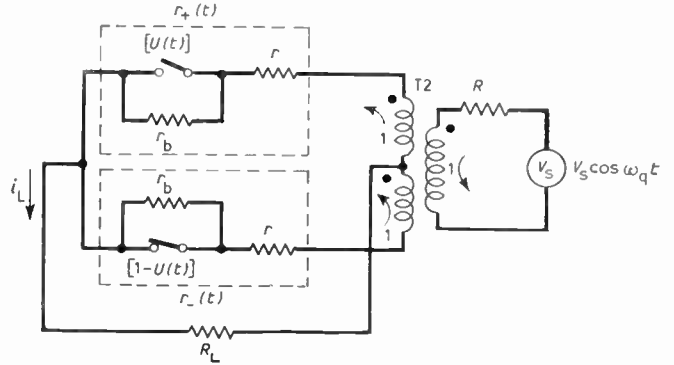
On the positive half-cycle of the carrier, D1 and D2 conduct and the i.f. currents flowing in T2 appear as a common-mode signal across the balanced windings of T1 and so are shunted to the centre-tap, assuming tight coupling of the windings. Thus the i.f. circuit is closed through the load impedance Z_L as in the equivalent circuit. Similarly D3 and D4 conduct on the negative half-cycle.

The equivalent switches in Fig. 1(b) therefore represent two diode branches in parallel, the value of r_b being equal to half the diode reverse resistance and resistor r half the sum of the linearizing resistor R and the forward diode resistance r_f .



(a) Diode-ring modulator.

Fig. 1.



(b) Equivalent circuit of double-balanced mixer of (a).

3 Analysis of Balanced Mixer

Referring to Fig. 1(b), and representing the lossy diode switches by the time-varying resistors:

$$r_+(t) = r + r_b U(t)$$

$$r_-(t) = r + r_b(1 - U(t))$$

where

$$r = \frac{(r_f + R)}{2}$$

Assuming a 1 : 1 : 1 transformer

$$i_L = V_s \cos \omega_q t \left[\frac{1}{R_s + R_L + r_+(t)} - \frac{1}{R_s + R_L + r_-(t)} \right]$$

after substitution for $r_+(t)$ and $r_-(t)$ and simplification

$$i_L = \frac{V_s \cos \omega_q t}{R_s + R_L} [1 - 2U(t)] \times \left[\frac{1}{1 + \frac{R_s + R_L}{r_b} + \frac{r}{R_s + R_L} + \frac{2r}{r_b} + \frac{r^2}{r_b(R_s + R_L)}} \right]$$

where L = loss due to non-ideal switches:

$$i_L|_{\omega = \omega_q - \omega_c} = \frac{2}{\pi} \frac{1}{(R_s + R_L)} V_s \sin(\omega_q - \omega_c)t \left[\frac{1}{L} \right]$$

$$\text{insertion loss} = \frac{\text{max. available input power}}{\text{load power of wanted sideband}}$$

$$= \frac{V_s^2/4R_s}{V_s^2 \frac{4}{\pi^2} \frac{R_L}{(R_s + R_L)^2} \frac{1}{L^2}}$$

$$= 10 \log_{10} \left[\frac{\pi^2 (R_s + R_L)^2}{16 R_s R_L} \right] + 20 \log_{10} [L] \text{ dB}$$

When $R_s = R_L = R_0$

insertion loss = 3.92 +

$$+ 20 \log_{10} \left[1 + \frac{2R_0}{r_b} + \frac{r}{2R_0} + \frac{2r}{r_b} + \frac{r^2}{2R_0 r_b} \right] \text{ dB} \quad (2)$$

If $r_b \gg R_0$ and r , then

$$\text{insertion loss} = 3.92 + 20 \log_{10} \left[1 + \frac{r}{2R_0} \right] \text{ dB} \quad (3)$$

and

$$Z_{in} = (R_L + r) \quad (4)$$

The additional loss due to included 'linearizing' resistors in the diode bridge, can therefore be calculated from equation (3). The fixed loss of 3.92 dB is the fundamental loss of a commutating mixer operating with resistive source and load impedances and results from power dissipated in sidebands at harmonics of the carrier frequency, ω_c , in addition to the unwanted fundamental sideband.

By reflecting this power with respectively short and open circuits at the input and output of the modulator, the unwanted products can be remodulated and then appear at the wanted sideband frequency. When correctly matched this is known as the 'zero-loss' mixer.⁷

In the absence of linearizing resistors, the insertion loss of a practical ring-mixer using hot carrier diodes and working between 50 Ω impedances is 5.8–6.0 dB, the additional loss occurring in the diodes and transformers.

4 Intermodulation

In the ideal modulator, analysed in the previous Section, the input signal is translated to a new centre-frequency without impairing the contained information. In practice distortion of the signal occurs during translation, due to non-linearity in the switching element and due to phase modulation of the carrier signal⁴ resulting from imperfect switching.

In order to quantify this non-linearity, it is usual to apply two closely spaced sinusoidal signals, f_1 and f_2 , and measure the level of intermodulation and harmonic products. These products will be of the form⁴ $f_c \pm (nf_1 \pm mf_2)$, and will be either even-order products when $(m \pm n)$ is even, or odd when $(n \pm m)$ is odd. In normal use where relatively low levels of intermodulation are expected, it is only necessary to consider second- and third-order products of the form

$f_c \pm (f_1 \pm f_2)$, $f_c \pm (2f_1 \mp f_2)$, $f_c \pm (2f_2 \mp f_1)$. In receiver design, the third-order products $f_c \pm (2f_2 - f_1)$ and $f_c \pm (2f_1 - f_2)$ are the most serious since they lie close to the wanted signals and could fall within the i.f. bandwidth.

The intermodulation performance of the mixer is usually measured in terms of the third-order intercept which is the imaginary intersection of the output power (10 dB/10 dB) and third-order intermodulation product power (30 dB/10 dB) plotted against the input power.⁹ The intermodulation level for any input power can then be calculated using the equation:

$$P_{13} = 3(TOI - P_{in}) \text{ dBm} \quad (5)$$

In common with other push-pull circuits, the balanced mixer should cancel even-order distortion products but in practice the degree of suppression will be dependent on the balance. In the following Sections, the measures for improving the balance will be described, and the sources of third-order distortion will be analysed for the double balanced ring modulator.

4.1 Balance of Even-order Products

Even-order products, like the odd-order products, arise due to device non-linearity and imperfect switching, but as is well known^{1, 4, 8, 9} cancellation occurs in the balanced circuit. This can be seen, for example, in the analysis of diode non-linearity derived in Appendix 1 and discussed in the next Section. Measures to reduce odd-order distortion will also reduce even-order products provided the balance is undisturbed.

Full suppression of all even-order products is not possible in a practical circuit due to imbalance in the transformers and mismatching of the diodes. The balance can be improved by using a matched quad of hot-carrier diodes and precision resistors in the ring. At v.h.f., the transformer design is quite critical and usually transmission line transformers are used comprising several turns of tightly twisted bifilar or trifilar wire on a ferrite toroid. The trifilar winding ensures tight coupling and a balance of 40–50 dB can be achieved in a centre-tapped section. The design of these transformers is described in Ref. 10.

The inputs of T1 and T2 in Fig. 1(a) are fed directly from an unbalanced source with one side earthed. This causes a capacitive unbalance in the secondary winding, but can be overcome by connecting unbalanced-to-balanced transformers (baluns)¹⁰ to the inputs.

Attempts to provide adjustment of the balance by means of potentiometers or trimmers have not been successful at high frequencies, and best results have been obtained by keeping the mixer structure as simple as possible with a symmetrical layout and short printed circuit tracks. This also improves the switching speed which as shown in Section 4.3 is a major factor in determining the mixer performance.

4.2 Non-linearity of the Switching Element

Even if the switching action of the modulator were perfect and represented by equation (1), distortion would still arise due to the variation of diode slope

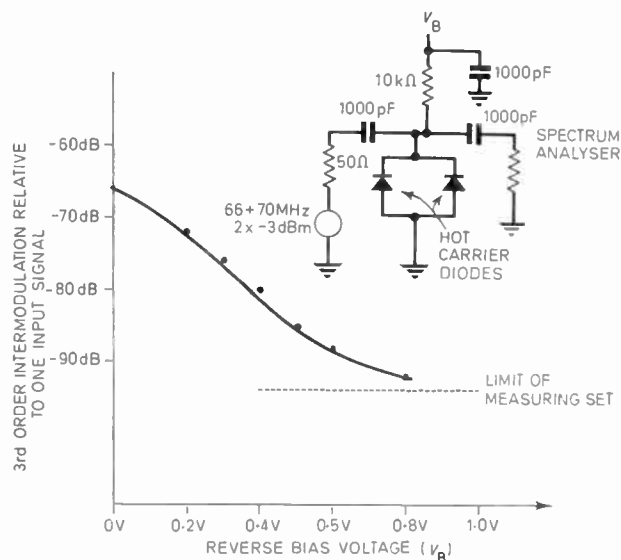


Fig. 2. Intermodulation distortion in reverse-biased diodes.

resistance with applied voltage. The effect of device non-linearity has been discussed in a paper by Christiansen¹ where it is shown that minimum distortion is obtained when contributions from forward and reverse biased diodes are equal. It is assumed that perfect switching could be achieved, and the practical results relate to an audio-frequency modulator where ideal square-wave switching is feasible.

The source of distortion in reverse-biased hot-carrier diodes is due mainly to the voltage-dependent reverse capacitance (provided the signal voltage is insufficient to forward-bias the diode) and so will only become important at high frequencies and small reverse bias. The level of this distortion will depend on the doping-profile of the diode junction. For the diodes used and at the frequencies of interest, approximately 70 MHz, the relationship between third-order intermodulation and reverse bias voltage was measured and is shown in Fig. 2.

The non-linearity in the forward direction^{2, 11} can be determined by considering the equivalent signal circuit (Fig. 3), during a half-cycle of the carrier. The instantaneous voltages across the diodes can be calculated using the diode equation:¹²

$$V_f \approx \frac{kT}{q} \ln \left[\frac{I_f}{I_s} \right] \quad (6)$$

and hence, as shown in Appendix 1, the two-tone third-order intermodulation intercept is given by

$$10 \log_{10} \left[\frac{2(R_s + R_L + R/2)^3}{R_s} \frac{8q}{kT} I^3 \times 10^3 \right] \text{ dBm} \quad (7)$$

where R = linearizing resistor in bridge,

I = peak current of carrier square wave.

It can be seen that the intercept is proportional to the cube of the carrier current and so as the carrier level is increased this source of distortion rapidly becomes negligible, e.g. in a 50 Ω system at $I = 20$ mA, the third-order intercept is 47 dBm.

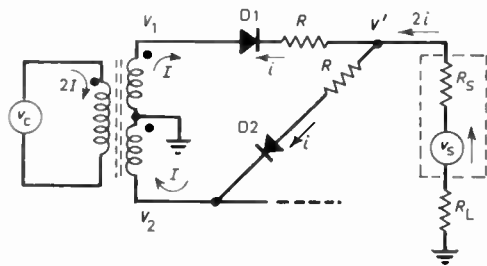


Fig. 3. Equivalent signal circuit during half-cycle of carrier.

In Fig. 4, the predicted and measured values of third-order intercept are plotted against forward current. The above calculations assume ideal square wave switching so that the diodes can be considered in either the fully 'on' or fully 'off' states and a 'quasi-static' equivalent circuit can be used. A sinewave local oscillator drive would involve much more complex analysis.¹³

4.3 Phase Modulation of the Switching Function

The phase modulation of the carrier switching-function by signal voltages and currents is a fundamental characteristic of switching modulators using ideal bi-linear devices controlled by applied voltages. The effect in the case of a sinusoidal carrier has been analysed in several papers^{3, 14, 15} and the level of intermodulation calculated in terms of the ratio, k , of applied signal voltage to carrier voltage. The instant of switching, determined by the zero-volt condition across the ideal switch, is modulated at a rate equal to the difference frequency of local oscillator and input signals, the depth of modulation being determined by the ratio k . It is shown¹⁵ that the relative level of a third-order intermodulation product to wanted sideband is approximately

$$20 \log_{10} \left[\frac{k^2}{8} \right] \text{ dB} \quad (8)$$

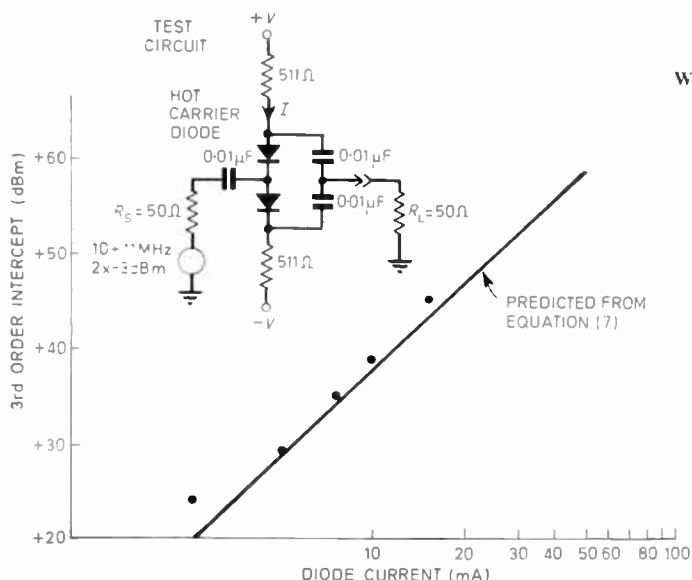


Fig. 4. Third-order intercept versus forward current.

Gardiner,¹⁴ by using a more accurate representation of the diode switch to include the forward voltage as an offset, has identified two voltage overload conditions:

- (a) When the sum of input signals is less than the diode offset voltage so the phase modulation occurs at a point when all the diodes are non-conducting and the full open-circuit carrier voltage is present.

$$k = \left[\frac{V_s}{V_c} \right]$$

- (b) Once the diodes have started to conduct, the forward voltage of the conducting diodes will then determine the reverse bias voltage on remaining diodes, and hence the maximum signal voltage beyond which the second overload condition will apply once reverse-biased diodes are turned on. The second overload point can be raised by including a bias network of parallel resistor and capacitor in series with each diode to enhance the offset voltage.

At normal working levels, the source of distortion is limited to the first overload condition and could be eliminated completely with ideal square-wave switching. The case of ideal switching is considered in a later paper by Gardiner.⁵

At high frequencies, ideal square-wave switching is not possible due to the limitations of switching speed in practical devices. The effect of a signal voltage V_s superimposed on the carrier voltage V_c of finite rise and fall times is phase modulation of the switching function as shown in Fig. 5 and analysed in Appendix 2. The relative level of two-tone third-order intermodulation products is given by:

$$20 \log_{10} \left[\frac{(t_r \omega_{LO} \frac{V_s}{V_c})^2}{8} \right] \text{ dB} \quad (9)$$

and the third-order intercept defined in terms of the total input power given by

$$10 \log_{10} \left[\frac{2 \times 10^3 V_c^2}{t_r^2 \omega_{LO}^2 R_s} \right] \text{ dBm} \quad (10)$$

where V_c = peak-to-peak carrier voltage appearing across one arm of the bridge,

V_s = peak voltage of each input signal,

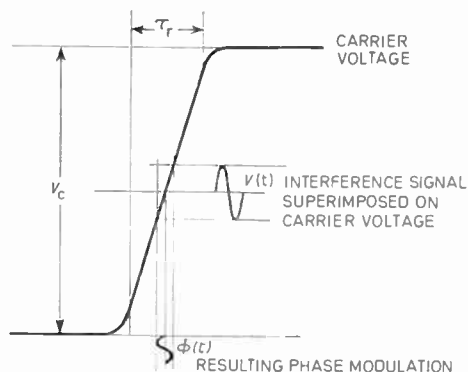


Fig. 5. Phase modulation of the switching function.

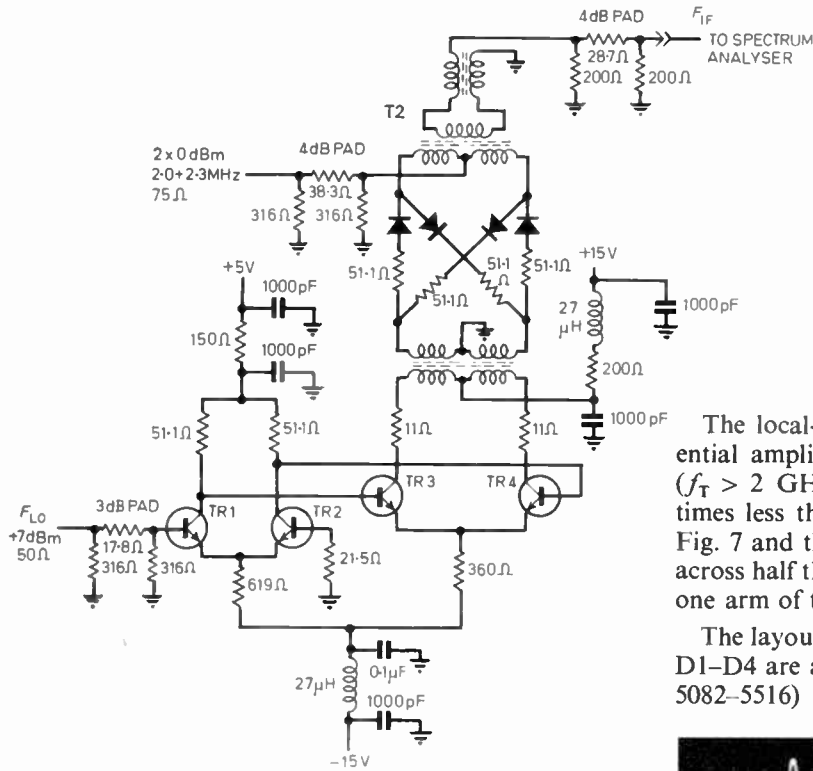


Fig. 6. High-frequency mixer.

The local-oscillator signal is processed by two differential amplifiers using high-speed switching transistors ($f_T > 2$ GHz) to give a square wave of rise and fall times less than 1 ns. A typical waveform is shown in Fig. 7 and this voltage of 2.5 V peak-to-peak appears across half the secondary winding of T1 and hence across one arm of the bridge.

The layout of the practical circuit is depicted in Fig. 8. D1-D4 are a matched quad of hot-carrier diodes (HPA 5082-5516) and the included 51 Ω linearizing resistors

- R_s = source impedance,
- t_r = rise- and fall-time,
- ω_{LO} = local oscillator frequency.

The terms in equation (9) show that the distortion level is related to the signal voltage and not to the signal power, so the linearity could be improved by reducing the source impedance, as is also indicated by equation (10). It can be seen also, from equation (9), that for a given ratio of carrier-to-signal voltage, the product of local-oscillator frequency and rise-time determines the level of intermodulation, faster rise-time being required at higher frequencies. For a fixed rise-time, the relative level of intermodulation products will rise at 12 dB/octave of local oscillator frequency.

5 Practical Mixer Circuit

The circuit of the input mixer design for an instrumentation receiver† is shown in Fig. 6. The input frequency band, 10 kHz to 25 MHz, is applied to the centre tap of T2, and the local oscillator covers the frequency range 61.2 to 86.1 MHz giving a first intermediate frequency of 61.1 MHz. Because of the wide bandwidth required at the input of the mixer and the required insertion loss flatness of approximately 0.1 dB, broad-band resistive terminations are used although this causes higher insertion loss than would be obtained with tuned terminations.^{7, 16} Also the insertion loss can be reduced by shunting the linearizing resistors with capacitors,^{9, 14} but this was also found to affect the flatness adversely.

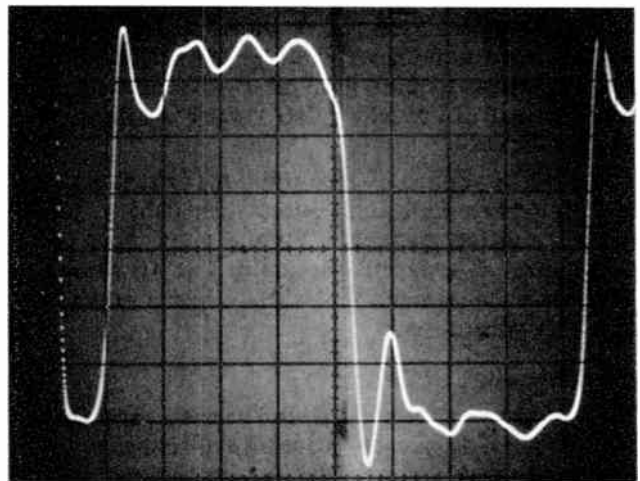


Fig. 7. Local oscillator waveform.

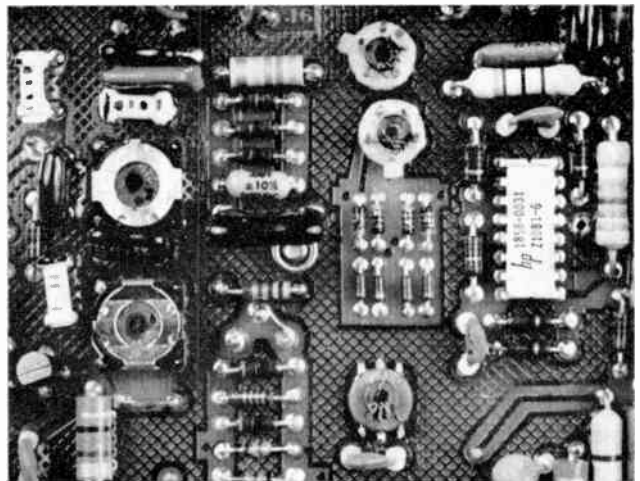


Fig. 8. Practical mixer layout.

† Hewlett Packard 3745A Selective Level Measuring Set.

are miniature 1% tolerance components. Hot-carrier diodes are capable of switching in fractions of a nano-second due to the absence of charge-storage effects,¹² and so will operate entirely under the control of applied voltages at the switching speeds of the local oscillator drive.

The load impedance presented by the 61.1 MHz i.f. amplifier is a broadband 50 ohms termination and thus, with linearizing resistors of 51 ohms, the input impedance, defined by equation (4), is approximately 75 ohms, and the insertion loss 8–9 dB. The carrier leak at the i.f. output is approximately –25 dBm.

5.1 Measurements

To check the theory of Section 4.3, intermodulation measurements were made for different rise- and fall-times controlled by connecting capacitors between the collectors of TR3 and TR4. The peak-to-peak voltage swing appearing across a diode branch is approximately 2.5 V. Predicted and measured results are shown in Fig. 9 and demonstrate reasonable agreement. The dip in the plot for $t_r = 1$ ns is probably due to cancellation caused by other effects at this relatively low intermodulation level.

The current being switched in the diode ring is 30–35 mA, which, from Fig. 4, would give an intercept, due to diode non-linearity, of greater than 55 dBm (and an intermodulation level of < –100 dB at the test levels), so one can conclude that voltage overload is the dominant effect.

This can be verified by measuring the intermodulation level for various input and output impedances, defined by minimum loss pads, and for the same input power to the mixer. The results plotted in Fig. 10 show that the higher voltages associated with the higher impedances cause more distortion.

5.2 Discussion of Results

It is evident therefore that, for a given rise-time and local oscillator frequency, reducing the source and load impedance would improve the linearity by reducing the signal voltage as indicated by equations (9) and (10). Alternatively the carrier voltage V_c could be increased either by increasing the included linearizing resistors in the bridge or by raising the local oscillator drive current.

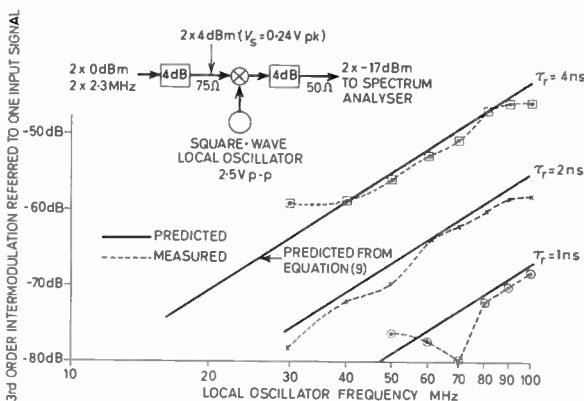


Fig. 9. Predicted and experimental results for effect of finite rise-time in local oscillators.

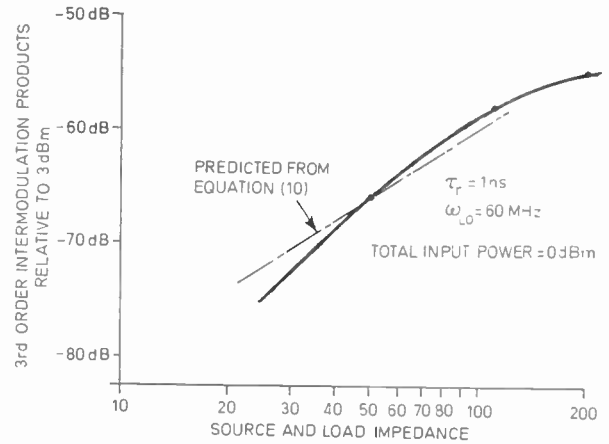


Fig. 10. Intermodulation level versus source and load impedance for a fixed power level.

Unfortunately, reducing the impedance level or increasing the linearizing resistors also increases the insertion loss defined by equation (3) and so would reduce the advantage of improved linearity since a higher input signal level would be required for the same signal/noise ratio at the output of the mixer. In order to estimate the true improvement in linearity the third-order intercept should be defined in terms of the total output power by subtracting equation (3) from equation (10).

$$\text{output intercept} = 10 \log_{10} \left[\frac{2 \times 10^3 (V_f + I_c R)^2}{t_r^2 \omega_{LO}^2 R_s} \right] - 3.92 - 20 \log_{10} \left[1 + \frac{R}{4R_0} \right] \quad (11)$$

where $V_c = V_f + I_c R$

and $V_f =$ diode forward voltage ≈ 1 V,

$I_c =$ peak-to-peak local oscillator current in one arm of bridge.

for large R , when $I_c R \gg V_f$.

Output intercept approximates to

$$10 \log_{10} \left[\frac{2 \times 10^3 I_c^2 R_0}{t_r^2 \omega_{LO}^2} \right] - 3.92 - 20 \log_{10} \left[\frac{R_0}{R} + \frac{1}{4} \right] \text{ dBm} \quad (12)$$

which for $R \rightarrow \infty$ gives

$$10 \log_{10} \left[\frac{2 \times 10^3 I_c^2 R_s}{t_r^2 \omega_{LO}^2} \right] + 8 \text{ dBm} \quad (13)$$

The calculated values of input and output third-order intercept and mixer insertion-loss are plotted in Fig. 11 for a set of typical parameters and a range of linearizing resistors. The results indicate a true improvement in dynamic range, in terms of the output intercept, by inclusion of linearizing resistors provided sufficient input signal power can be supplied by a preceding amplifier.

In practice it is often desirable to minimize the insertion loss of the mixer so it is preferable to increase the local oscillator voltage V_c by an increase in current drive rather than larger included resistance. Furthermore,

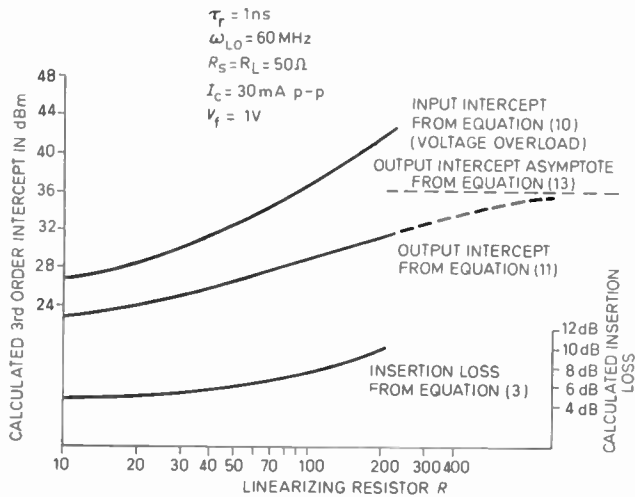


Fig. 11. Variation of third-order intercept and insertion loss with linearizing resistors.

due to stray capacitance, higher resistance could also result in a poorer rise- and fall-time which would correspondingly affect the intermodulation level.

6 Conclusion

It has been shown that for a practical diode-ring mixer working at v.h.f. that the major source of distortion is due to voltage overload resulting from finite switching time. The effect can be reduced by speeding up the local-oscillator transitions or by increasing the local-oscillator drive.

The same results could, of course, be achieved by supplying a sufficiently large sinusoidal carrier signal, but the particular advantage of the square-wave drive is that high performance can be achieved at much lower local-oscillator power. In Appendix 3 it is shown that, for the same transition time in the vicinity of diode switching, the ratio of sinewave to square-wave power would be

$$\frac{2}{(t_r \omega_{LO})^2}$$

which for a rise time of 1 ns at a carrier frequency of 60 MHz would mean about 15 times the square-wave power. The ratio of peak-to-peak voltages is

$$\frac{2}{(t_r \omega_{LO})}$$

With modern switching transistors it is relatively easy to achieve rise- and fall-times of 1–2 ns and the use of a non-saturating differential amplifier for limiting and supplying the local-oscillator power is more efficient than a linear amplifier supplying a sinewave drive.

The effect of diode non-linearities in a practical high-level mixer is not significant except at much lower frequencies.

7 Acknowledgments

The author wishes to thank Hewlett Packard Limited for permission to publish this paper.

8 References

- Christiansen, L., 'Über der kubischen Verzerrungen am Ringmodulator', *Frequenz*, 5, No. 11/12, pp. 298–303, 1951.
- Stewart, R. V. and Gardiner, J. G., 'Contribution to mixer intermodulation distortion of nonlinearity in the diode forward characteristics', *Electronics Letters*, 7, No. 10, pp. 279–81, 20th May 1971.
- Belevitch, V., 'Non-linear effects in ring modulators', *Wireless Engineer*, 26, p. 177, May 1949.
- Tucker, D. G., 'Intermodulation distortion in rectifier modulators', *Wireless Engineer*, 31, pp. 145–52, June 1954.
- Gardiner, J. G., 'The signal-handling capacity of the square-wave switched ring modulator', *The Radio and Electronic Engineer*, 41, No. 10, pp. 465–70, October 1971.
- Poultney, A. E. J., 'Trends in h.f. communications receiver design', Conference on Radio Receivers and Associated Systems, Swansea, 1972, pp. 69–76 (IERE Conference Proceedings No. 24).
- Gardiner, J. G., 'Front end mixer problems: considerations in the achievement of optimum linearity and conversion efficiency', *ibid.*, pp. 45–60.
- Tucker, D. G., 'Unbalance effects in modulators', *J. Brit. Instn Radio Engrs*, 15, pp. 199–207, April 1955.
- Cheadle, D., 'Selecting mixers for best intermod performance', *Microwaves*, November 1973, pp. 48–52; December 1973, pp. 58–62.
- Ruthroff, C. L., 'Some broadband transformers', *Proc. IRE*, 47, pp. 1337–42, August 1959.
- Herishen, J. T., 'Diode mixer coefficients for spurious response prediction', *IEEE Trans. on Electromagnetic Compatibility, EMC-10*, No. 4, pp. 355–63, December 1968.
- 'The hot-carrier diode: theory, design and application', Hewlett Packard, Application Note No. 907.
- Maurer, R. E., 'Analysis of intermodulation distortion in double balanced diode ring modulators', IEEE Intl Conf. on Communication, 11–13th June 1973, Conference Record, Part II, pp. 51.21–51.26.
- Gardiner, J. G., 'An intermodulation phenomenon in the ring modulator', *The Radio and Electronic Engineer*, 39, No. 4, pp. 193–7, April 1970.
- Gardiner, J. G., 'The relationship between cross-modulation and intermodulation distortions in the double balanced modulator', *Proc. IEEE*, 56, No. 11, pp. 2069–71, November 1968.
- Kurth, C., 'Analysis of diode modulators having frequency-selective terminations, using computers', *Electrical Communication*, 39, No. 3, pp. 369–78, 1964.
- Abramovitz, M. and Stegun, I. A., 'Handbook of Mathematical Functions with Formulas, Graphs and Mathematical Tables' (U.S. Department of Commerce, U.S. Government Printing Office, Washington D.C., June 1964).

9 Appendix 1: Analysis of Diode Non-linearity

From the equivalent circuit of Fig. 3, during one half-cycle of the local oscillator, the voltages at either side of the transformer secondary with respect to the node V are:

$$V_1 - V' = \left[(I - i)R + \frac{kT}{q} \ln \left[\frac{I - i}{I_s} \right] \right]$$

$$V_2 - V' = - \left[(I + i)R + \frac{kT}{q} \ln \left[\frac{I + i}{I_s} \right] \right]$$

These branch voltages may be considered as composed of a differential component due to the carrier current which appears across the balanced windings of the transformer, and a common-mode component due to

the signal current.

$$\begin{aligned} V_1 - V' &= V_{diff} + V_{cm} \\ V_2 - V' &= -V_{diff} + V_{cm} \end{aligned}$$

Since no common-mode voltage can appear across the transformer secondary:

$$\begin{aligned} V' &= V_{cm} \\ &= \frac{1}{2} \left[2iR - \frac{kT}{q} \ln \left[\frac{I-i}{I+i} \right] \right] \\ V' &= iR + \frac{kT}{2q} \ln \left[\frac{1+i/I}{1-i/I} \right] \end{aligned}$$

For the signal circuit,

$$V_s - V' = (R_s + R_L)2i$$

therefore

$$V_s = (R_s + R_L + R/2)2i + \frac{kT}{2q} \ln \left[\frac{1+i/I}{1-i/I} \right]$$

Let

$$(R_s + R_L + R/2) = R_x$$

Series expansion of logarithmic term,¹⁷ neglecting terms higher than third-order:

$$\begin{aligned} V_s &= 2iR_x + \frac{kT}{2q} \left[\left(\frac{i}{I} - \frac{1}{2} \left[\frac{i}{I} \right]^2 + \frac{1}{3} \left[\frac{i}{I} \right]^3 \dots \right) - \right. \\ &\quad \left. - \left(-\frac{i}{I} - \frac{1}{2} \left[\frac{i}{I} \right]^2 - \frac{1}{3} \left[\frac{i}{I} \right]^3 \dots \right) \right] \end{aligned}$$

Therefore

$$V_s = i \left[2R_x + \frac{kT}{qI} \right] + \frac{1}{3} \frac{kT}{q} \left[\frac{i}{I} \right]^3$$

since the second-order terms cancel.

By reversion of series (ref. 17, p. 16),

$$i = \frac{V_s}{2R_x - \frac{kT}{qI}} - \frac{\left[2R_x - \frac{kT}{qI} \right] \frac{1}{3} \frac{kT}{qI^3} V_s^3}{\left[2R_x - \frac{kT}{qI} \right]^5}$$

if $2R_x \gg kT/qI$ (always true in a practical circuit),

$$i = \frac{V_s}{2R_x} - \frac{1}{3} \frac{kT}{q} \frac{1}{(2R_x)^4 I^3} V_s^3 \tag{14}$$

For two-tone testing, $V_s = V \cos \omega_1 t + V \cos \omega_2 t$. The non-linearity can be represented by the polynomial:

$$i = aV_s + bV_s^2 + cV_s^3 + \dots$$

For small levels of distortion (neglecting higher-order terms), relative levels of distortion products to one fundamental:

$$\begin{aligned} \text{second harmonics} & \frac{bV}{2a} \\ \text{second-order intermodulation} & \frac{bV}{a} \\ \text{third harmonics} & \frac{cV^2}{4a} \\ \text{third-order intermodulation} & \frac{3cV^2}{4a} \end{aligned}$$

From equation (14), relative level of third-order intermodulation

$$k_{I_3} = 20 \log_{10} \left[\frac{kT}{4q} \frac{1}{8R_x^3} \frac{V^2}{I^3} \right] \text{ dB} \tag{15}$$

From equation (5),

$$k_{I_3} = -2(\text{TOI} - P_{in}) \text{ dB}$$

$$\text{third-order intercept} = \left(P_{in} - \frac{k_{I_3}}{2} \right) \text{ dBm}$$

Referring the third-order intercept to the total input power of both signals,

$$\begin{aligned} \text{TOI} &= 10 \log_{10} \left[10^3 \left(\frac{V^2}{8R_s} + \frac{V^2}{8R_s} \right) \right] - \\ &\quad - 10 \log_{10} \left[\frac{kT}{4q} \frac{1}{8R_x^3} \frac{V^2}{I^3} \right] \\ &= 10 \log_{10} \left[\frac{R_x^3}{R_s} \frac{8q}{kT} I^3 \times 10^3 \right] \text{ dBm} \tag{16} \end{aligned}$$

When $R_x = 2R_s$ (i.e. no linearizing resistors),

$$\text{TOI} = 10 \log_{10} \left[64R_s^2 \frac{q}{kT} I^3 \times 10^3 \right] \text{ dBm} \tag{17}$$

10 Appendix 2: Distortion Due to Finite Switching Time in a Ring Modulator

It has been shown by Tucker,⁴ that the ratios of distortion products to wanted fundamental sideband is the same for the ring modulator as the single diode, provided the appropriate voltages are considered. At the instant when all four diodes are non-conducting, the full input signal voltage, $v(t)$, will appear across each diode in addition to the full carrier voltage V_c . Thus the instant of switching, determined by the zero volt condition, will be shifted in time as shown in Fig. 5, and the resulting phase modulation of the carrier frequency ω_c can be seen by inspection to be:

$$\Phi(t) = v(t) \frac{t_r}{V_c} 2\pi \frac{\omega_c}{2\pi} = v(t) \frac{t_r}{V_c} \omega_c$$

Assuming a sinusoidal input signal of peak value V_s , frequency ω_1 , the modulated switching function is given by:

$$U(t) = \frac{1}{2} + \frac{2}{\pi} \sum_{n=1}^{\infty} \frac{\cos [(2n-1)(\omega_c t + x \sin \omega_1 t)]}{(2n-1)}$$

For first-order of modulation, i.e. products around ω_c ,

$$U(t) = \frac{1}{2} + \frac{2}{\pi} [\cos \omega_c t \cos (x \sin \omega_1 t) - \sin \omega_c t \sin (x \sin \omega_1 t)]$$

where

$$x = t_r \omega_c \frac{V_s}{V_c}$$

Using the Fourier expansions:

$$\begin{aligned} \cos (x \sin \omega_1 t) &= J_0(x) + 2J_2(x) \cos 2\omega_1 t + \\ &\quad + 2J_4(x) \cos 4\omega_1 t + \dots \end{aligned}$$

and

$$\begin{aligned} \sin (x \sin \omega_1 t) &= 2J_1(x) \sin \omega_1 t + 2J_3(x) \sin 3\omega_1 t + \dots \end{aligned}$$

and noting that in the double balanced mixer, d.c. and

even-order products cancel, the switching function becomes:

$$U(t) = \frac{2}{\pi} [-\sin \omega_c t (2J_1(x) \sin \omega_1 t + 2J_3(x) \sin 3\omega_1 t)]$$

neglecting higher-order terms.

Therefore,

$$U(t) = -\frac{2}{\pi} [J_1(x) \sin (\omega_c - \omega_1)t + J_1(x) \sin (\omega_c + \omega_1)t + J_3(x) \sin (\omega_c - 3\omega_1)t + J_3(x) \sin (\omega_c + 3\omega_1)t]$$

hence

$$\text{ratio of fundamental to third harmonic} = \frac{J_3(x)}{J_1(x)}$$

For small x (ref. 17, p. 256, p. 360),

$$J_m(x) = \frac{(\frac{1}{2}x)^m}{\Gamma(m+1)}$$

$$\Gamma(m+1) = \Pi(m) = m!$$

Therefore,

$$J_0(x) = x/2, \quad J_2(x) = x^2/8, \quad J_3(x) = x^3/48.$$

Hence

$$k_3 = \frac{x^2}{24}$$

Thus the ratio of third harmonic to fundamental due to finite switching time

$$= \frac{\left[t_r \omega_c \frac{V_s}{V_c} \right]^2}{24}$$

For polynomial of the form

$$V_{out} = aV_{in} + bV_{in}^2 + cV_{in}^3 + \dots$$

$$\text{third harmonic ratio} = \frac{c}{4a} V_{in}^2$$

third-order intermodulation ratio

$$= \frac{3c}{4a} V_{in}^2 \quad (\text{see Appendix 1})$$

Thus ratio of third-order intermodulation to fundamental signal is, by analogy,

$$k_{13} = 20 \log_{10} \frac{\left[t_r \omega_c \frac{V_s}{V_c} \right]^2}{8} \quad \text{dB}$$

$$\text{Third-order intercept} = P_{in} - \frac{k_{13}}{2} \text{ dBm} \quad (\text{see Appendix 1})$$

Referring the third-order intercept to the total input power,

$$\text{TOI} = 10 \log_{10} \left[\frac{V_s^2}{8R_s} + \frac{V_s^2}{8R_s} \right] - 10 \log_{10} \frac{\left[t_r \omega_c \frac{V_s}{V_c} \right]^2}{8} \quad \text{dBW}$$

$$\text{third-order intercept} = 10 \log_{10} \left[\frac{2 \times 10^3 V_c^2}{t_r^2 \omega_c^2 R_s} \right] \quad \text{dBm}$$

11 Appendix 3: Relative Power Consumption of Square-wave and Equivalent Sine-wave Drive

Considering the carrier voltage appearing across one arm of the diode bridge, find the equivalent sine-wave voltage to give the same rate of change of voltage at the zero crossing point as with the square-wave.

For sine-wave

$$\frac{dV}{dt} = V_0 \omega \cos \omega t = V_0 \omega \Big|_{\text{at } t=0}$$

For square-wave

$$\frac{dV}{dt} = \frac{V_c}{t_r}$$

where V_c = peak-to-peak voltage.

Equating dV/dt ,

$$V_0 = \frac{V_c}{t_r \omega_c}$$

Load impedance seen at primary of $T_1 \simeq R/2$.

Therefore,

$$\text{square-wave power} = \frac{(V_c/2)^2}{R/2}$$

$$\text{sine-wave power} = \frac{V_0^2}{2R/2} = \frac{V_c^2}{t_r^2 \omega_c^2 R}$$

$$\text{ratio} = \frac{2}{(t_r \omega_c)^2}$$

$$\text{ratio of peak-to-peak voltages} = \frac{2}{t_r \omega_c}$$

Manuscript received by the Institution on 22nd July 1975. (Paper No. 1719/MI 3.)

© The Institution of Electronic and Radio Engineers, 1976

IERE News and Commentary

Pre-1974 Graduate Members of the Institution

There are still a number of Graduate members elected before the end of 1973 whose qualifications do not meet the present academic requirements for Corporate Membership, and who must therefore pass the CEI Part 2 Academic Test before an application for transfer to the grade of Member can be considered. It is expected that this Test (which consists of two approved Technical Papers from Part 2 of the CEI examination) will be withdrawn in a few years' time. The rules for the Test permit two attempts but require that both subjects should be passed at the same sitting and present indications are that the last date at which the *first* attempt can be made will be May 1979.

Since applications by overseas Graduates to sit at this time must be received by the Institution not later than 15th November 1978, it is thought necessary to give this early notice, in order that preparatory study can be commenced in good time. For candidates sitting the examination in the UK, the last date for receipt of entries will be 15th January 1979. There is, of course, no reason why those affected should not sit before the dates mentioned if they wish.

Any Graduate member elected before 31st December 1973 who is aware that he needs to pass the Part 2 Academic Test or who is uncertain whether this is necessary, should get in touch with the Institution to obtain any further information or advice required.

Engineers' Voice should be heard in Public Policy

In his Graham Clark Lecture, 'The Voice of the Engineer in Public Policy', Sir Alan Cottrell, Master of Jesus College, Cambridge, and a former chief scientific adviser to the Government, said that he thought professional engineers should speak out loudly on those aspects of public issues in which they were expert. The quality of technical decision-making in Britain since the Second World War had suffered through the failure of Government to engage more than a fraction of the brain power and expertise of the nation. He believed that in technical decisions there was a clear separation between government and governed, with little communication between them at policy-making level except through Parliament which had little understanding of, or interest in, technical matters. Few matters emptied the Commons more quickly than a debate on a scientific or engineering subject.

Although a great technical feat, *Concorde* had been a 'tragic misdirection of resources', said Sir Alan. Its major casualties were those engineers and workmen who had given half a lifetime's skills and energies to a commercially unsound project. Had the voice of the whole engineering industry

been heard, loud and clear, on aircraft policy, it was possible that the aircraft industry would be in a much sounder position today.

Copies of the lecture, in booklet form, are available from CEI, 2 Little Smith Street, London SW1P 3DL, price 40p.

Digital Network Testing Summer School

The Department of Electronics, Southampton University, in conjunction with Membrain Limited, is organizing a three-day residential summer school on 'The Theory and Practice of Digital Network Testing'. The course will be held at Southampton University from Wednesday, 7th to Friday, 9th July 1976 and will cover such topics as the limitations of exhaustive testing and the use of fault-effect models; automatic test pattern generation using Boolean difference or D-algorithm techniques; use of simulators to generate and evaluate test patterns; and design of easily-tested logic networks. The course will also include a demonstration of and a practical session on a Membrain 2400 Series Automatic Test System for digital networks.

The registration fee for the course will be £55.00 and accommodation will be available in one of the University Halls of Residence (approximate cost—£5.00 per night).

Further details and registration form from Dr. R. G. Bennetts (REE/1), Department of Electronics, University of Southampton, Southampton SO9 5NH. Tel: 0703 559122, Ext. 580/2493.

Solid State Devices—Research Support

The development of the electronics industry over the past twenty-five years has been dramatic, and the results of its technological advances are ubiquitous. Central to this growth has been the development of solid-state devices, allowing ever more complex circuitry to be contained in ever smaller spaces. This rapid rate of change has resulted from high R & D expenditure, which depends on large and assured markets and it is in this respect that UK industry has been at a disadvantage.

A report examining these problems, prepared by a panel chaired by Professor W. E. J. Farvis of Edinburgh University and entitled 'Solid-state Devices: a strategy for SRC research support', was recently published by the Science Research Council.

The Panel argues that this rapid growth and the resulting highly competitive market situation has meant that industrial research aimed at the fundamental understanding of existing materials and effects currently utilized in devices has, to some extent, been neglected. It suggests that research in universities and polytechnics could play an important role for British industry by 'underpinning' device R & D through the provision of this basic data and also in looking for new effects and materials which industry might exploit several years from now. There is also seen to be a need to encourage the concentration of effort in particular aspects of this research, in order to maximize its effectiveness.

Research requires materials and devices of the highest industrial standard and since these are often not commercially available, the Report proposes that SRC should set up centralized facilities in a small number of locations to provide a high-quality service. This service needs to be paralleled by research in specialized aspects of device fabrication such as diffusion, crystal growing, epitaxy, mask-making, etc. The Report also recommends an overall increase in funds spent on solid-state devices research, if necessary at the expense of other areas of electrical and electronic engineering.

In publishing the report for comment the SRC also seeks proposals for the establishment of material and devices centres. Copies are available free of charge from Miss Joyce Iruo, S.R.C., State House, High Holborn, London WC1 (tel. 01-242 1262, extension 215).

Applications of Charge Coupled Devices

A two-day residential Summer School on 'Applications of Charge Coupled Devices' is being held at the University of Southampton on 15th/16th July 1976. Following an introductory session, the School will cover the main areas of imaging, analogue signal processing and digital applications. Lectures are from industrial, government and university establishments. Further details may be obtained from the organizer, Dr. J. D. E. Beynon, Department of Electronics, The University of Southampton SO9 5NH (Telephone Southampton 559122, extension 777).

ENGINEER OFFSHORE 76 Exhibition

An exhibition showing the vital role played by engineers in a wide range of activities—and especially in developing offshore resources of oil, gas and other minerals around Britain's own coasts—is to be held in London during June. Organized by the British National Committee on Ocean Engineering, a committee of the Council of Engineering Institutions, ENGINEER OFFSHORE 76 will be open to the public daily (except Sunday) from Tuesday, 22nd June to Friday, 2nd July, at the Institution of Civil Engineers, Great George Street, London, SW1. Times of opening will be 10.00 a.m. to 6.00 p.m. (8.00 p.m. Tuesdays and Thursdays) and admission is free.

The large oil companies, British Gas Corporation, construction firms, consultants, engineering institutions and others are contributing money, graphic material and models to create a vivid picture of how engineering expertise, manpower, research and finance are being utilized to exploit the benefits from offshore development. Additionally the exhibition will show how the engineers' skills are being used in developing and managing fisheries resources; in the building and operation of our worldwide maritime transport fleet; in preventing sea pollution and coastline desecration; and in the design, contracting and supporting services needed for safe and efficient operations. The exhibition will also portray the role of government engineers in regulating offshore activities and that of research teams in meeting current challenges with new ideas, for example in alternative energy sources such as tides and waves.

Scientific Instrument Achievement Award

The Achievement Award of the Worshipful Company of Scientific Instrument Makers is made annually for an outstanding British or Commonwealth achievement in the scientific instrument field, including contributions to research, development and design, a new application or technique, or any other outstanding meritorious effort in aspects of scientific instrumentation. It is expected that the presentation this year will be made at the Installation Court Dinner on 26th October. CEI institutions have been invited to submit full details of any achievement which, in their opinion, is suitable for consideration, and the IERE Council will be pleased to receive nominations from members.

Conference on Digital Processing of Signals in Communications

The continued rapid advances in Digital Circuit Technology over the past few years have led to more and more complex devices being available at relatively low cost and of extremely small size. This advance has influenced engineers to consider systems which would have been uneconomical with discrete components. Many new communications systems are being introduced as a direct result of the availability of medium and large scale integration devices and in particular the microprocessor. These advances in the communications and television field form the theme of the forthcoming conference organized by the IERE with the association of the Institution of Electrical Engineers and the Institute of Electrical and Electronics Engineers and to be held at the University of Technology, Loughborough, from 6th to 8th September 1977. A similar conference was held at Loughborough in 1972.

The Organizing Committee, which is under the chairmanship of Professor J. W. R. Griffiths and includes representatives of the sponsoring organizations drawn from industry, Government research establishments and universities, now invites papers for this Conference. In the first instance synopses of proposed contributions are requested. Preference will be given to those describing original work, new systems, or new applications. For guidance a non-exclusive range of subjects is offered:

- Digital Television
- Digital Processing of Speech and Music Signals
- Computer/Data Communication
- Digital Filters in Communications

- Computer Processing of Images
- Digital Studio Techniques
- Coding Techniques for Television Transmission
- Digital Data Transmission Techniques including Error Detection and Correction
- Automatic Equalization
- Underwater Acoustic Communication
- Telemetry
- Simulation of Communication Systems
- Instrumentation for Digital Communication
- Signal Design

A synopsis (typically about 200 words) should be long enough to enable the Committee to assess the scope of the proposed paper, and should be sent to the Secretary, Organizing Committee for the Conference on Digital Processing of Signals, Institution of Electronic and Radio Engineers, 8-9 Bedford Square, London, WC1B 3RG. Synopses should be submitted as soon as possible but not later than 14th July 1976.

Final papers may be either in short form or full length, i.e. containing either 2000 words or 4000 words approximately. Papers will be pre-printed, and are therefore required in final form by 25th March 1977.

Further information and registration forms for the Conference will be available in due course from the Conference Registrar at the Institution.

Conference on Computer Systems and Technology

University of Sussex—29th to 31st March 1977

To keep pace with the rapid advances in computer architecture and its associated technology this conference, organized by the IERE with the association of the Institution of Electrical Engineers and the British Computer Society, will embrace both the hardware and software aspects of computer systems ranging from switching theory and computer languages through to devices and peripheral equipment. The Organizing Committee, which is under the Chairmanship of Professor D. W. Lewin, has decided that to contain this vast subject area the 1977 conference, in contrast to earlier conferences, will concentrate on the themes of Microprocessors, Reliable Systems and Interactive Systems.

It is intended that each session will embrace both hardware and software considerations in an endeavour to bring together specialists in equipment and software design, as well as application and systems designers, thus enabling common problem areas to be highlighted and new solutions proposed.

Review and survey papers as well as papers on research and applications will be included. Considerable emphasis will be given to the formation of Round Tables and Discussion Groups to be led by experts in the field.

Papers are invited along the lines of the conference theme given above. The following list of suggested topics are not intended to be exhaustive. Contributions which embrace more than one theme will be of particular interest.

1. Microprocessors

- Hardware design
- Microprocessor architecture
- Distributed and dedicated systems
- Microprogramming techniques
- Peripheral systems and interfacing
- Systems software, including macro-assembly languages and compilers, emulation
- Applications of microprocessors
- System design using microprocessors
- Impact on education/society/industry
- Other related topics

2. Reliable Systems

- Hardware and software aspects of software reliability
- Fault-tolerant systems and economic aspects
- Fail safe philosophy and techniques
- System modelling and simulation
- Fault diagnosis and test generation
- Error-coding and redundancy techniques
- Design verification, performance testing and evaluation
- Reliable software, including recovery procedures etc.
- Hardware monitoring and maintenance
- Software tools for system and program development
- Other related topics

3. Interactive Systems

- Man-machine systems, machine-machine interaction
- Theoretical principal and methodology of design
- Security, protection and reliability
- Design for extensibility
- Data-base structure and management
- User languages for interaction

Interfacing and communication aspects

Application areas

Other related topics

In the first instance a synopsis should be submitted. This should be long enough (typically about 200 words) to enable the committee to assess the scope of the proposed paper, and should be sent to the Joint Conference Secretariat at the IERE. Synopses should be submitted as soon as possible but not later than 31st July 1976.

Final papers may be either in short form or full length, i.e. containing either 2000 words or 4000 words approximately. They will be pre-printed and are, therefore, required in final form by 5th January 1977.

Further information and registration forms for the conference will be available in due course from the Conference Registrar, Institution of Electronic and Radio Engineers, 8-9 Bedford Square, London WC1B 3RG (Telephone 01-637 2771).

Standard Frequency Transmissions—March 1976

(Communication from the National Physical Laboratory)

March 1976	Deviation from nominal frequency in parts in 10 ⁸ (24-hour mean centred on 0300 UT)	Relative phase readings in microseconds NPL—Station (Readings at 1500 UT)		
		Droitwich 200 kHz	*GBR 16 kHz	†MSF 60 kHz
1	-0.1	697.8	612.3	
2	-0.1	696.9	612.1	
3	-0.1	696.9	612.2	
4	-0.1	697.0	612.1	
5	-0.1	697.0	612.0	
6	-0.1	697.0	611.9	
7	-0.1	697.3	611.9	
8	-0.1	697.8	612.1	
9	-0.1	697.2	612.3	
10	-0.1	696.5	612.1	
11	-0.1	696.0	612.1	
12	-0.2	697.0	612.1	
13	—	—	612.2	
14	—	—	612.2	
15	-0.2	697.2	612.1	
16	-0.2	696.7	612.1	
17	-0.2	696.2	611.9	
18	-0.2	696.6	611.9	
19	-0.2	696.4	611.9	
20	-0.2	696.3	611.8	
21	-0.1	696.0	611.7	
22	0	696.0	611.7	
23	0	696.0	611.7	
24	0	696.4	611.5	
25	0	695.8	611.7	
26	—	695.9	611.7	
27	-0.4	695.7	611.7	
28	-0.4	697.0	611.7	
29	-0.4	697.2	611.8	
30	-0.4	698.5	612.0	
31	—	698.3	612.2	

All measurements in terms of H-P Caesium Standard No. 344, agrees with the NPL Caesium Standard to 1 part in 10¹¹.

* Relative to UTC Scale; (UTC_{NPL}-Station)
= +500 at 1500 UT 31 December 1968.

† Relative to AT Scale; (AT_{NPL}-Station)
= +468.6 at 1500 UT 31 December 1968.

Members' Appointments

CORPORATE MEMBERS

Mr. S. A. Aziz, M.Sc., M.S. (Fellow 1953) is now a consultant in radio and telecommunications with Messrs Noon Qayum & Co., Lahore. Mr. Aziz worked for All-India Radio from 1938 to 1945, and following two years in the United States, joined



Radio Pakistan. He retired as Chief Engineer in 1973 and then served as Director of Engineering for the newly formed Pakistan Broadcasting Corporation for a year. He has been associated with the Institution's Karachi Section for many years and has been its Chairman since 1961.

Mr. Peter Huggins (Fellow 1961, Member 1952, Associate 1945) is now working as a consulting engineer on measurement and data acquisition techniques. From 1973 to 1975 he was Technical Director of Mangood Ltd. of Pontypool, and previously was with Girling Ltd. at Cwmbran;



in both capacities he was mainly concerned with electronic weighing techniques. Mr. Huggins is a Past Chairman and member of the Committee of the West Midlands Section and he has contributed several papers on automation and associated subjects to the Journal.

Mr. A. G. Barnes (Member 1969, Graduate 1964) has been appointed an Assistant Electronics Engineer with the British Airports Authority. After holding appointments in industry he first joined the Authority as Works Engineer (Electronics).

Colonel J. F. Blake (Member 1969) has taken up an appointment as Commanding Officer, Engineering Wing, School of Signals, Blandford Camp. For the past 18 months he was with NICSMA, NATO.

Mr. P. F. Branagan (Member 1973, Graduate 1970), who has been with Radio Telefis Eireann since 1968, is now Senior Project Engineer in the Network Design and Development Department.

Mr. Alan Breeze (Member 1971, Graduate 1969), previously Marketing Manager of Tellurometer (UK) Ltd., has been appointed Technical Consultant, Hydrographic Systems, with Sea and Land Services, Ltd. of Glasgow.

Mr. G. V. Caley (Member 1973, Graduate 1972) who went to Manama, Bahrain, as an Assistant Engineer with Cable and Wireless Ltd. a year ago, has moved to Dubai and is engaged on the installation of an international telephone switching centre and maintenance centre.

Mr. Ahmad Fadami, M.S. (Member 1973) who is with National Iranian Radio and Television, has been appointed Director, Logistics and Maintenance, in which capacity he is in charge of these aspects for all radio and television stations within the Company.

Mr. S. J. Harris (Member 1970) has moved to Plymouth to take up the post of Principal Engineer, Radio and Audio Development, with Rank Radio International. He joined the Company in 1950 and was latterly with the laboratories in Chiswick.

Mr. D. S. Hooker (Member 1973, Graduate 1968), an Executive Engineer in the Post Office, has been appointed Head of the Register-Translator Development Group at Telecommunications Headquarters in London.

Mr. Stanley Lowther (Member 1971, Graduate 1964) who is with the Ministry of Defence Procurement Executive, has been appointed Quality Officer (P & TO II) with the Electrical Quality Directorate in Edinburgh. He was previously Deputy Quality Manager.

Mr. John Lowry, B.Sc. (Member 1970) who has been with the BBC since 1963, latterly as an engineer with the Transmitter Group of the Engineering Department in London, has been appointed Transmitter Manager at the Holme Moss Station in Yorkshire.

Mr. G. E. Myers (Member 1972, Graduate 1967) has been appointed Senior Telecommunications Officer in the Department of Civil Aviation, Nadi Airport, Fiji. For the past five and a half years he has been Engineer-in-Charge, Air Traffic Control, at the Aircraft and Armament Experimental Establishment, Boscombe Down.

Mr. R. J. Newton (Member 1973, Graduate 1970) has been appointed Production Director with L.C. Automation Ltd., Preston, Lancashire; he was previously Drawing Office Manager with the Company.

Sqn. Ldr. T. S. Page, RAF (Member 1973, Graduate 1967) who was appointed Officer Commanding 112 Signals Unit, RAF Stornoway, in 1973, has moved to the Ministry of Defence, Air Engineering 14c (RAF) as Staff Officer for avionic systems.

Mr. S. K. Randev, B.Sc. (Member 1972) who has been with the Fertilizer Corporation of India Ltd., since 1960, has been promoted to Assistant Chief Engineer Instrumentation, and is now at the Ramagundam Planning and Development Site Office.

Mr. S. M. Romm (Member 1973, Graduate 1965) has been appointed General Manager (Manufacturing) with Foster Cambridge, Eaton Socon, Huntingdonshire. He was formerly Works Manager with Fielden Electronics Ltd., Manchester.

Mr. P. A. Rozier (Member 1974, Graduate 1969) has joined Ferranti Semiconductors as Field Sales Engineer. His previous appointment was as a Project Engineer with Evans Electro Selenium Ltd.

Mr. Philip Scargill (Member 1965, Graduate 1962) who has been with the Union Carbide Corporation for the past ten years, since 1971 as Product Manager with the Company's subsidiary in Geneva, has been appointed Marketing Manager, Consumer Electronics, at the plant in Simpsonville, South Carolina, USA.

Mr. B. B. Streater (Member 1973, Graduate 1972) who was with Diablo Systems S.A. as Sales Manager for the United Kingdom and Scandinavia, has joined LogAbax Ltd., London, as Sales Manager of the OEM Division.

Mr. K. Walker, Dip.El. (Member 1969, Graduate 1955) who joined Mullard's Southampton Works in 1955, has been appointed Head of the Electronics Department of Albury Laboratories Ltd., near Guildford.

Mr. C. R. Wheeler (Member 1972, Graduate 1969), formerly with NCR Terminal Systems Division, Dayton, Ohio, has been appointed MOS Applications Engineer with Advanced Micro Devices Inc., Sunnyvale, California, where he is responsible for microprocessor and m.o.s. memory applications.

Mr. S. P. Wong, B.Sc. (Member 1974, Graduate 1967) has been appointed Manager of INFA Corporation Ltd., Kowloon, a trading company for telecommunications, electronics and building automation systems. He was formerly a public lighting engineer with the China Light and Power Company Ltd.

NON-CORPORATE MEMBERS

Mr. A. C. Bentley (Companion 1968) has retired from the post of Director of the Radio and Electronic Component Manufacturers' Federation after more than thirty years' service with the Federation. Two years ago Mr. Bentley was appointed an Honorary Life Member of the Committee of European Associations of Electronic Components (CEMEC) in recognition of the part which he played in the formation of CEMEC and its predecessor CEPEC, of which he was President from 1969 to 1970. He is succeeded at BREMA by Mr. William Barrett, formerly Director of the Scientific Instrument Manufacturers' Association.

Mr. F. O. Adophy (Graduate 1966) who has been with the Nigerian Broadcasting Corporation since 1958, has been promoted to Senior Engineer at Port Harcourt.

Lt. M. W. Buggy, RN (Graduate 1970) has been posted to HM Dockyard, Portsmouth, as Data Processing Officer and Weapons Electrical Information Specialist in the Ship Maintenance Authority. His previous appointment was as Radio Section Officer in HMS *Hermes*.

Mr. D. C. Butt (Graduate 1970) has been appointed Field Sales Manager for the Ignition and Control Systems Unit at Plessey Windings, Titchfield. He was formerly with the Honeywell Temperature Control Group, latterly as Senior Sales Engineer.

Mr. S. H. Cramer (Graduate 1965) has completed a year's tour of duty as Technical Instructor at the Pontoise factory of

Burroughs Corporation and has returned to Burroughs Machines Ltd. as Senior Technical Representative based at Ruislip, Middlesex.

Mr. A. J. Fisher (Graduate 1967) has been appointed Technical Sales Engineer with Transformers and Rectifiers Ltd., Guildford. He was previously Chief Projects Engineer with RSM Transformers Ltd., Redditch.

Mr. B. J. Foale (Graduate 1970) who is with the Post Office, has been promoted to Executive Engineer within the External Telecommunications Executive Division.

Mr. Brian Gill (Graduate 1966) has been appointed a Principal Development Engineer with Plessey Semiconductors, Swindon.

Mr. S. W. Kelly (Graduate 1973) has joined the Flight Automation Research Laboratories of Marconi-Elliott Avionics at Chatham as a Development Engineer. His previous appointment was as Physicist/Engineer at the Applied Research Laboratories of Thorn Radio Valves and Tubes at Rochester.

Mr. A. J. Turk (Graduate 1968), formerly Training Officer with Marconi Space and Defence Systems Ltd., Applied Electronics Laboratories, Portsmouth, is now working as a Spacecraft Systems Engineer.

Flt. Lt. P. A. Wheeler, RAF (Graduate 1971) has been posted from RAF Lossiemouth, where he was Officer Commanding, No. 1 Engineering Line Flight, *Jaguar* OCU, to be Electrical Engineering Task Programmes Officer at the Radio Engineering Unit, RAF Henlow.

Mr. A. A. A. Olaoya (Associate Member 1974) has been appointed Technical Manager of the Electronics Instrumentation Ltd., Ibadan, Nigeria. He was previously Manager for Radio, Audio and Domestic Appliances with the OGT Group of Companies Ltd., Lagos.

Captain E. S. Tan, RSAF (Associate Member 1974) has taken up the post of Officer Commanding, Electrical Engineering Squadron, RSAF Changi Air Base. He was previously Officer Commanding, Air Radar and Communication Flight at RSAF Tengah Air Base.

Mr. J. C. Wise (Associate Member 1975) has left the RAF after completing nine years' service term and has been appointed Head of the Electronics and Bio-medical Engineering Department at Copthorne Hospital, Shrewsbury.

Mr. R. O. Yussuf (Associate Member 1974) who is with the Civil Aviation Authority, has been promoted to Air Traffic Manager Grade II at Gatwick Airport.

Mr. E. C. Bowen (Associate 1963) is now Managing Director of MBM Associates International, Uxbridge, engineering consultants for broadcasting and communications.

Sqn. Ldr. L. A. Bull, MBE, RAF (Rtd.) (Associate 1967) has joined Plessey Marine Research Unit as DDS Engineer. His last service appointment was as Officer Commanding, Electrical Engineering Squadron, Ground Radio Servicing Centre, RAF North Luffenham.

A New European Scientific Association

The first meeting of the European Incoherent Scatter Facility (EISCAT) Council took place in January at Kiruna, Sweden. The facility will probe the ionosphere using high power radar techniques and the agreement establishing the organization, which will build and operate the facility, has recently been signed by the Science Research Council (SRC) and scientific research councils in Finland, France, the Federal Republic of Germany, Norway and Sweden. EISCAT will be funded by the six member agencies and will operate from three bases inside the Arctic Circle—at Kiruna, at Tromsø in Norway and at Sodankylä in Finland. The Headquarters will be at Kiruna.

EISCAT will be governed by a Council, under which will be a scientific advisory committee. The cost of the SRC at current prices and exchange rates will be about £2.4M towards the capital cost of the facility and about £160K annually towards running costs; approximately equal financial contributions will be made by France, Germany, the UK and the Nordic countries as a group.

At Tromsø will be installed two high-powered radar transmitters operating at frequencies of 224 MHz and 933 MHz, with a number of receivers at the three sites capable of detecting the radio signals scattered from charged

particles in the ionosphere at heights between about 80 km and 2000 km.

Incoherent scatter, as a method of probing the ionosphere from the ground, has proved its worth in other parts of the world—including the UK, where a successful incoherent scatter experiment was recently concluded. The purpose of EISCAT is to give detailed information about the ionosphere in high latitudes, where the interaction between the solar wind and the Earth's magnetic field creates many striking natural phenomena—notably the aurora—that are of interest to scientists in a wide range of disciplines. EISCAT offers an excellent method of tackling the complex scientific problems of the aurora, magnetic storms and their effects on the ionosphere, and how the ionosphere is linked with the lower atmosphere and with the magnetosphere—a tenuous region that surrounds the Earth to a distance of several Earth radii.

Observing time on the EISCAT facilities will be divided between a programme common to all members, in which UK scientists will be fully involved, and other programmes in which UK research workers will be entitled to a share of the remaining observing time for their own experiments. At least ten groups of UK scientists are expected to make use of EISCAT, which should become operational in 1979 with a life of at least 10 years.

Obituary

The Council has learned with regret of the deaths of the following members:

Wing Commander Henry Brian Alty, RAF (Ret.) (Member 1944) died on 24th December 1975, aged 65 years. He was unmarried.

After receiving his early technical education at Radcliffe Technical College, Manchester, while working in the electrical and radio industries, in 1935 he entered the RAF and took courses at the Electrical and Wireless School. In the years just before and at the beginning of the War he specialized in u.h.f. techniques and later lectured at No. 1 Radio School and, after commissioning as a Signals Officer in the Technical Branch, at the Officers Signals School. In the later years of the War he was Technical Liaison Officer to the Beam Approach Technical Training School. He subsequently received a permanent commission and held a variety of overseas and staff posts, including tours of duty at RRE Malvern from 1962 to 1964 and at the Ministry of Defence up to his retirement on medical grounds in 1965.

Gordon Mervyn Wilfred Cork (Graduate 1967) died suddenly on 2nd February 1976, aged 48 years. He leaves a widow.

Following National Service in REME Gordon Cork entered industry and between 1949 and 1960 first worked with the Automatic Telephone and Electric Company as a student engineer and then with the Flight Simulator Departments of the Weapons Research Divisions of English Electric and of A. V. Roe and, from 1957 to 1960, as a Technical Assistant with Bruce Peebles. During this period he embarked on studies at the Heriot-Watt and Napier Colleges for the Higher National Certificate which he completed with endorsements in industrial electronics and microwave engineering in 1967. He then joined the Astronomical Instrumentation Division of the Royal Observatory, Edinburgh, and in 1965 was successful in the Open Competition for Experimental Officer posts in the Scientific Civil Service. He remained at the Observatory up to the time of his death and during these years was responsible for developing electronic control and instrumentation techniques for such highly sophisticated astronomical equipment as the Schmidt Telescope, interferometers and a spectrophotometer.

Ronald Richard French (Fellow 1959) died after a short illness on 31st December 1975, aged 61 years. He leaves a widow and a son and daughter.

'Bob' French received his technical education at the Polytechnic, Regent Street, London, where he studied full time for the Higher National Diploma in electrical and radio engineering. He worked first for Murphy Radio from 1934 to 1936, being in charge of Production Quality Control and Check Test Departments, and in 1936 moved to Standard Telephones and Cables, North Woolwich, ultimately becoming a senior section head in charge of research and development of specialized testing apparatus for telephone and radio transmission systems. In 1951 Mr. French joined the Ministry of Supply as a Professional Engineer I at the Fort Halstead Armament Research Establishment. He developed special power supply equipment for the first British atomic bomb test and subsequently with the Atomic Weapons Research Establishment he took charge of the electronics engineering section and prototype workshops in support of the Trials Division and later Applied Physics.

Edward Malcom Leonard (Member 1967, Student 1962) died on 2nd January 1976, aged 50 years. He leaves a widow and two sons.

Born in Cardiff, Edward Leonard received his early technical education at the Army Technical School, Chepstow, between 1939 and 1942 and he then served in the REME. From 1949 to 1953 he was a Staff Sergeant in charge of a workshop section and on leaving the Army he joined STC as an Electrical Inspector in the Transmission Department. In 1959 he was appointed a Technical Assistant with the Independent Television Authority and for the next sixteen years his work was in the operation and maintenance of attended and unattended transmitting stations. Mr. Leonard's first post was as Shift Engineer at the Emley Moor transmitter and on promotion to Senior Shift Engineer in 1963 he went to the Moel-y-Parc Station; he was promoted Assistant Engineer-in-charge five years later. In March 1975 Mr. Leonard left the Authority to take up an engineering appointment with Trans World Airlines in Saudi Arabia where he died suddenly as a result of a heart attack.

Air Commodore Lawrence Patrick Moore, C.B.E., RAF (Ret.) (Fellow 1961) died on 15th January 1976, aged 69 years. He leaves a widow.

Patrick Moore was in the Royal Air Force from when he joined as an Aircraft Apprentice in 1922 until his retirement in 1961. He was commissioned as a Signals Officer in 1924, later qualifying as a pilot,

and held staff appointments in the 'thirties with Coastal Command. Among his wartime postings was as Command Signals Officer in West Africa and he was Senior Air Staff Officer HQ No. 27 Group from 1944 to 1946. For the two years immediately after the war he was Officer in Charge of writing the Signals History of World War II in the Air Historical Branch of the Air Ministry. From 1950 to 1955 Air Commodore Moore held appointments as Chief Signals Officer at HQ Coastal Command and HQ Far East, and he returned to the UK as Senior Technical Staff Officer HQ No. 41 Group. His final appointment was Director of Telecommunications at the Air Ministry; during this period he was assessor on the Radio Research Board of D.S.I.R.

Air Commodore Robert Cecil Wansbrough, M.A., RAF (Ret.) (Fellow 1944) died on 27th February 1976, aged 79 years.

Robert Wansbrough was born in Lincoln and educated at King Edward's High School, Birmingham. He was apprenticed to Igranic Electrical Company, Bedford, in 1912 but left to serve initially with Army and later in the Royal Flying Corps. On demobilization in 1919 he re-entered industry, working for a time in the General Electric Company as Technical Secretary to the Managing Director at Witton and later in Kingsway. In 1921 he rejoined the RAF subsequently taking the Long Signals Course and gaining a B.A. degree at Cambridge University. After holding posts in research and development establishments in the 'thirties he was appointed to the staff of the Director of Communications Development in 1940 with the rank of Wing Commander. Subsequently as Group Captain he served in Deputy Director posts in the Ministry of Aircraft Production concerned particularly with the radio repair organization. Shortly after the end of the War Air Commodore Wansbrough joined the Institution's Membership Committee on which he served until 1957, apart from a break of some eighteen months when he was on the staff of RAF Headquarters, Middle East Land Forces, Cairo. From 1948 to his retirement in 1949 he was Director of Radio at the Air Ministry and he then joined E.M.I. Sales and Services as Personal Assistant to the Managing Director. For several years prior to his final retirement Air Commodore Wansbrough was a Senior Technical Assistant with E. G. Brisch & Partners, where he was concerned with classification and coding of electrical and electronic components.

IERE Golden Jubilee Convention—'ELECTRONICS IN SOCIETY'

University of Cambridge, 28th June—1st July 1976

Programme

Monday, 28th June

14.00 Welcome by Prof. W. GOSLING, *Convention Chairman*.
Introductory Address by Sir LEONARD ATKINSON, K.B.E.

Keynote Address by Prof. Sir HERMANN BONDI, K.C.B., F.R.S.
(*Chief Scientific Adviser, Ministry of Defence.*)

Following the paper by Sir Hermann Bondi there will be a discussion.

16.30 Visit to Swaffham Prior Church to hear a lecture by C. C. H. WASHTELL (Fellow) on 'The Electrophonic Organ—The Organ of the Future?'; this will be followed by a short demonstration of the electrophonic instrument installed in the church.

A Sherry Reception will be given by EMI in King's College for all delegates between 18.00 and 19.15.

20.30 Organ Recital in King's College Chapel by GLYN JENKINS of St. Catharine's College.

Tuesday, 29th June

SESSION 1—COGNITIVE SCIENCE AND SIGNAL PROCESSING

Chairman: Prof. W. A. GAMBLING (*University of Southampton*)

'The present and possible future of intelligent machines'
By Dr. J. R. PARKS (*Department of Industry*)

'Applications of pattern recognition and scene analysis to the electronics industry'
By J. A. WEAVER (*Mullard Research Laboratories*)

'Digital signal processing'
By Prof. J. W. R. GRIFFITHS (*University of Loughborough*)

Keynote Address by BERNARD ASHER (*National Economic Development Office*)

SESSION 2—COMMUNICATIONS

Chairman: Prof. J. W. R. GRIFFITHS (*University of Loughborough*)

'Future telecommunications services'
By Dr. A. A. L. REID (*Post Office*)

'Broadcast and wired teletext systems'
By P. L. MOTHERSOLE (*V. G. Electronics*)

'Optical fibres—the new transmission line'
By Prof. W. A. GAMBLING (*University of Southampton*)

'Computer communication networks'
By D. W. DAVIES (*National Physical Laboratory*)

TWO HISTORICAL LECTURES (delivered in parallel sessions)

'Some personal recollections of automatic control'
By Prof. K. A. HAYES with an introduction by Prof. D. R. TOWILL (*University of Wales Institute of Science and Technology*)

'Hunting for Hertzian waves—a history of early radio detectors'
By Dr. V. J. PHILLIPS (*University College of Swansea*) with an introduction by Prof. W. GOSLING (*University of Bath*)

19.00 Reception by the Mayor of the City of Cambridge for Overseas Delegates. (At the Guildhall)

Wednesday, 30th June

SESSION 3—ADVANCES IN DATA PROCESSING

Chairman: Prof. D. W. LEWIN (*Brunel University*)

'Microprocessor applications'
By P. H. HAMMOND (*Warren Spring Laboratory*)

'Microprocessor technology and architecture'
By L. A. CRAPNELL (*Ferranti*)

'Towards nanosecond digital data processing'
By P. M. THOMPSON (*Thompson Foss*)

Keynote Address by Sir IEUAN MADDOCK, C.B., O.B.E., F.R.S.
(*Immediate Past President IERE and Chief Scientist, Department of Industry*)

SESSION 4—MEDICAL ELECTRONICS

Chairman: I. D. JEFFERIES (*Cossor Electronics*)

'Seeing inside the human body by computer'
By G. HOUNSFIELD (*EMI*)

'Aids for the handicapped—rehabilitation engineering'
By K. COPELAND (*University College London*)

'The 8-bit medicine man'
By Dr. G. H. BYFORD (*RAF Institute of Aviation Medicine*)

THE NINTH CLERK MAXWELL MEMORIAL LECTURE

to be given by Dr. H. B. G. CASIMIR (*Philips*)

Sherry Reception in Trinity College

Thursday, 1st July

SESSION 5—MICROELECTRONICS

Chairman: Prof. D. S. CAMPBELL (*University of Loughborough*)

'New linear analogue circuit techniques'
By C. S. DEN BRINKER (*Mackintosh Consultants*) and Prof. W. GOSLING (*University of Bath*)

'The present and future of microelectronics'
By W. HOLT (*Plessey*)

'LSI realization of digital filters for signal processing'
By Dr. G. P. EDWARDS (*Pye-TMC*)

Keynote Address by the Hon. CHRISTOPHER LAYTON (*Commission for European Communities*)

SESSION 6—CONTROL AND AUTOMATION

Chairman: Brig. R. KNOWLES (*Institute of Quality Assurance*)

'An overview of tracking control systems'
By Prof. D. R. TOWILL (*UWIST*)

'Aircraft landing systems'
By G. C. HOWELL (*Royal Aircraft Establishment, Bedford*)

'Automated design of control systems'
By P. ATKINSON (*University of Reading*)

'Future electronic control and communications in guided land transport systems'
By M. S. BIRKIN (*British Rail*)

Sherry Party given by Pye/Philips in King's College

Convention Banquet in King's College

The programme of addresses and papers will be supported by an Exhibition. Residential accommodation has been arranged at King's College and several social events will take place there and elsewhere. Fuller details of the programme may be obtained from the Conference Department, IERE, 9 Bedford Square, London WC1B 3RG.

Conference on 'Video and Data Recording'

Organized by THE INSTITUTION OF ELECTRONIC AND RADIO ENGINEERS with the association of The Institution of Electrical Engineers, The Royal Television Society, The Institute of Electrical and Electronics Engineers, The Society of Motion Picture and Television Engineers and The Institute of Physics.

University of Birmingham—20th to 22nd July 1976

Provisional Programme

Tuesday, 20th July

Introductory Lecture 'Trends in data recording'
By C. D. MEE (*IBM, USA*)

THEORY OF RECORDING PROCESSES

'Transfer characteristics of a magnetic tape channel'
By Dr. H. KÖHLER and H. WEILER (*Institut für Technische Elektronik, Germany*)

'Experiments on the writing process in magnetic recording'
By Dr. G. BATE and L. P. DUNN (*IBM, U.S.A.*)

'The development and application of a simple model of digital magnetic recording to thick oxide media'
By Dr. B. K. MIDDLETON and P. L. WISELY (*Manchester Polytechnic*)

'Deriving the replay pulse from the magnetic and physical characteristics'
By W. R. NAYLAND (*Burroughs Machines*)

NEW RECORDING TECHNIQUES AND MEDIA

'Video recording by optical means: the videodisk'
By J. P. LACOTTE, B. BLONDET and S. KRETSCHMER (*Thomson-CSF, France*)

'Holographic data storage and processing in photosensitive electro-optic crystals'
By J. P. HUIGNARD, J. P. HERRIAU and F. MICHÉRON (*Thomson-CSF, France*)

'Charge coupled device shift registers'
By J. F. DICKSON (*Plessey*)

'A small magnetic bubble memory system'
By D. J. HUNTER (*Plessey*)

'Domain tip memories'
By C. BATTAREL and M. HANAUT (*Crouzet S.A. France*)

'Domain tip propagation devices'
By I. L. SANDERS and Dr. A. J. COLLINS (*Wolfson Centre for Magnetism Technology*)

'Optical digital recording'
By J. T. RUSSELL (*Digital Recording Corporation, USA*) and R. A. WALKER (*Battelle Pacific Northwest Laboratories, USA*)

Wednesday, 21st July

VIDEO AND COMPUTER

Introductory Lecture: 'The future of recording'
Dr. G. BATE, (*IBM, USA*)

'Digital video-tape data handling in a CAMAC System'
By Dr. S. CITTOLIN and Dr. B. G. TAYLOR (*NP Division, CERN, Switzerland*)

'Interfacing an analogue video tape recorder and a digital processor,
By Dr. H. KÖHLER and H. WEILER (*Institut für Technische Elektronik, Germany*)

'Multi-channel digital sound recorder'
By F. A. BELLIS (*BBC Research*)

'Improved techniques for measuring phase and gain in digitised video signals'
By M. T. SALTER and M. O. FELIX (*Ampex, USA*)

INSTRUMENTATION

'Advances in high density digital recording and reproduction'
(*Bell & Howell*)

'Assessment of tapes and channel responses for pulse code modulation recording'
By W. VIGAR (*EMI, SE Laboratories*)

'High bit-rate, high-density magnetic-tape recording'
By Dr. C. F. SPITZER, A. JENSEN and J. M. UTSCHIG (*Ampex, USA*)

CODING AND MODULATION

'Optimal codes for digital magnetic recording'
By J. C. MALLINSON and J. W. MILLER (*Ampex USA*)

'Analytical techniques for application to data waveform analysis and equaliser network design.'
By G. A. CRAWFORD (*Teesside Polytechnic*)

'Signal processing in optical video recording'
By Dr. M. R. De HAAN (*Philips, Netherlands*)

'Colour television recording and playback with channels of limited bandwidth or poor timing stability'
By F. A. GRIFFITHS (*The Decca Record Co.*)

'An environmentally hardened airborne video tape recording and playing machine'
By J. ELLIOTT (*EMI*)

Thursday, 22nd July

RECORDING AND REPLAY HEADS

'Wear in recorder heads by magnetic tape'
By Dr. D. A. CASH (*Fulmer Research Institute*) and R. PAGEL (*Government Communications HQ*)

'The magnetic field near the side edge of narrow magnetic recording heads'
By A. VAN HERK and D. L. A. TJADEN (*Philips, Netherlands*)

'Track width on integrated heads'
By J. DESSERRE, M. HELLE and J. P. LAZZARI (*CII, France*)

'Performance of conductor strip and thin film recording heads'
By Dr. A. S. MARWAHA and D. J. C. M. PROSPER (*Polytechnic of North London*)

'Magneto-resistive read heads and their combination with thin film write heads'
By F. W. GORTER (*Philips, Netherlands*)

'Suppression of thermally induced pulses in magnetoresistive heads
By F. B. SHELEDY and S. D. CHEATHAM (*IBM, USA*)

'Design considerations for helical scan recording head contour'
By F. W. HAHN (*IBM, USA*)

TRANSCRIPTION

'Digital television comb filter with adaptive features'
By J. P. ROSSI (*CBS Technology Centre, USA*)

'A new system of cassette type consumer VTR'
By N. KIHARA (*Sony, Japan*)

'Rapid transmission and storage system'
By B. BENSON (*Goldmark Communications*)

'A new approach to helical scan recording'
By W. SCULLION (*Ampex, USA*)

Applicants for Election and Transfer

Meeting: 13th April 1976 (Membership Approval List No. 220)

GREAT BRITAIN AND IRELAND CORPORATE MEMBERS

Transfer from Member to Fellow

MEDLAND, Roy North. *Berwick, East Lothian.*

Transfer from Graduate to Member

BRETT, Michael David. *Croydon, Surrey.*
LEWIS, Peter John. *Pontypool, Gwent.*

Direct Election to Member

BERRY, Peter Raymond. *Maidstone, Kent.*
PASSMORE, Raymond. *Portsmouth, Hampshire.*
PHILLIPS, Barry Roger. *Wellington, Somerset.*
RHODES, John G. L. *Malmesbury, Wiltshire.*
SMITH, Arnold Moses. *Addington, Surrey.*

NON-CORPORATE MEMBERS

Direct Election to Companion

KROCH, Henry J. *Abercynon, Mid-Glamorgan.*

Transfer from Student to Graduate

ASH, Geoffrey. *Dunstable, Bedfordshire.*
EDGAR, Thomas H. *Blaydon, Tyne and Wear.*

THE MEMBERSHIP COMMITTEE at its meeting on 13th April 1976 recommended to the Council the election and transfer of the following candidates. In accordance with Bye-law 23, the Council has directed that the names of the following candidates shall be published under the grade of membership to which election or transfer is proposed by the Council. Any communication from Corporate Members concerning the proposed elections must be addressed by letter to the Secretary within twenty-eight days after publication of these details.

Direct Election to Graduate

WAI, Fung-Man. *West Ealing, London.*

Direct Election to Associate Member

JUSTIN, Peter Williams. *North Harrow, Middlesex.*
MATTHEWS, Stephen E. *Ilford, Essex.*
PETHERS, Joseph D. *Bampton, Oxfordshire.*
WILLIAMS, Kenneth. *Stokenchurch,, Buckinghamshire.*
WATTS, James H. C. *Ruardean, Gloucestershire.*

Direct Election to Associate

VALENTINE, Mark St. John. *Rockbourne, Hampshire.*

STUDENTS REGISTERED

CHAWDA, Rameshbbhai D. *Leicester.*

OVERSEAS

CORPORATE MEMBERS

Transfer from Graduate to Member

SOO, Kok Kee. *Singapore.*
WILMOT, Phyllis C. *Unterhaching, West Germany.*

Transfer from Student to Member

CARDLE, Peter A. *Paris.*

NON-CORPORATE MEMBERS

Transfer from Student to Graduate

CHEUNG, Chee Hsun. *Hong Kong.*

Direct Election to Graduate

SABARATNAM, Pasupathy. *Chunnakam, Sri Lanka.*

Transfer from Student to Associate Member

WANG, Shaw-Thang. *Singapore.*

Direct Election to Associate Member

LEUNG, Pak Chuen. *Hong Kong.*

STUDENTS REGISTERED

KWOK, Chee Mun. *Singapore.*
RAJU, Kulara Mama. *Dubai, U.A.E.*
WU, Tek Ming. *Singapore.*
YAP, Chee Kian. *Singapore.*
YEUNG, Kwong-Leung. *Hong Kong.*

Go-ahead for Euronet

A new network for the transmission of scientific and research data throughout the Common Market countries is to be jointly established by the Post Office and the other PTT Administrations of the nine members of the European Economic Community. The network, known as Euronet, is sponsored by the EEC and the important job of designing, planning and implementing the telecommunications element will be carried out by the British Post Office.

The most important advantages of the network are that it will enable incompatible documentation systems to communicate with each other. It will also reduce duplication which could arise in creating a comprehensive system of computer information stores (database) for the Community.

The network will serve some 700 data terminals at research centres, public bodies and other organizations by the end of the decade, giving them immediate access to scientific and technical information stored in the databases. Due to start in about two years' time, Euronet will initially be a private network but it might eventually form the basis of a European public data-transmission network.

Formal agreement to set up the telecommunications element of the network was reached in December by the PTT Administrations of the nine EEC countries. Acting as a Consortium, they authorized the French Department of Posts and Telecommunications to sign an agreement with the EEC on their behalf to cover the development, planning and implementation of the telecommunications element.

The Consortium has also set up a Management Committee whose task will be to bring Euronet into being. The work is to be carried out through two Sub-committees, one to deal with commercial problems and the other to oversee the implementation of the network. The latter is chaired by Mr Philip Kelly, a senior British Post Office Engineer.

One of the Management Committee's first decisions—made at its inaugural meeting on Friday, 6th February—was to agree on the need for a study contract to prepare a precise definition of the proposed Euronet system. This will be placed by the French Administration on behalf of the Management Committee when a specification for the definition stage contract has been drawn up. Producing this specification will be the first job of the Implementation Sub-Committee.

The telecommunications network will use the method of data transmission known as packet switching, in which the data are sent as a series of self-contained addressed blocks. Euronet's packet-switching technology will be based on that to be used in another European data system—the European Informatics Network (EIN). Each user's terminal will be connected to equipment which will assemble data into packets for onward transmission to one of the databases linked into the network. This equipment will also breakdown packets received from a database into a continuous data stream.

The network will be based initially on four packet switching centres in London, Frankfurt, Paris and Rome. These nodal centres will provide access to databases for users in those countries and will also be linked to network access centres (concentrators) in Amsterdam, Brussels, Copenhagen and Dublin to provide database access for users in the Netherlands, Belgium, Denmark and the Irish Republic. Access will also be provided in Luxembourg, the EEC Commission's data centre.

Information will be stored on two computers—in Cologne, Germany and Frascati, Italy—containing a score of data files which will be accessible to users. These cover such diverse fields as physics, chemistry, aerospace, energy, nucleonics, metallurgy, medicine, agriculture, economics, statistics and law.